University of Jiroft

**Biospecies Research**

Journal homepage: bsr.ujiroft.ac.ir

Iranian Biology Society

# Intravenous glucose tolerance test in Baluchi ewe lambs receiving dietary supplemental selenium-methionine and chromium-methionine

Amir Mousaie[1,2*], Reza Valizadeh[2], Abbas Ali Naserian[2], Mohammad Heidarpour[3], Hossein Kazemi Mehrjerdi[3]

https://doi.org/10.22034/bsr.2025.559992.1001

[1] *Department of Animal Science, Faculty of Agriculture, University of Jiroft, Jiroft, Iran*

[2] *Department of Animal Science, Faculty of Agriculture, Ferdowsi University of Mashhad, Mashhad, Iran*

[3] *Department of Clinical Science, Faculty of Veterinary Medicine, Ferdowsi University of Mashhad, Mashhad, Iran*

**ARTICLE INFO**

**Article Type**
Original Article

**Article History**
Received: 21 November 2025
Accepted: 22 December 2025
Published: 15 February 2026


***Corresponding author**
a.mousaie@ujiroft.ac.ir

**ABSTRACT**

The impact of dietary supplementation of 1.5 mg of Selenium/kg of diet as Selenium-methionine (Se-Met) and 0.8 mg of Chromium/kg of diet as Chromium-methionine (Cr-Met) and their combination (Se-Cr-Met) on glucose and insulin responses during intravenous glucose tolerance test (IVGTT) was examined on 24 Baluchi ewe lambs (18-20 weeks of age) with 6 replicates per treatment. Blood samples were collected before (time 0) and 2, 10, 20, 30, 45, 60, 90, 120 and 180 min after IVGTT. The supplementation of Se- and/or Cr-Met resulted in a lower peak glucose concentration at 2 minutes and a diminished concentration at 180 minutes following the infusion ($P < 0.05$). Additionally, lambs receiving Cr-Met and Se-Cr-Met exhibited lower serum glucose levels at 120 minutes in comparison to the control group ($P \leq 0.05$). Furthermore, animals consuming diets supplemented with Se-Met and/or Cr-Met showed a reduced area under the curve (AUC) for glucose and insulin at 180 minutes following the IVGTT ($P < 0.05$). The quantity of circulating malondialdehyde, which serves as an indicator of oxidative stress, was reduced in lambs supplemented with Se-Met and/or Cr-Met ($P < 0.05$). It can be concluded that the supplementation of organic Se-Met and/or Cr-Met enhanced glucose clearance and insulin sensitivity in growing Baluchi ewe lambs, with these effects possibly mediated by a decrease in systemic oxidative stress.

**Keywords**: Chromium, Ewe lamb, Glucose tolerance test, Insulin, Selenium

**How to cite this paper**

Mousaie, A., Valizadeh, R., Naserian, A., Heidarpour, M., Kazemi Mehrjerdi, H., 2026. Intravenous glucose tolerance test in Baluchi ewe lambs receiving dietary supplemental selenium-methionine and chromium-methionine. *Biospecies Research*, 1, pp. 1-9.

## Introduction

Insulin, produced by the pancreatic beta cells, is the hormone that plays a crucial role in reducing blood glucose levels and promoting energy storage. It aids in the synthesis and storage of glycogen, lipids, and proteins (Rahman et al., 2021; Qiao et al., 2024). Research indicated that insulin sensitivity diminishes with maturation and aging in both animals and humans; however, the timing and degree of compensatory

hyperinsulinemia, along with its effects on glucose tolerance, remain inadequately understood (Gatford et al., 2004). Additionally, insulin resistance (IR) may impair weight gain in developing animals. Insulin facilitates cellular glucose uptake, stimulates glycolysis, and encourages the synthesis of hepatic and muscle glycogen, adipose triglycerides, and skeletal muscle protein, while also inhibiting their degradation (Baumgard et al., 2015). Furthermore, a decline in insulin sensitivity is observed during the first year of life in sheep (Clarke et al., 2000).

Selenium (Se), recognized as an essential micronutrient, exerts its beneficial impacts through selenoproteins such as glutathione peroxidase (GPX1), which acts as an inhibitor of reactive oxygen species (Vonnahme et al., 2010, Mousaie, 2021). Ezaki (1990) illustrated that Se induced various insulin-like effects in rat adipocytes, including the stimulation of glucose transport activity. McNeill (1991) built upon Ezaki's findings, demonstrating that selenium functioned as an insulin-mimetic agent in vivo. A study highlighted the positive effects of antioxidants, including Se, on glucose tolerance and insulin sensitivity in dairy cows (Abuelo et al., 2016). Nevertheless, limited information exists regarding the effects of dietary Se supplementation on glucose tolerance in ruminant animals, particularly in sheep. Similarly, chromium (Cr) intake is associated with diverse metabolic functions in both humans and livestock. The trivalent form of chromium ($Cr^{+3}$), which is a component of low-molecular-weight chromium-binding substance (LMWCr) or *chromodulin*, is crucial for metabolism as it enhances glucose tolerance by amplifying insulin action and is involved in the metabolism of proteins, lipids, and carbohydrates (Vincent, 2007). While the organic source of Cr as chromium-methionine (Cr-Met) has been reported to improve the growth performance of Baluchi lambs (Mousaie et al., 2014), there exists contradictory evidence concerning the glucose-reducing effects of Cr supplements in ruminant animals. The glucose tolerance test provides a more accurate assessment of an animal's insulin status compared to basal insulin and glucose levels. Moreover, to the authors' knowledge, there is a lack of research examining the impacts of Se and Cr administration on the intravenous glucose tolerance test (IVGTT) in sheep particularly ewe lambs. The aim of this study was to evaluate the effects of dietary organic selenium and chromium supplementation on the insulin sensitivity of growing ewe lambs using IVGTT, representing the first investigation of its kind in this sheep breed.

## Materials and methods

### Animals and experimental treatments

This experiment was carried out at the Research Station of the Department of Animal Science, Ferdowsi University of Mashhad, Iran. Animals were managed in accordance with the protocols established by the Iranian Council of Animal Care (1995). A total of four experimental diets were randomly allocated to 24 nulliparous fat-tailed Baluchi ewe lambs, aged 18-20 weeks and with an average live weight of 24.2 ± 0.4 kg, utilizing a completely randomized design with six replications for each experimental group. The experimental period spanned 11 weeks during the summer months.

Following a 2-week acclimatization phase to a control diet and the experimental conditions, the lambs were randomly assigned to one of four dietary treatments: 1) Basal diet (Control group); 2) Basal diet supplemented with 1.5 mg of Selenium (Se) per kg of diet in the form of selenium-methionine (Se-Met; Availa®Se 1000, containing a minimum concentration of 1000 mg of Se per kg from a selenium-L-methionine complex, Zinpro Corporation, USA); 3) Basal diet supplemented with 0.8 mg of Chromium (Cr) per kg of diet in the form of chromium-methionine (Cr-Met; Availa®Cr 1000, which includes a minimum concentration of 1000 mg/kg of Cr from a chromium-L-methionine complex, Zinpro Corporation, USA); and 4) Basal diet supplemented with both 1.5 mg of Se, as Se-Met and 0.8 mg of Cr as Cr-Met per kg of dry matter (Se-Cr-Met). The composition of diet ingredients and nutrients is presented in Table 1.

Table 1. Ingredients and chemical composition of the experimental diet

| Ingredient | g /kg DM |
|---|---|
| Alfalfa hay mid-bloom | 100 |
| Corn silage | 100 |
| Wheat straw | 50 |
| Barely grain | 300 |
| Soybean meal | 90 |
| Extruded linseed | 80 |
| Wheat bran | 150 |
| Beet pulp-shreds | 115 |
| Mineral-vitamin mixture [a] | 10 |
| Salt | 5 |
| Chemical composition | |
| Crude protein | 157 |
| Ether extract | 50 |
| Neutral detergent fiber (NDF) | 360 |
| Ash | 70 |
| Calcium | 8.5 |
| Phosphorous | 5.9 |
| Metabolizable energy (Mcal/kg) [b] | 2.57 |

[a] Mineral and vitamins g/kg supplement: Se, 0.01g (Na2Seo3); Mn, 2 g; Zn, 3 g; Co, 0.1g; I, 0.1g; Ca, 195g; P, 90g; Mg, 20g; Fe, 3g; Antioxidant, 0.4g; Vit. A, 500,000 IU; Vit. D3, 100,000; Vit. E 0.1 g. [b] Calculated with Small Ruminant Nutrition System (SRNS) software.

### Intravenous glucose tolerance test

An intravenous glucose tolerance test (IVGTT) was conducted at the end of the experiment. All ewe lambs underwent an overnight fasting period, during which they were weighed. Jugular veins were catheterized using Certofix trio 720 catheters (14-gauge, 20 cm length, B-Braun, Melsungen, Germany) under local anesthesia and in accordance with aseptic procedures. The animals were permitted a recovery period of 24 hours' post-catheterization to minimize the potential influence of stress hormones on blood glucose and insulin levels. The animals were provided with unrestricted access to water and feed throughout the recovery period. Then, the animals underwent an overnight fasting prior to the IVGTT. Subsequently, a bolus dose of glucose (dextrose solution; Merck Co., Germany) was administered (50% wt/vol; 0.50 g of glucose/kg of body weight), following the methodology outlined by Kitchalong et al. (1995).

### Blood samples collection and analysis

Blood samples for the analysis of glucose and insulin were collected at baseline and at 2, 10, 20, 30, 45, 60, 90, 120, and 180 minutes following the infusion. Catheters were thoroughly flushed with saline after the glucose infusion and each blood sampling. Blood samples were centrifuged at 3000 × g for 10 minutes, and the serum was stored at -80°C until further analysis. Glucose concentration was determined using the glucose oxidase/peroxidase method (Pars Azmoon Co., Tehran, Iran), while insulin levels were measured using an ELISA kit (Monobind Inc., Lake Forest, CA, USA). The glucose and insulin responses to the glucose tolerance test were assessed by calculating the areas under the curve (AUC) for the periods of 0 to 60, 0 to 90, 0 to 120, and 0 to 180 minutes' post-infusion. Additionally, the concentrations of malondialdehyde (MDA) as thiobarbituric acid-reactive substances and the total antioxidant capacity of serum

were evaluated using the ferric reducing antioxidant power (FRAP) assay, following the protocol established in a prior study (Mousaie et al., 2017).

### Statistical analysis

Data were analyzed using a mixed model that incorporated fixed effects for treatment, time of sampling, and the interaction between treatment and time, as well as the random effect of the animal within each treatment group (SAS 9.2). The body weight of the lambs prior to the IVGTT was included as a covariate in the models to enhance the precision of the analysis. The AUC for glucose and insulin during the IVGTT was calculated utilizing the trapezoidal method alongside actual concentration values, after excluding the baseline concentration. Basal glucose and insulin concentrations, measured immediately before the IVGTT, were derived by averaging values from samples collected 10 and 0 minutes prior to the test.

$$AUC = (t_b\text{-}t_a) \times ([t_a + t_b]/2).$$

Where $[t_a]$ is the concentration of metabolite at time a ($t_a$), and $[t_b]$ represents the concentration of the metabolite at time point b ($t_b$). To account for the differing correlations of repeated measures within the same subject, mixed models with various covariance structures (e.g., compound symmetry, heterogeneous compound symmetry, autoregressive (1), heterogeneous autoregressive (1), and unstructured) were evaluated to identify the structure yielding the best fit criteria. The autoregressive (1) model was determined to be the most suitable option. The data are presented as least square means ± standard error (SE). Statistical significance was established at $P \leq 0.05$, while trends were noted at $P \leq 0.10$.

## Results

### Blood glucose and insulin concentrations

Based on the findings of this study, no significant differences were observed among treatments in serum glucose levels at time 0 (prior to the glucose administration). However, the average serum glucose levels during the IVGTT for the Se-Met (254.0 mg/dl), Cr-Met (254.2 mg/dl), and Se-Cr-Met (255.0 mg/dl) groups were lower than that of the control group, which had an average of 284.0 mg/dl ($P < 0.05$, Figure 1). After the glucose infusion, serum glucose concentrations increased, with the Se-Met and/or Cr-Met groups exhibited significantly lower quantities than the control lambs at both 2 minutes (the peak of glucose concentration) and 180 minutes following the IVGTT ($P < 0.05$). At the 120-minute mark, the Cr-Met ($P = 0.045$) and Se-Cr-Met ($P = 0.04$) groups presented lower serum glucose levels compared to the control, while the Se-Met animals demonstrated a tendency toward reduced serum glucose concentration ($P = 0.06$). The data related to the AUC for glucose are detailed in Table 2. Lambs receiving the Se-Cr-Met supplementation had a lower AUC at the 120-minute interval ($P = 0.02$), while all lambs given Se-Met and/or Cr-Met supplemented diets exhibited a reduced AUC of glucose at the 180-minute point in comparison to the control ($P < 0.05$). Serum insulin concentrations, as illustrated in Figure 2, did not show significant differences among the experimental groups. However, lambs received diets supplemented with Se-Met ($P = 0.02$) and Cr-Met ($P = 0.02$) had a lower AUC of insulin at the 180-minute mark following the IVGTT, as indicated in Table 2.

### Blood antioxidant biomarkers

Serum MDA concentrations (mean ± SEM) for the control, Se-Met, Cr-Met, and Se-Cr-Met groups were recorded at 7.68 ± 0.260, 5.80 ± 0.260, 5.48 ± 0.260, and 5.52 ± 0.260 nmol/ml, respectively. The MDA levels in lambs fed Se- and/or Cr-Met supplements were significantly lower than those observed in the control group ($P < 0.05$). Total antioxidant capacity, as measured by FRAP values, was recorded at 110 ± 14.37, 147 ± 14.37, 127 ± 14.37, and 145 ± 14.37 µmol/ml for the control, Se-Met, Cr-Met, and Se-Cr-Met groups, respectively. Despite the elevated FRAP values observed in the Se- and/or Cr-Met groups, no significant differences were noted between the serum FRAP values of the treated animals and those of the control group.

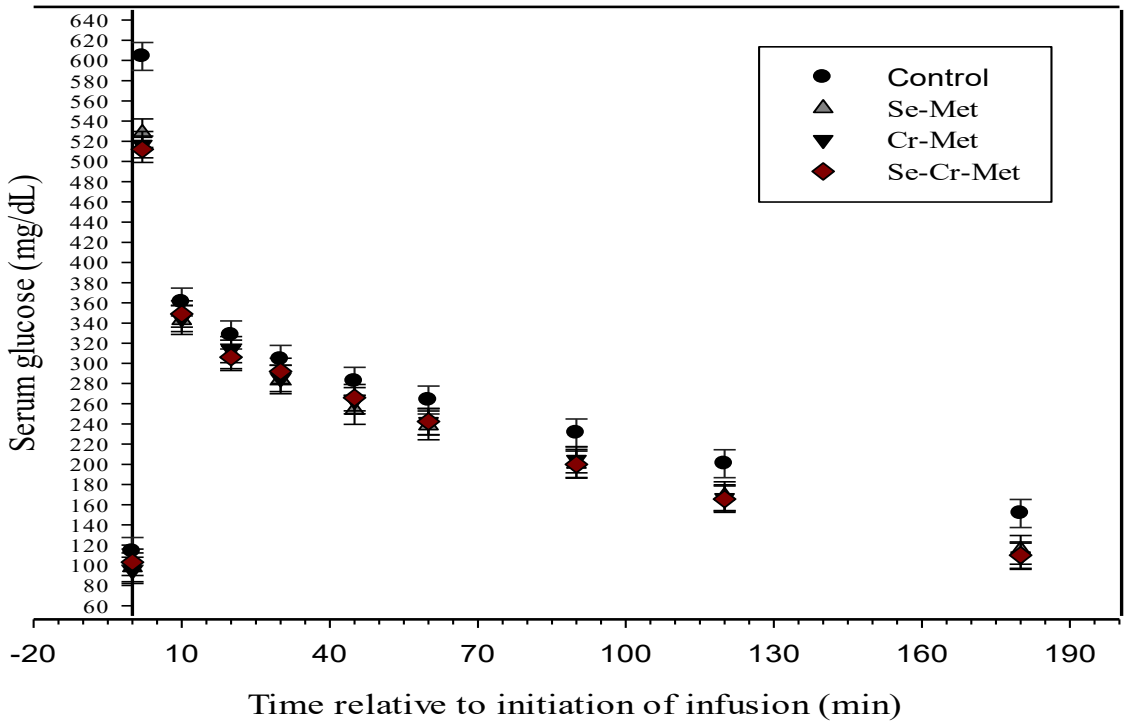


**Figure. 1** Serum glucose concentration in response to an intravenous glucose infusion of ewe lambs fed Se-Met and/or Cr-Met supplements. n = 6 in each experimental group. Time 2: Se/Cr-Met vs Control $P < 0.05$; Time 120: Cr-Met & Se-Cr-Met vs. Control $P < 0.05$. Time 180: Se/Cr-Met vs Control $P < 0.05$

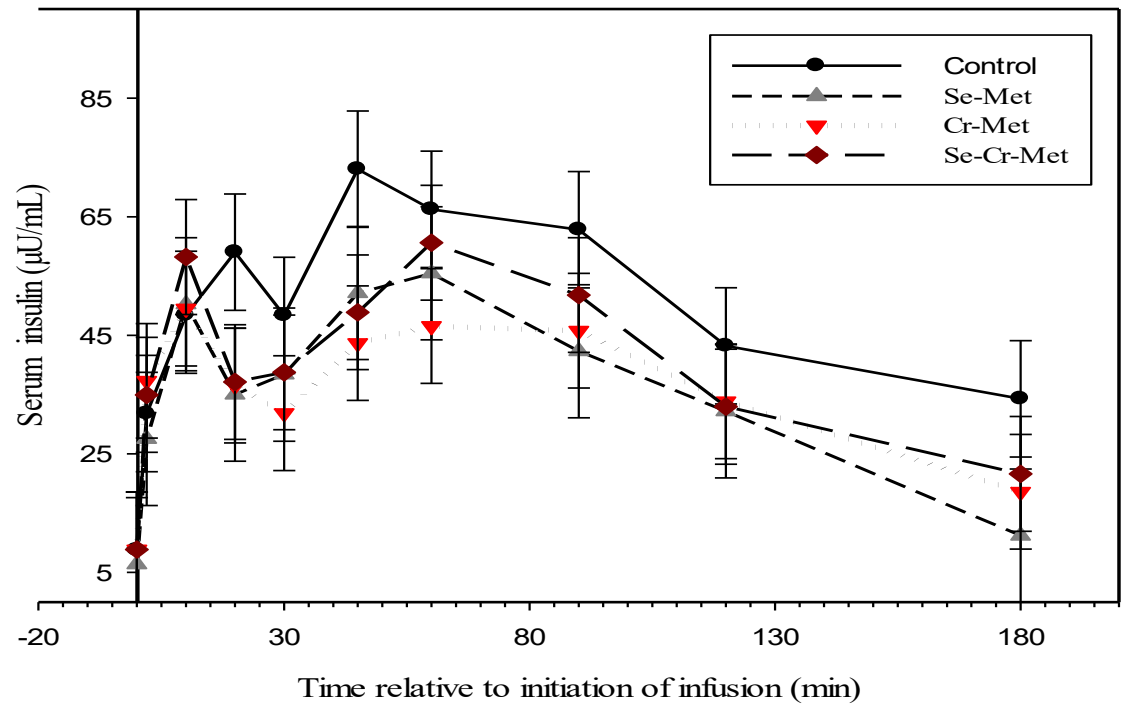


**Figure. 2** Serum insulin concentration in response to an intravenous glucose infusion of ewe lambs fed Se-Met and/or Cr-Met supplements. n = 6 in each experimental group

Table 2 Effects of feeding Se-Met and/or Cr-Met supplements on serum glucose and insulin kinetics following an intravenous glucose infusion of Baluchi ewe lambs.

| | Experimental group | | | |
|---|---|---|---|---|
| Area under the curve | Control | Se-Met | Cr-Met | Se-Cr-Met |
| Glucose | | | | |
| $AUC_{60}$ | 13384 | 12998 | 12686 | 12310 |
| $AUC_{90}$ | 17363 | 16643 | 16491 | 15775 |
| $AUC_{120}$ | 20408 [a] | 19238 [ab] | 19290 [ab] | 18168 [b] |
| $AUC_{180}$ | 24135 [a] | 21870 [b] | 21996 [b] | 20155 [b] |
| SEM | 848.7 | 882.2 | 771.6 | 776.9 |
| Insulin | | | | |
| $AUC_{60}$ | 1917 | 1319 | 1467 | 1690 |
| $AUC_{90}$ | 3598 | 2597 | 2593 | 3112 |
| $AUC_{120}$ | 4933 | 3523 | 3524 | 4120 |
| $AUC_{180}$ | 6778 [a] | 4443 [b] | 4565 [b] | 5229 [ab] |
| SEM | 806.3 | 882.6 | 710.5 | 720.0 |

SEM: Standard error of means

n = 6 in each experimental group

$AUC_{60}$ = area under the curve during the first 60 min of IVGTT [(mg/dL) × 60 min].

$AUC_{90}$ = area under the curve during the 90 min of IVGTT [(mg/dL) × 90 min].

$AUC_{120}$ = area under the curve during the 120 min of IVGTT [(mg/dL) × 120 min].

$AUC_{180}$ = area under the curve during the 180 min of IVGTT [(mg/dL) × 180 min].

Different superscripts within a row indicate statistical significance at $P < 0.05$.

## Discussion

A reduction in insulin sensitivity has been observed between 1 and 12 months of age in sheep, indicating that insulin sensitivity declines throughout the first year of life in lambs (Clarke et al., 2000). Glucose serves as the primary or exclusive source of cellular energy in various tissues, including red blood cells, immune cells, and the brain (Ravelo et al., 2025). The glucose tolerance test serves as an effective method for diagnosing glucose intolerance in both humans and animals. However, the establishment of catheters and the IVGTT pose challenges in sheep and goats. In this study, we opted to utilize a catheter designed for human cardiovascular surgery, despite its higher cost, to facilitate the IVGTT, thereby reducing the stress typically associated with catheterization. Dietary supplemental Se and Cr from organic sources showed favorable outcomes on glucose tolerance in ewe lambs. According to Ezaki's study (1990), Se enhances glucose tolerance in experimental animals. Vonnahme et al. (2010) demonstrated the positive effects of maternal high Se feeding in sheep on the insulin sensitivity of offspring. Nonetheless, research regarding the influence of Se on glucose and insulin dynamics in sheep remains limited. In the present investigation, serum MDA, a reliable index of lipid peroxidation (Mousaie, 2021), decreased in Se-supplemented lambs. Supporting these findings, Abuelo et

al. (2016) indicated that cows receiving antioxidant supplementation (vitamin E and Se) experienced improved insulin sensitivity by enhancing the antioxidant system. Regarding the effects of Cr on insulin sensitivity, Kitchalong et al. (1995) reported no change in glucose tolerance in lambs fed diets supplemented with Cr. Conversely, Kegley et al. (1997) observed a reduction in plasma glucose concentration following intravenous insulin infusion in calves that received chromium chloride or the chromium-nicotinic acid complex, aligning with our results. Emami et al. (2014) also documented a significant decrease in glucose AUC in goat kids after the inclusion of 1.5 mg of Cr/kg diet as chromium-methionine. The variation in studies' outcomes may be attributed to differences in animal breeds, physiological conditions, and the types and levels of minerals supplied. Insulin lowers circulating glucose levels by promoting its uptake in insulin-sensitive tissues, enhancing glycogen synthesis, and decreasing gluconeogenesis. The lower plasma glucose and insulin levels observed in chromium-supplemented lambs in this study suggest that less insulin was necessary to clear glucose from the bloodstream, indicating an increased tissue sensitivity to insulin (Emami et al., 2014). Consequently, the significantly lower peak of serum glucose at 2 minutes following glucose infusion may serve as an indicator of improved insulin responsiveness in lambs receiving dietary selenium-methionine and/or chromium-methionine supplements. A greater AUC would indicate higher peripheral glucose intolerance, while a lower insulin AUC would imply enhanced insulin efficiency or a diminished requirement for insulin to facilitate effective and timely peripheral glucose uptake (Hayirli et al., 2001). The concentration of MDA is commonly employed as a marker of lipid peroxidation. In accordance with the previous study (Mousaie et al., 2017), serum MDA levels were reduced through the administration of selenium-methionine and/or chromium-methionine, which may corroborate the hypothesis regarding the advantageous effects of decreased oxidative stress on insulin sensitivity in lambs supplemented with these compounds. The mechanisms that contribute to insulin resistance in ruminants remain inadequately elucidated. From a physiological standpoint, this condition bears some resemblance to human types I and II diabetes; however, a key distinction lies in the fact that ruminants exhibit lower glucose concentrations than humans. In the context of human type II diabetes, substantial evidence indicates that oxidative stress is instrumental in the onset and progression of insulin resistance, which can be significantly mitigated through the administration of antioxidant supplements (Chalmeh et al., 2021). The results of this study suggest a heightened insulin sensitivity, indicating that a reduced amount of insulin was required to remove glucose from the bloodstream of lambs fed with the Se- and Cr-supplemented diets.

## Conclusion

The responses of glucose tolerance and insulin secretion to an intravenous glucose load in ewe lambs receiving diets supplemented with Se-Met and/or Cr-Met exhibited differences compared to those on a control diet. Specifically, animals on Se- and/or Cr-supplemented diets showed reduced serum glucose levels at 2- and 180-minutes' post-glucose infusion, along with a lower AUC for glucose and insulin at 180 minutes after the infusion. These findings suggest potential beneficial effects of these supplements on insulin sensitivity. Nonetheless, additional research is required to elucidate the precise mechanisms through which Se-Met and/or Cr-Met supplements influence insulin resistance in sheep.

## Acknowledgements

The authors express their gratitude to the Department of Animal Science at the Faculty of Agriculture, Ferdowsi University of Mashhad, as well as to Sana Dam Pars and Yasna Mehr Co. (Tehran, Iran) for their partial financial support of this research.

## Conflict of interest

The authors declare that there is no conflict of interest.

## Ethical Statement

The authors confirm their adherence to the ethical standards specified in the journal's author guidelines.

They also confirm that all procedures concerning animal care, experimental methods, and sampling were carried out in compliance with the regulations established by the Iranian Council of Animal Care (1995). Moreover, all research protocols, including the use of facilities and sampling procedures, received approval from the Department of Animal Science at the Faculty of Agriculture, Ferdowsi University of Mashhad, Iran.

**References**

Abuelo, A., Alves-Nores, V., Hernandez, J., Muino, R., Benedito, J.L., Castillo, C., 2016. Effect of parenteral antioxidant supplementation during the dry period on postpartum glucose tolerance in dairy cows. *Journal of Veterinary Internal Medicine,* 30: 892-898.

Baumgard, L.H., Hausman, G.J., Sanz Fernandez, MV., 2015. Insulin: pancreatic secretion and adipocyte regulation. *Domestic Animal Endocrinology*, 54: 76-84.

Chalmeh, A., Pourjafar, M., Badiei, K., Mirzaei, A., Jalali, M., Mazrouei Sebdani, M., 2021. Effects of dietary antioxidants on glucose and insulin responses to glucose tolerance test in transition dairy cows. *Domestic Animal Endocrinology*, 75: 106602. DOI: 10.1016/j.domaniend.2020.106602.

Clarke, L., Firth, K., Heasman, L., Juniper, D.T., Budge, H., Stephenson, T. Symonds, ME., 2000. Influence of relative size at birth on growth and glucose homeostasis in twin lambs during juvenile life. *Reproduction, Fertility and Development*, 12: 69-73.

Emami, A., Ganjkhanlou, M., Zali, A., 2014. Effects of Cr methionine on glucose metabolism, plasma metabolites, meat lipid peroxidation, and tissue chromium in Mahabadi goat kids. *Biological Trace Element Research*, 164: 50-57.

Ezaki, O., 1990. The insulin-like effects of selenate in rate adipocytes. *Journal of Biological Chemistry*, 265: 1124-1128.

Gatford, K.L., De Blasio, M.J., Thavaneswaran, P., Robinson, J.S., McMillen, IC., Owens, J.A., 2004. Postnatal ontogeny of glucose homeostasis and insulin action in sheep. *American Journal of Physiology-Endocrinology and Metabolism*, 286: 1050-1059.

Hayirli, A., Bremmer, D.R., Bertics, S.J., Socha, M.T., Grummer, R.R., 2001. Effect of chromium supplementation on production and metabolic parameters in periparturient dairy cows. *Journal of Dairy Science*, 84: 1218-1230.

Iranian Council of Animal Care., 1995. Guide to the care and use of experimental animals. vol 1. Isfahan University of Technology, Isfahan, Iran.

Kegley, E.B., Spears, J.W., Brown, T.T., 1997. Effect of shipping and chromium supplementation on performance, immunity response, and disease resistance of steers. *Journal of Animal Science*, 75: 1956-1964.

Kitchalong, L., Fernandez, J.M., Bunting, L.D., Southern, L.L., Bidner, T.D., 1995. Influence of chromium tripicolinate on glucose metabolism and nutrient partitioning in growing lambs. *Journal of Animal Science*, 73: 2694-2705.

McNeill, J.H., Delgatty, H.L.M., Battell, M.L., 1991. Insulin-like effects of sodium selenate in streptozotocin-induced diabetic rats. *Diabetes*, 40: 1675-1679.

Mousaie, A., Valizadeh, R., Naserian, A.A., Heidarpour, M., Kazemi Mehrjerdi, H., 2014. Impacts of feeding selenium-methionine and chromium-methionine on performance, serum components, antioxidant status and physiological responses to transportation stress of Baluchi ewe lambs. *Biological Trace Element Research*, 162: 113-123.

Mousaie, A., Valizadeh, R., Chamsaz, M., 2017. Selenium-methionine and chromium-methionine supplementation of sheep around parturition: impacts on dam and offspring performance. *Archives of Animal Nutrition*, 71: 134-149.

Mousaie, A., 2021. Dietary supra-nutritional supplementation of selenium-enriched yeast improves feed efficiency and blood antioxidant status of growing lambs reared under warm environmental conditions. *Tropical Animal Health and Production*, 53: 138.

Qiao, K., Jiang, R., Contreras, G.A., Xie, L., Pascottini, O.B., Opsomer, G., Dong, Q., 2024. The Complex interplay of insulin resistance and metabolic

inflammation in transition dairy cows. *Animals*, 14: 832. DOI: 10.3390/ani14060832.

Rahman, M.S., Hossain, K.S., Das, S., Kundu, S., Adegoke, E.O., Rahman, M.A., Hannan, M.A., Uddin, M.J., Pang, M.G., 2021. Role of insulin in health and disease: An update. *International Journal of Molecular Sciences*, 22: 6403. DOI: 10.3390/ jms22126403.

Ravelo, A.D., Matamoros, C., Harvatine, K.J., Salfer, I.J., 2025. Daily rhythms of glucose, insulin, and nonesterified fatty acid responses to an intravenous glucose tolerance test in dairy cows. *Journal of Dairy Science*, 108: 5462-5474.

Vincent, J.B., 2007. The nutritional biochemistry of chromium (Ⅲ). *Elsevier*, First edition. 293 pp.

Vonnahme, K.A., Luther, J.S., Reynolds, L.P., Hammer, C.J., Carlson, D.B., Redmer, D.A., Caton, J.S., 2010. Impacts of maternal selenium and nutritional level on growth, adiposity, and glucose tolerance in female offspring in sheep. *Domestic Animal Endocrinology*, 39: 240-248.

University of Jiroft

**Biospecies Research**

Journal homepage: bsr.ujiroft.ac.ir

Iranian Biology Society

# Effect of *Pteropyrum aucheri* Jaub. & Spach shrub on desert soil seed banks, application for restoring the medicinal plant *Pergularia tomentosa* L.

Reza Erfanzadeh[1]*; Fatemeh-al-Sadat Hosseini[2]

https://doi.org/10.22034/bsr.2025.561903.1002

[1] *Rangeland Management Department, Faculty of Natural Resources, Tarbiat Modares University, Tehran, Iran.*

[2] *Rangeland Management Department, Faculty of Natural Resources, Tarbiat Modares University, Tehran, Iran.*

**ARTICLE INFO**

**Article Type**
Original Article

**Article History**
Received: 24 November 2025
Accepted: 28 December 2025
Published: 15 February 2026


***Corresponding author**
rezaerfanzadeh@modares.ac.ir

**ABSTRACT**

*Pergularia tomentosa*, a medicinally valuable species in arid regions, persists at critically low densities in recently years in Iran, demanding some conservation action. Its frequent coexistence with *Pteropyrum aucheri*, a shrub known to enhance its aboveground growth, prompted our investigation into *P. aucheri*'s influence on soil seed bank (SSB) dynamics for potential restoration applications. Greenhouse germination of soil samples (beneath vs. outside shrub canopies) revealed 2,164 seedlings, with 68% (1,486) emerging from sub-canopy soils. *P. aucheri* significantly enhanced SSB density at 0-5 cm depth across functional groups: annuals (3,431 vs. 999), perennials (412 vs. 147), forbs (1,835 vs. 726), and grasses (2,048 vs. 424). Poaceae dominated the SSB composition (8 species). The complete absence of *P. tomentosa* germinants, despite its coexistence with *P. aucheri*, reveals a critical restoration constraint. This suggests that SSBs contributes minimally to *P. tomentosa* persistence and canopy-associated SSB enrichment doesn't benefit this target species. While *P. aucheri* creates favorable microsites for general SSB enrichment, its facilitation doesn't extend to *P. tomentosa* recruitment via seed banks. Restoration protocols must therefore combine shrub-retention (to maintain beneficial microhabitats) with active *P. tomentosa* reintroduction to ensure species recovery in degraded arid ecosystems. Active restoration such as direct seeding is essential.

**Keywords**: Facilitation effects, Medicinal plants, Passive restoration, Seed germination, Iran.

**How to cite this paper**

Reza Erfanzadeh., Fatemeh-al-Sadat Hosseini., 2026. Effect of *Pteropyrum aucheri* Jaub. & Spach shrub on desert soil seed banks, application for restoring the medicinal plant *Pergularia tomentosa* L. ***Biospecies Research***, 1, pp. 10-23.

## Introduction

An evergreen perennial shrub from the Apocynaceae family, *Pergularia tomentosa* L. has a characteristic scent. Classified as a xerophyte, it grows well in arid and semiarid environments across the globe, especially in sand and gravel plains (Feulner, 2016). The plant usually reaches under one meter in height and is common in various African nations, including Egypt, Jordan, and Kenya, as well as in Asian countries like Iran, Afghanistan, and Saudi Arabia (Babaamer et al., 2013). Notably, *P.*

*tomentosa* is recognized for its substantial enzyme content, antifungal characteristics, and milk-clotting capabilities (Benyahia et al., 2021). The leaves, in particular, have been noted as a significant source of flavonoids and cardenolides, providing a rich supply of natural antioxidants and antitumor agents (e.g., Lahmar et al., 2022). While *P. tomentosa* offers many benefits, it is classified as endangered with very low population densities in the arid rangelands of the United Arab Emirates, Lebanon, and Iran, necessitating immediate ecological intervention (Allen et al., 2021; Hosseini Kahnuj et al., 2017). In response, restoration initiatives have been suggested in Iran. Hosseini Kahnuj et al. (2017) specifically advocated for dedicated conservation measures, proposing the planting of this species under shrub canopies or alongside waterways to support its preservation and recovery. Commonly used restoration approaches in degraded areas include passive restoration, which leverages the soil seed bank after removing grazing animals, and active restoration, such as replanting. Due to its lower expense, some ecologists argue that passive restoration should be the first strategy attempted. This method depends on a regressive ecosystem's natural succession to restore target species and plant communities without direct human involvement (e.g., Zahawi et al., 2014; Miao et al., 2016). Consequently, prior to engaging in the often-expensive active restoration process, we evaluated the soil seed bank (SSB) in the native habitat of *P. tomentosa* to determine its potential for the passive restoration of this species.Of the Earth's total land area, 36% consists of arid and semi-arid ecosystems, where shrubs function as essential foundation species. Their presence critically shapes ecosystem structure and function (Lortie et al., 2017; Jones et al., 2023). As a fundamental part of these environments, shrubs substantially alter habitat conditions by driving the spatial distribution of soil nutrients (Yang et al., 2024; Soubry et al., 2022). Research indicates that woody plants in such regions can increase mycorrhizal colonization (Armenta Calderón et al., 2019), boost soil microbial activity (Chandregowda et al., 2018), alter patterns of runoff and sediment discharge (Lu et al., 2019), and affect the soil seed bank (SSB) (e.g., Hadinezhad et al., 2021). Specifically, shrubs enrich the SSB under their canopies via two key processes: firstly, the direct trapping of seeds, especially those dispersed by wind, and secondly, by altering the local environment to boost seed production in the understory (Hadinezhad et al., 2021). Acting as ecological facilitators, they generate favorable microsites that aid in seed retention, survival, and germination. The buildup of shrub litter and foliage improves underlying soil quality, which in turn can lead to higher seed production and a greater density of buried seeds (e.g., Gomaa et al., 2023). Consequently, analyzing the SSB and its spatial and temporal dynamics in association with shrubs may provide a useful framework for the targeted conservation and restoration of other species in arid landscapes.The shrub *Pteropyrum aucheri* Jaub. & Spach is among the most significant plants found in arid and semiarid rangelands. Within Iran, this species is distributed across numerous provinces in the Irano-Turanian region, where it can grow up to 1.5 meters, making it one of the tallest shrubs in its habitat (Rechinger and Schiman-Czeika, 1968). It serves as a dominant shrub species on plains, along riversides, and in seasonal waterways (Khosravi Mashizi, 2019). Earlier research has indicated that *P. aucheri* improves soil fertility factors, including total organic matter, though its positive impact on soil is somewhat weaker relative to other shrub species (Motamedi et al., 2013; Erfanzadeh et al., 2016). This study specifically aimed to examine the influence of *P. aucheri* on the density and richness of the soil seed bank (SSB) in its environment, with a focus on assessing its facilitative role on the SSB of *P. tomentosa* for restoration objectives. Both species are indigenous and occur naturally in the region without human cultivation (Ghahreman and Attar, 1999). In the study area, they grow in close proximity, with *P. aucheri* being the dominant species and *P. tomentosa* present in scarce numbers.

Therefore, the objectives of this study were, first, to determine whether *P. aucheri* increases the density and species richness of the total soil seed bank beneath its canopy, and second, to evaluate its potential role in

conserving *P. tomentosa* by assessing whether its facilitative effects enhance the SSB of this species. Previous reports have shown that both above and belowground parts of *P. tomentosa* beneath the canopy of *P. aucheri* were significantly larger than those outside the canopy cover (Hosseini Kahnuj et al., 2017), indicating positive facilitative effects on *P. tomentosa*.

## Materials and Methods

### Study area

The research was conducted in the semi-arid rangeland surrounding Kahnuj city, situated in Kerman province, Iran (57°, 42' E and 27°, 57' N) (Fig. 1). The average annual temperature is 25.5°C, ranging average monthly from 13°C in January to 38°C in July. The elevation is 490 meters above sea level, and mature soils are not prevalent in the area, which is predominantly occupied by lithosol and regosol. The average annual 30-years precipitation is 171.8 mm (Nezhad Afzali and Bayatani, 2018). Precipitation has an occasionally distribution in this district. The only rainfall takes place in May, December, January and February. Mean humidity in this district changed irregularly ranging between 31% in early summer and 56% in late autumn and early winter (Vatandoost et al., 2010). According to our analysis of the ten-year meteorological data from Kahnuj Meteorological Station, the average annual precipitation in 2017 was only 44.4 mm, indicating severe drought conditions. This contrasts sharply with the adjacent years (137.9 mm in 2016 and 146.56 mm in 2018) and is about the quarter of the average annual precipitation, underscoring the extremity of the 2017 drought. The flora of the province mirrors its climatic contrast. The highlands feature remnants of a dry natural forest made up of shrubs and trees like *Pistacia atlantica* and *Amygdalus scoparia*. The lowlands are sparsely covered with steppe-like vegetation. *P. aucheri* is a dominant shrub species at certain sites and a co-dominant species at other lowland locations (Dehbandi and Aftabi, 2016). The natural vegetation has suffered degradation due to human activities such as excessive grazing by goats and sheep, approximately 2 animal units per hectare. The primary livestock breeds in the area are the Raeini Cashmere goat and the Kermani sheep (Ansari-Renani et al., 2013).

### Morphological characteristics of *Pergularia tomentosa*

*P. tomentosa* has young branches that twine around older ones. The leaves are pubescent, cordate, petiolate, and opposite, measuring 1.5–30 cm in length. The fruits are 3–6 cm long, consisting of paired spiny follicles that are inflated at the base. The flowers are pedicellate and arranged in umbelloid cymes. The seeds are ovate, truncate at the apex, and densely velvety-pubescent on both sides, with a dark brown coloration. The pappus of the seeds plays a vital role in the wind-aided dispersal of its seeds. The root system comprises woody main roots with small rootlets and lateral branches (Al-Said, 1988; Hosseini et al., 2022).

### Site selection and soil sampling

In the rangelands of Sehchah village (Kahnuj city), we identified habitats where *P. tomentosa* and *P. aucheri* co-occur. Within these habitats, three sites were selected, and at each site, five *P. aucheri* individuals were randomly chosen. The distance between two neighboring shrubs of *P. aucheri* was at least 150 meters. Ten soil cores were randomly collected beneath each shrub individual at depths of 0-5 cm and 5-10 cm using a metal soil sampler (5 cm in diameter). Similarly, ten soil cores were randomly gathered from outside the canopy of *P. aucheri* (control) within an area of approximately 0.6 square meters inside a quadrat measuring 0.8 m × 0.8 m (the average diameter of the *P. aucheri* canopy was about 90 cm, covering a soil surface area of 0.6 square meters). Due to the dominant northwestern winds in the study area (and across central Iran), we collected soil cores from the southeastern side of shrubs, opposite the prevailing wind direction, to minimize the influence of shrub litterfall on soil and vegetation in the control samples. Additionally, we ensured that sampling locations were beyond the influence zone of any neighboring shrubs, maintaining a minimum distance of 3 m from shrub canopies at each site (Casals et al., 2013; Erfanzadeh et al., 2021). For each shrub location (under or outside the canopy), soil from

the ten cores was combined into a single composite sample per depth (0-5 cm and 5-10 cm). This resulted in an average of 0.98-liter soil sample in each sample for each layer, which exceeds the recommended 0.8-liter soil necessary to determine the species composition of the seed bank (Hutchings, 1986) and applied by researchers in desert ecosystems (e.g. Li et al., 2022). Following the methods of Jiang et al. (2013) and Lee et al. (2024), we collected soil samples once during early autumn (October) after the growing and seeding season. The samples were labeled and transported to the laboratory for cold stratification at 1- 4°C. Following this, they were taken to the greenhouse for a germination test (Miller and Cummins, 2003).

**Greenhouse experiment**

In the greenhouse, the samples were spread in a thin layer (4 mm) on 40 cm × 40 cm trays filled with sand. The sand was collected from the Caspian Sea beach, ensuring it was free of seeds and other contaminants. Each shrub individual had four trays assigned: one placed under the canopy and one outside the canopy for 'each' soil depth (a total of 60 trays for both soil depths). These trays were randomly positioned on shelves in the greenhouse, exposed to natural light, and were kept moist through tap watering. Additionally, six control trays filled with the same sand but without field soil samples were randomly placed on shelves to detect potential greenhouse and sand contamination (Hazhir et al., 2024). Seedlings were identified upon germination using the nomenclature specified by Rechinger (1964), counted, and either removed or transplanted into pots for further growth and identification if they could not be identified at that stage. After 15 weeks, with no further germination observed, the trays were allowed to dry for two weeks to crumble the samples and expose buried seeds to light. Subsequently, watering recommenced for approximately two months. Germinated seedlings were identified and incorporated into the existing greenhouse data. Finally, the residual soil was inspected for any remaining seeds by examining small random samples from the trays under a microscope and testing seeds with a needle to differentiate between firm (viable) and empty (non-viable) seeds (Erfanzadeh et al., 2010). No viable ungerminated seeds were detected during microscopic examination. Furthermore, the control trays showed zero germination during the entire greenhouse experiment.

**Statistical analyses**

To analyze the distribution and composition of species in the SSB, non-metric multidimensional scaling (NMDS) ordination (method = Bray-Curtis dissimilarity, k = 2) was applied. The analysis grouped the samples into four categories, each representing a specific depth within a distinct location, where soil samples were collected *under* and *outside* the shrub. Significance of differences were assessed with permutational multivariate analysis of variance (PERMANOVA) using "adonis2" function with 999 permutations and Bray-Curtis distances. In addition, we used "pairwise.adonis" function to statistically compare species composition of SSB between for categories including two sampling locations (under and outside the cushion) and two depths. The NMDS and PERMANOVA analyses were calculated in the R statistical environment (version 4.5.0; R Core Team, 2025) using the 'vegan' package (Oksanen et al., 2020).
Additionally, the total seed density, SSB density of each plant functional group (annuals, perennials, forbs, grasses, and woody species) per square meter and total species richness per soil sample were calculated (Hazhir et al., 2024).

The Shapiro-Wilk test was used to check data normality distribution. For SSB comparisons between sampling location (inside and outside the shrub) and depths, we fitted generalized linear mixed models (GLMMs) with a log-link function and Poisson distribution (Sun et al., 2023). Overdispersion was checked; if present, a negative binomial distribution would have been used. Separate models were fitted for each individual SSB characteristics, with each characteristic serving as response variables and sampling location and depth as fixed effects. All GLMM analyses were performed using the *glmmTMB* package (v1.1.2.3) in R 4.5.0. Additionally, we conducted pairwise comparisons of SSB characteristics

between sampling locations in each depth via the *emmeans* package.

## Results

### Soil seed bank composition and similarity

In total, 2164 seeds were germinated in the greenhouse. Of these, 1486 seeds were discovered under the *P. aucheri* canopy, with 1156 seeds at 0-5 cm and 330 seeds at 5-10 cm soil depths. Additionally, 678 seeds were observed outside the shrub canopy, comprising 341 seeds at 0-5 cm and 337 seeds at 5-10 cm depths. Overall, a total of 37 species from 18 families were detected in the SSB. The largest number of species belonged to the Poaceae and Asteraceae families, with 8 and 6 species, respectively. 29 species were commonly found beneath and outside the shrub canopy, while 3 species were exclusively found under the canopy and 5 species exclusively outside the canopy. A total of 32 species from 17 families were identified in soil samples collected beneath the shrub canopy, while 34 species from 16 families were germinated in soil samples collected outside the shrub canopy (see Appendix 1). Annual species, including *Bromus rechingeri* H. Scholz, *Asteriscus pygmaeus* (DC.) Coss. & Durieu, *Stipa capensis* Thunb., and *Setaria glauca* (L.) Beauv., dominated the SSB composition. The results on the NMDS1 and NMDS2 axes and PERMANOVA test indicated that there were significant differences in scores among the four categories ($F = 20.25$, $p = 0.000$) (Fig. 2). Furthermore, pairwise comparisons among the four categories revealed significant differences in SSB composition between areas under and outside the shrub canopy at the 0-5 cm depth (Table 1).

### Soil seed bank density and richness

The results of GLMMs indicated that the main effect of sampling location on total richness and density and, annual and forb densities was significant, with the highest richness and densities observed beneath the canopy. A main effect of depth on total richness, total density and SSB densities of functional groups was observed, with the highest richness and densities found at the surface depth. The interaction effect of sampling location and depth on total richness, total density and density of all functional groups (excluding woody species) was found to be significant (Table 2). The pairwise comparison results revealed that at depth of 0-5 cm, the highest total richness, total density, as well as the density of annuals, forbs, and grasses, were present underneath the shrub canopy (See Fig. 3). There was no significant difference at the density of the SSB of perennials and woody species between underneath and outside the shrub canopy (Fig. 3). Furthermore, at depth of 5-10 cm, only the density of perennials differed significantly between underneath and outside the shrub canopy, with the highest density observed underneath the shrub canopy. The total richness, total density and SSB density of other functional groups did not show significant differences at this depth between underneath and outside the shrub canopy (Fig. 3). Our target species, *Pergularia tomentosa*, was not observed in either greenhouse germination trials, nor was it detected during microscopic analysis of soil samples.

## Discussion

Our results partially supported the initial hypothesis: while *Pteropyrum aucheri* exhibited positive facilitative effects on SSBs by increasing total seed richness, density, and functional group densities, these effects were species-specific. Notably, no significant enhancement was observed for our target species, *Pergularia tomentosa* (consistent with species-specific SSB dynamics reported by Suleiman et al., 2023). The findings suggest that shrubs like *P. aucheri* can act as critical seed reservoirs, supporting passive recovery of herbaceous species in degraded arid sites (Auffret et al., 2024). SSBs are essential for ecosystem resilience and reflect regeneration potential, particularly in harsh desert environments where active restoration is often costly due to extreme temperatures and low precipitation (Suleiman et al., 2023). While SSBs enable passive restoration at the community level (Auffret et al., 2024), their efficacy varies across species. For taxa like *P. tomentosa*, showing limited SSB persistence, active restoration may be necessary to ensure (re)colonization post-disturbance.

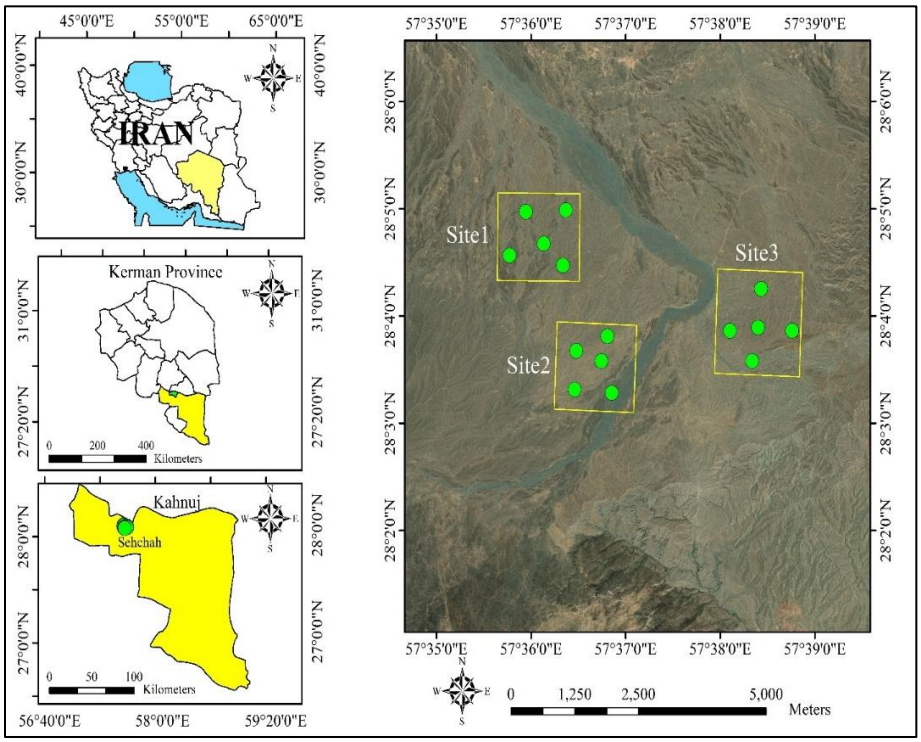


**Figure 1.** Geographical location of the study area in Kahnuj county, Kerman Province, Iran

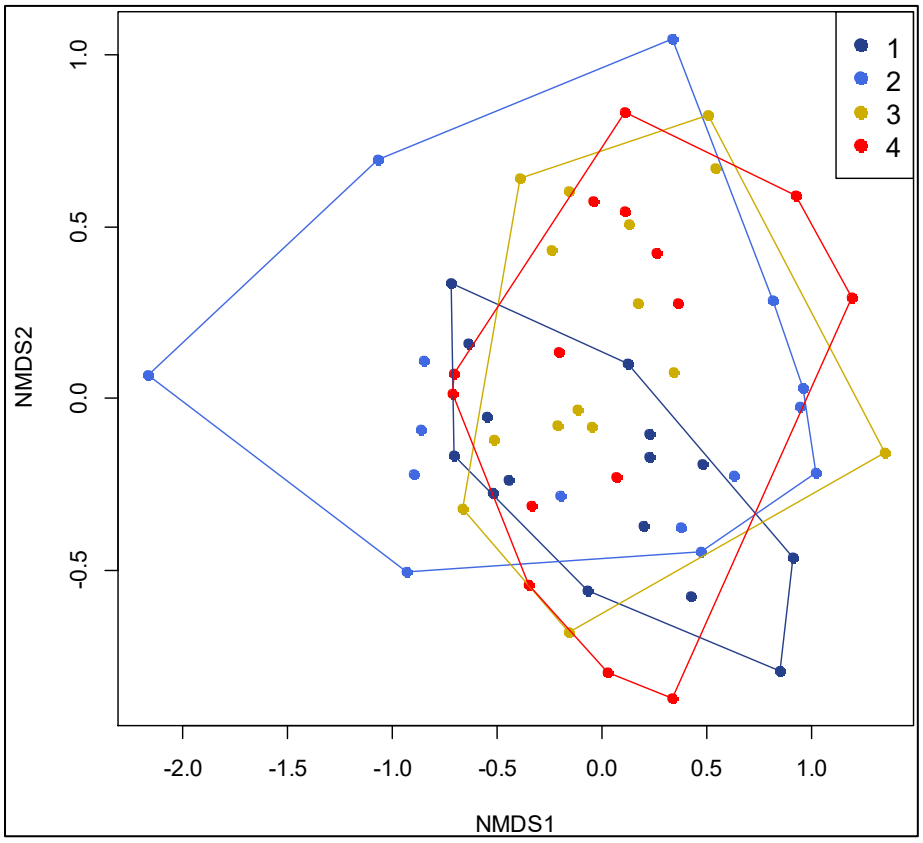


**Figure 2.** Non-metric multidimensional scaling (NMDS) of the soil seed bank (SSB) composition (Stress = 0.018). 1: Soil samples under *Pteropyrum aucheri* canopy at 0-5 cm depth, 2: Soil samples under *P. aucheri* canopy at 5-10 cm depth, 3: Soil samples outside *P. aucheri* canopy at 0-5 cm depth, 4: Soil samples outside *P. aucheri* canopy at 5-10 cm depth.

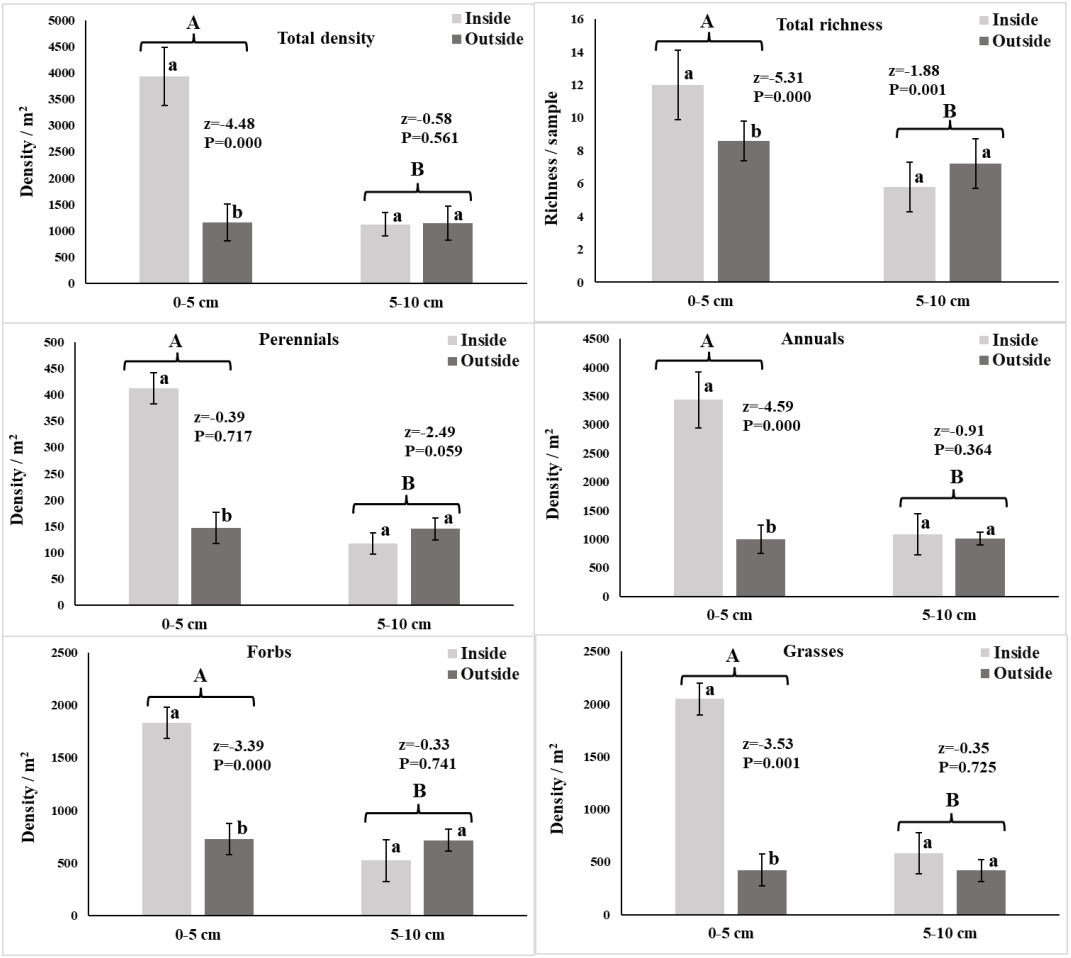


**Figure 3.** Total density, species richness, and functional group densities of the soil seed bank beneath and outside *Pteropyrum aucheri* canopy. Lowercase letters denote significant differences between microsites (beneath vs. outside canopy) within each soil depth separately, and uppercase letters indicate significant differences between soil depths (main effect of depth).

**Table 1.** Pairwise comparisons of soil seed bank composition conducted among four categories (beneath vs. outside *Pteropyrum aucheri* canopy at two soil depths) using PERMANOVA with the 'pairwise.adonis' function in the vegan package. InUp: Soil samples under *P. aucheri* canopy at 0-5 cm depth, InLow: Soil samples under *P. aucheri* canopy at 5-10 cm depth, OutUp: Soil samples outside *P. aucheri* canopy at 0-5 cm depth, OutLow: Soil samples outside *P. aucheri* canopy at 5-10 cm depth.

| Pairs | df | Sum of Square | F. Model | R2 | p value |
|---|---|---|---|---|---|
| InUp vs. InLow | 1 | 0.51 | 1.49 | 0.05 | 0.161 |
| InUp vs. OutUp | 1 | 0.77 | 2.56 | 0.08 | 0.004 |
| InUp vs. OutLow | 1 | 0.71 | 2.25 | 0.07 | 0.010 |
| InLow vs. OutUp | 1 | 0.5 | 1.41 | 0.05 | 0.154 |
| InLow vs. OutLow | 1 | 0.32 | 0.85 | 0.03 | 0.606 |
| OutUp vs. OutLow | 1 | 0.04 | 0.11 | 0.01 | 0.997 |

**Table 2.** The effects of sampling location (beneath and outside the *Pteropyrum aucheri* canopy) and soil depth (0-5 cm and 5-10 cm) and their interactions on total richness, total density, and soil seed bank density of functional groups.

| | | Chi-square | p value |
|---|---|---|---|
| Total density | Sampling location | 29.59 | 0.000 |
| | Soil depth | 29.47 | 0.000 |
| | Location × depth | 27.09 | 0.000 |
| Total richness | Sampling location | 6.77 | 0.021 |
| | Soil depth | 152.10 | 0.000 |
| | Location × depth | 25.21 | 0.000 |
| Annual density | Sampling location | 40.15 | 0.001 |
| | Soil depth | 27.50 | 0.002 |
| | Location × depth | 25.87 | 0.000 |
| Perennial density | Sampling location | 2.49 | 0.124 |
| | Soil depth | 22.07 | 0.000 |
| | Location × depth | 6.69 | 0.046 |
| Forb density | Sampling location | 5.81 | 0.033 |
| | Soil depth | 8.08 | 0.000 |
| | Location × depth | 6.19 | 0.043 |
| Grass density | Sampling location | 0.39 | 0.537 |
| | Soil depth | 11.85 | 0.000 |
| | Location × depth | 10.56 | 0.000 |
| Shrub density | Sampling location | 0.69 | 0.418 |
| | Soil depth | 11.16 | 0.000 |
| | Location × depth | 0.69 | 0.418 |

In this study, the total density of SSB plants is relatively high, aligning with research in Asian deserts (Hadinezhad et al., 2021; Li et al., 2022) and American deserts (e.g. Luis et al., 1998).However, the overall SSB density differs from the observations in other desert regions (e.g. Zhang and Li, 2018), potentially due to the presence of higher cover of woody plants in those areas. Given that the NMDS and PERMANOVA results show distinct groupings for samples from outside and beneath the shrub canopy in the upper soil layer, our findings indicate that *P. aucheri* alters SSB composition while also increasing SSB density under the canopy. Previous studies, such as Tessema et al. (2017), Foronda et al. (2020), and Hadinezhad et al. (2021), have documented how shrubs can augment the number of buried seeds in the soil through direct seed trapping or indirect mechanisms involving other animal or plant species, resulting strong changes in SSB composition. Our research reveals a greater richness and abundance of seeds within shrub canopies compared to open areas in arid ecosystems. Therefore, conservation efforts could prioritize woody species, such as *P. aucheri*, which can bolster population and community regeneration by fostering abundant SSBs for some species within desert communities.

We found that annual plant species accounted for the largest proportion of species in the study area. This finding is consistent with studies on SSBs in the desert ecosystem in China (Zhang and Li, 2018), the Hexi Corridor desert in China (Lu et al., 2019), the grassland

desert Sevilleta National Wildlife Refuge in the USA (Loydi and Collins, 2021), and the Ulan Buh desert in Inner Mongolia (Li et al., 2022). Annuals are well-known for their ability to produce persistent SSBs.

In deserts, they exhibit strong tolerance to water deficiency and have a larger niche breadth compared to perennials (Jia et al., 2017). Most annual plants complete their entire life cycle during a short period of rainy times and produce a large number of tiny seeds. Additionally, heavy grazing may contribute to the prevalence of annuals in the SSBs in our area. Li et al. (2024) demonstrated that heavy grazing significantly increased annual plants in the top 5 cm of soil. In addition to producing large quantities of seeds that are dispersed shortly after maturation, annuals employ an "escape" strategy by falling into cracks and depressions in the soil to avoid seed consumption (Li et al., 2008). Consequently, annuals play a crucial role in mitigating species extinction and vegetation degeneration in severe desert environments through their abundant SSBs (Li et al., 2008).

Analysis of the soil seed bank in the study area revealed that the Poaceae family was predominant. This outcome is consistent with earlier investigations in the African savanna (Savadogo et al., 2017) and semi-arid grasslands of China (Li et al., 2024). In the African savanna context, genera like *Aristida* and *Eragrostis* were common in SSBs, whereas *Leymus chinensis*, *Stipa grandis*, and *Cleistogenes squarrosa* were identified as the most abundant Poaceae species in the Chinese study (Li et al., 2024). Further supporting this pattern, De Andrade and Miranda (2014) noted that Poaceae species (64%) often dominate post-disturbance in savanna environments, and Li et al. (2014) recorded *Eragrostis pilosa* as a frequent SSB component. Grasses are known for forming highly persistent seed banks, a trait linked to their production of numerous small seeds (Erfanzadeh, 2020). In contrast, the abundance of shrub seeds in the SSB was remarkably low, with greenhouse trials yielding only eight germinants from three species—a pattern frequently observed in desert seed bank research. Woody plants typically form transient seed banks; their seeds are often attractive to predators, struggle to incorporate into the soil due to their larger size, and are produced in limited quantities (Erfanzadeh, 2020).

Surprisingly, no of *P. tomentosa* seeds germinated in the greenhouse, despite their efficient wind-mediated dispersal via pappus, which facilitates trapping by shrub canopies. Furthermore, meteorological data revealed significant variations in seed production conditions for this species. Notably, no germinants emerged, whether in soil collected from open areas or beneath *P. aucheri*, suggesting that seed bank germination alone is insufficient for restoring all plant species in SSBs. While this species likely forms a transient seed bank similar to other woody plants, its absence in the SSB may reflect methodological limitations in seed detection due to sampling constraints. Practical limitations often result in only sampling a small percentage of the total area of a study site, leading to an underestimation of species richness and density within the seed bank for a particular species (Bossuyt and Honnay, 2008). Consequently, there is a need for more comprehensive future studies to validate methodologies and increase the number of soil samples collected in the desert.

## Conclusion

Of particular significance in desert ecosystems, this research underscores the vital role of preserving facilitator shrub species, which substantially increase both the density and richness of the soil seed bank to the advantage of herbaceous plant communities. The results highlight the crucial function these shrubs serve in restoring overgrazed landscapes by enriching the SSB. *P. tomentosa*, however, represents a significant exception to this pattern. Despite the general enhancement of the SSB beneath shrubs, this medicinal species does not sustain a viable seed bank, even with facilitation. Its absence from both the SSB and the standing vegetation is concerning and suggests a risk of extinction, as natural regeneration seems improbable. Therefore, although the conservation of shrubs is fundamental for broader ecosystem recovery, the persistence of *P. tomentosa* likely depends on targeted, active measures such as direct seeding or transplantation.

Appendix 1. Soil seed bank density (seeds/m$^2$) for each plant species beneath and outside *Pteropyrum aucheri* canopy at two soil depths in Kerman Province, Iran. A: annual, B: biennial, P: perennial; Cr: cryptophyte, He: hemicryptophyte, Ph: phanerophyte, Th: therophyte.

| | | | | | Under the canopy | | Outside the canopy | |
|---|---|---|---|---|---|---|---|---|
| Plant Species | Plant Family | Growth form | Growth span | Growth form | 0-5 cm | 5-10 cm | 0-5 cm | 5-10 cm |
| Anagallis arvensis | Primulaceae | Forb | A | Th | 7 | 7 | 10 | 7 |
| Anthemis austro-iranica Rech.f., Aellen&Esfand. | Asteraceae | Forb | A | Th | 0 | 0 | 3 | 0 |
| Asphodelus tenuifolius Cav. | Xanthorrhoeaceae | Forb | A | Th | 662 | 340 | 302 | 336 |
| Asteriscus pygmaeus (DC.) Coss. & Durieu | Asteraceae | Forb | A | Th | 132 | 34 | 92 | 78 |
| Biscutella didyma L. | Brassicaceae | Forb | A | Th | 10 | 0 | 3 | 0 |
| Bromus rechingeri H. Scholz | Poaceae | Grass | A | Th | 808 | 170 | 187 | 170 |
| Bromus tectorum L. | Poaceae | Grass | A | Th | 65 | 20 | 3 | 3 |
| Calotropis procera (Aiton) W.T.Aiton | Asclepiadaceae | Shrub | P | Ph | 7 | 0 | 7 | 0 |
| Digitaria nodosa Parl. | Poaceae | Grass | P | He | 3 | 0 | 0 | 0 |
| Erodium cicutarium (L.) L'Hér. | Geraniaceae | Forb | A | Th | 78 | 24 | 10 | 14 |
| Festulolium miliaceum L. | Poaceae | Grass | A | Th | 0 | 0 | 10 | 10 |
| Filago desertorum Pomel | Asteraceae | Forb | A | Th | 3 | 0 | 0 | 3 |
| Forsskaolea tenacissima L. | Urticaceae | Forb | P | He | 17 | 3 | 51 | 61 |
| Galium uperceratum L. | Rubiaceae | Forb | A | Th | 3 | 3 | 10 | 10 |
| Helichrysum sp. | Asteraceae | Forb | P | He | 3 | 0 | 3 | 0 |
| Herniaria hirsuta subsp. cinerea (DC.) Arcang. | Caryophyllaceae | Forb | A | Th | 163 | 44 | 61 | 61 |
| Hyparrhenia hirta (L.) Stapf | Poaceae | Grass | P | He | 14 | 10 | 10 | 7 |
| Lappula sinaica (A.DC.) Asch. & Schweinf. | Boraginaceae | Forb | A | Th | 7 | 3 | 0 | 3 |
| Leptaleum filifolium (Willd.) DC. | Brassicaceae | Forb | A | Th | 7 | 14 | 3 | 7 |
| Lepyrodiclis sp. | Caryophyllaceae | Forb | A | Th | 0 | 3 | 14 | 20 |
| Lycium edgeworthii Sch.-Tem. | Solanaceae | Shrub | P | Ph | 0 | 0 | 3 | 0 |

| | | | | | | | | |
|---|---|---|---|---|---|---|---|---|
| Malva sylvestris L. | Malvaceae | Forb | P | Cr | 3 | 0 | 0 | 0 |
| Medicago sativa L. | Leguminosae | Forb | P | Cr | 14 | 20 | 0 | 0 |
| Misopates orontium (L.) Raf. | Scrophulariaceae | Forb | A | Th | 68 | 71 | 34 | 34 |
| Notoceras bicorne (Aiton) | Brassicaceae | Forb | A | Th | 20 | 3 | 3 | 3 |
| Paronychia arabica (L.) DC. | Caryophyllaceae | Forb | A | Th | 190 | 65 | 34 | 31 |
| Pimpinella barbata (DC.) Boiss. | Apiaceae | Forb | A | Th | 14 | 3 | 10 | 7 |
| Plantag opsyllium L. | Plantaginaceae | Forb | A | Th | 82 | 24 | 17 | 20 |
| Plantago trichophylla L. | Plantaginaceae | Forb | A | Th | 51 | 14 | 31 | 31 |
| Reichardia tingitana (L.) Roth | Asteraceae | Forb | A | Th | 0 | 0 | 3 | 0 |
| Setaria glauca (L.) Beauv. | Poaceae | Grass | A | Th | 459 | 109 | 61 | 65 |
| Sisymbrium irio L. | Brassicaceae | Forb | A | Th | 88 | 31 | 7 | 3 |
| Spergularia diandra (Guss.) Heldr. | Caryophyllaceae | Forb | A(B) | Th | 31 | 3 | 3 | 0 |
| Stipa capensis Thunb. | Poaceae | Grass | A | Th | 482 | 102 | 85 | 95 |
| Stipa parviflora Desf. | Poaceae | Grass | P | Cr | 431 | 0 | 71 | 65 |
| Urospermum picroides (L.) Scop. ex F.W.Schmidt | Asteraceae | Forb | P | He | 0 | 0 | 7 | 0 |
| Ziziphus nummularia (Burm.f.) Wight & Arn. | Rhamnaceae | Shrub | P | Ph | 3 | 0 | 7 | 0 |

## References

Allen, D.J., Westrip, J.R.S., Puttick, A., Harding, K.A., Hilton-Taylor, C. and Ali, H., 2021. UAE National Red List of Vascular Plants. Technical Report. *Ministry of Climate Change and Environment, United Arab Emirates, Dubai*.

Al-Said, M., Hifnawy, M., McPhail, A., McPhail, D., 1988. Ghalakinoside, a cytotoxic cardiac glycoside from Pergularia tomentosa. *Phytochemistry*, 27, 3245-3250.

Ansari-Renani, H.R. Rischkowsky, B., Mueller, J.P., Seyed Momen, S.M., Moradi, S., 2013. Nomadic pastoralism in southern Iran. *Pastoralism: Research, Policy and Practice* 3,11.

Armenta Calderón AD, Moreno-Salazar SF, Furrazola Gómez E, Ochoa-Meza A., 2019. Arbuscular mycorrhiza, carbon content and soil aggregation in Sonoran Desert plants. *Spanish Journal of Soil Science* 9, 42-53.

Auffret, A.G., Ladouceur, E., Haussmann, N.S., Daouti, E., Elumeeva, T.G., Kačergytė, I., Knape, J., Kotowska, D., Low, M., Onipchenko, V.G., Paquet, M., Rubene, D. & Plue, J., 2024. A global database of soil seed bank richness, density, and abundance. *Ecology*. 105(11): e4438.

Babaamer, Z., Sekhari, L., Al-Jaber, H., Al-Qudah, M., 2013. Extraction and identification of triterpenoids

from Pergularia tomentosa L. *Annales des Sciences et Technologie*, 5, 1-4.

Beatrijs, B., Olivier, H., 2008. Can the seed bank be used for ecological restoration? An overview of seed bank characteristics in European communities. *Journal of Vegetation Science* 19, 875-884.

Benyahia, F., Zitoun, O., Meghzili, B., Foufou, E., Zidoune, M., 2021. Use of Pergularia tomentosa plant enzymatic coagulant system in fresh cheese-making. *Food and Nutrition Sciences*, 12, 1028-1040.

BOSSUYT, B. & HONNAY, O. 2008. Heat shock increases the reliability of a temperate calcareous grassland seed bank study. Plant Ecology, 199, 1–7.

Casals, P., Romero, J., Rusch, G. M., Ibrahim, M., 2013. Soil organic C and nutrient contents under trees with different functional characteristics in seasonally dry tropical silvopastures. *Plant and Soil*, 374, 643-659.

Chandregowda, M.H., Murthy, K., Bagchi, S., 2018. Woody shrubs increase soil microbial functions and multifunctionality in a tropical semi-arid grazing ecosystem. *Journal of Arid Environments* 155, 65-72.

De Andrade, L.A.Z., Miranda, H.S., 2014. The dynamics of the soil seed bank after a fire event in a woody savanna in central Brazil. *Plant Ecol*, 215, 1199- 209.

Dehbandi, R., Aftabi, A., 2016. Geochemical provenance of soils in Kerman urban areas, Iran: Implications for the influx of aeolian dust. *Aeolian Research* 21(6),109-123.

Erfanzadeh, R. 2020. Soil seed bank ecology. *Tarbiat Modares University Press*, 271 p.

Erfanzadeh, R., Yazdani, M., Mosleh Arani, A., 2021. Effect of different shrub species on their sub-canopy soil and vegetation properties in semiarid regions. *Land Degradation and Development*, 32, 3236-3247.

Erfanzadeh, R., Bahrami, B., Motamedi, J., Dianati Tilaki, G.A., Abedi, M., 2016. Impact of dominant shrub species on soil organic matter content in dry grassland habitats. *Ecopersia*, 4(2), 1379-1393.

Erfanzadeh, R., Hendrickx, F., Maelfait, J.P., Hoffmann, M., 2010. The effect of successional stage and salinity on the vertical distribution of seeds in salt marsh soils. *Flora*, 205, 442-448.

FEULNER, G. R. 2016. The Flora of Wadi Wurayah National Park, Fujairah, United Arab Emirates: An annotated checklist and selected observations on the flora of an extensive ultrabasic bedrock environment in the northern Hajar Mountains. Tribulus, 24, 4–85.

Foronda, A., Pueyo, Y., Reiné, R., Arroyo, A.I., de la Luz Giner, M., Alados, C.L., 2020. The role of shrubs in spatially structuring the soil seed bank of perennial species in a semi-arid gypsum plant community. *Plant Ecology*, 221, 913–923.

Ghahreman A, Attar F., 1999. Biodiversity of plant species in Iran. vol. 1-14, *Tehran University press*, Iran.

Gomaa, N.H., Hegazy, A.K., Alhaithloul, H.A.S., 2023. Facilitation by Haloxylon persicum shrubs enhances density and richness of soil seed bank of annual plants in a hyper-arid ecosystem. *Plants*, 12(6), 1276.

Hadinezhad, M., Erfanzadeh, R., Ghelichnia, H., 2021. Soil seed bank characteristics in relation to different shrub species in semiarid regions. *Land Degrad. Dev*., 32, 2025-2036.

Hazhir, S., Erfanzadeh, R., Ghelichnia, H., Razavi, B.S., & Torok, P., 2024. Effects of livestock grazing on soil seed banks vary between regions with different climates. *Agriculture, Ecosystems and Environment*, 364, 108901.

Hosseini Kahnouj, S.H., Ayyari, M., Azarnivand, H., Piacente, S., Zare Chahouki, MA., 2017. Pergularia tomentosa, from traditional uses to ecology and phytochemistry. *Journal of Medicinal Plants*, 16(63), 1-11.

Hosseini, S.H., Ezzati Ghadi, F., Ramzani Ghara, A., Cerulli, A., Shakeri, A., Piacente, S., 2022. LC-MS-based metabolite profiling of aqueous extract of Pergularia tomentosa L. and its anti-hyperglycemic effect. *Iran J Basic Med Sci* 25,1433-1441.

Hutchings, M.J., 1986. Plant population biology. In: Moore, P.D., Chapman, S.B. (Eds.), Methods in Plant Ecology second ed. *Blackwell, Oxford*, pp. 377-435.

Jia, F., Tiyip, T.,Wu, N., Tian, C., and Zhang, Y., 2017. Characteristics of soil seed banks at different geomorphic positions within the longitudinal sand

dunes of the Gurbantunggut desert, China. *J. Arid. Land* 9 (3), 355-367.

Jiang, D., Wang, Y., Oshida, T., Luo, Y., Wang, H., Zhou, Q., 2013. Review of research on soil seed banks in desert regions. *Disaster Advances*, 6, 315-322.

Jones, S.A., Archer, S.R., Hartfield, K.A., Marsh, S.E., 2023. Topoedaphic constraints on woody plant cover in a semi-arid grassland. *Ecological Indicators*, 151, 110226.

Khosravi Mashizi, A., 2019. Physiological responses of Pteropyrum aucheri to short-term warming in semi-arid rangelands (case study: Kohpanj Region, Kerman Province, Iran). *Journal of Rangeland Science*, 9, 126-135.

Lahmar, I., Nasri-Ayachi, M.B., Belghith, K., 2022. Laticifer identification, rubber characterization, phenolic content, and antioxidant activity of Pergularia tomentosa latex extract. *BioMed Research International*, ID: 7158905.

Lee, S., Klinger, R., Brooks, M.L., Ferrenberg, S., 2024. Homogenization of soil seed bank communities by fire and invasive species in the Mojave Desert. *Front. Ecol. Evol*. 12:1271824.

Li, M., Xiao, H., Xin, Z., Li, X., Li, J., Miri, A., Cao, Q., 2022. Soil seed bank characteristics of Nitraria tangutorum Nebkhas in a Desert–Oasis Ecotone. *Front. Environ*. Sci. 10, 937257.

Li, X., Jiang, D., Zhou, Q., 2014. Soil seed bank characteristics beneath an age sequence of caragana microphylla shrubs in the Horqin sandy land region of northeastern China. *Land Degrad Dev*, 25, 236- 243.

Li, X., Li, X., Jiang, D., Liu, Z., Yu, Q., 2008. Annual plants in arid and semi-arid desert regions. *Front. Biol. China*, 3(3), 259–264.

Li, Y., Wang, H., Ma, Z., Xing, P., Wang, Y., Jin, Z., Zhou, Y., Li, F.Y., 2024. Adaptive grazing enhances plant species richness and density in the soil seed bank in a semi-arid grassland. *Ecological Indicators*.163, 112113.

Lortie CJ, Gruber E, Filazzola A, Noble T, Westphal M., 2017. The Groot Effect: plant facilitation and desert shrub regrowth following extensive damage. *Ecology and Evolution*. 8:706-715.

Loydi, A., Collins, S.L., 2021. Extreme drought has limited effects on soil seed bank composition in desert grasslands. *Journal of Vegetation Science*, 32, e13089.

Lu, R., Liu, Y.F., Jia, C., Huang, Z., Liu, Y., Hea, H., Liu, B.R., Wang, Z.J., Zhenga, J., Wua, G.L., 2019. Effects of mosaic-pattern shrub patches on runoff and sediment yield in a wind-water erosion crisscross region. *Catena* 174,199-205.

Lu, Y. F., Ma, L., Zhan, Y. F., Qian, W. J., Zhen, W. L., Teng, Y. F., 2019. A Review of the soil seed bank of artificial desert vegetation in the Hexi Corridor. *Fore. Sci. Technol*. 60 (11), 64–66.

Luis, M., Bertilde, E.R., Manuel, E.H., 1998. Timing and spatial patterning of seed dispersal and redistribution in a south American warm desert. *Plant Ecol*. 137 (2), 143–150.

Miao, R., Song, Y., Sun, Z., Guo, M., Guo, M., Zhou, Z., Liu, Y., 2016. Soil seed bank and plant community development in passive restoration of degraded sandy grasslands. *Sustainability*, 8(6), 581.

MILLER, G. & CUMMINS, R. 2003. Soil seed banks of woodland, heathland, grassland, mire and montane communities, Cairngorm Mountains, Scotland. Plant ecology, 168, 255–266.

Motamedi, J. Bahrami, B., Erfanzadeh, R., 2013. Assessing the impact of Pteropyrum aucheri species on particulate organic matter and soil aggregate dispersion. *Applied Soil Research*, 1: 84-93.

Nezhad Afzali, K., Bayatani, F., 2017. Determination of dry and wet periods in southern Kerman (Kahnouj) using moving average methods and standard index. *The 2nd National Conference on Meteorology and Climate in Iran*, Mashhad, Iran.

Oksanen, J., Blanchet, F. G., Friendly, M., Kindt, R., Legendre, P., Mcglinn, D., Minchin, P. R., O'hara, R., Simpson, G. L. & Solymos, P. 2020. vegan: Community Ecology Package. R package version 2.5-6. 2019.

Rechinger, K.H., 1964. Flora Iranica, *Akademische Druck- und Verlagsanstalt, Graz*. Iran, University of Tehran.

Rechinger, K.H. and Schiman-Czeika, H., 1968. Polygonaceae. – In: Rechinger, K.H. (ed.): Flora

Iranica, Lfg. 56. – *Akademische Druck- und Verlagsanstalt, Graz*.

Savadogo, P., Sanou, L., Dayamba, S.D., Bognounou, F., Thiombiano, A., 2017. Relationships between soil seed banks and above-ground vegetation along a disturbance gradient in the W National Park trans-boundary biosphere reserve, *West African Journal of Plant Ecology*, 10, 349–363

Soubry, I., Robinov, L., Chu, T. Guo, X., 2022. Mapping shrub cover in grasslands with an object-based approach and investigating the connection to topo-edaphic factors. *Geocarto International* 37, 16926-16950.

Suleiman, M.K., Bhatt, A., Jacob, S., Thomas, R.R., Sivadasan, M.T., 2023. Seed longevity in desert species and the possibility of forming a persistent soil seed bank. *Sustainability*, 15, 15904.

Sun, Y., Jia, W., Guo, H., Zhang, X., Wang, F., Zhao, H., Li, T., & Zhao, Z., 2023. Comparison of global and local Poisson models for the number of recruitment trees in natural forests. *Forests*, 14(4).

Tessema, Z.K., Ejigu, B., Nigatu, L., 2017. Tree species determine soil seed bank composition and its similarity with understory vegetation in a semi-arid African savanna. *Ecological Processes* 6, 9.

Thompson, K., Bakker, J., Bekker, R., 1997. The soil seed banks of North West Europe: methodology, density and longevity. *Cambridge University Press*, Cambridge, 276 pp.

Vatandoost, H., Akbarzadeh, K., Hanafi Bojd, A.A., Mashayekhi, M., Saffari, M., Malik, E., Kenyi, L., Abakar, J.B., Busaq, A., Esmailpour, M., Abuelgasim, H., Oshaghi, M.A., 2010. Malaria stratification in a malarious area, a field exercise. *Asian Pacific Journal of Tropical Medicine* 6, 807-811.

Yang, H., Yu, X., Song, J., Wu, J., 2024. Artemisia smithii patches form fertile islands and lead to heterogeneity of soil bacteria and fungi within and around the patches in alpine meadows of the Qinghai-Tibetan Plateau. *Frontiers in Plant Science Section of Functional Plant Ecology* 15: 1411839. https://doi.org/10.3389/fpls.2024.1411839.

Zahawi, W.A., Reid, J.L., Holl, K.D., 2014. Hidden costs of passive restoration. *Restor. Ecol*. 22, 284–287.

Zhang, Y., Li, J., 2018. Spatial pattern of seed bank and seedlings in Gurbantunggut desert soils the "protection effect" of scrub. *Arid. Zone Res*. 35 (05), 1138–1145.

University of Jiroft

**Biospecies Research**

Journal homepage: bsr.ujiroft.ac.ir

Iranian Biology Society

# Deciphering the molecular mechanisms of apoptosis: recent advances in controlled cell death pathways

Vajihe Saedi Marghmaleki[1*], Hamid Azizi-Malekabadi[2]

https://doi.org/10.22034/bsr.2025.562124.1003

[1] *Neuroscience Research Center, Baqiyatallah University of Medical Sciences, Tehran, Iran.*

[2] *Department of Medical BasicSciences,Isf.C.,Islamic Azad University, Isfahan, Iran.*

## ARTICLE INFO

**Article Type**
Review Article

**Article History**
Received: 25 November 2025
Accepted: 28 December 2025
Published: 15 February 2026


***Corresponding author**
Vajihe.saedi@yahoo.com

## ABSTRACT

Apoptosis is a genetically encoded and meticulously controlled cellular self-destruction program, fundamental to embryogenesis, tissue equilibrium, immune function, and the removal of compromised or dangerous cells. Unlike necrosis, apoptosis unfolds via a coordinated molecular cascade that maintains the plasma membrane's integrity and avoids inciting inflammation. Mechanistically, apoptosis is driven by a family of cysteine proteases called caspases. Their activation occurs primarily through two routes: the extrinsic pathway, triggered by death receptor activation, and the intrinsic pathway, regulated by mitochondrial events. A key regulatory checkpoint of the intrinsic pathway is mitochondrial outer membrane permeabilization (MOMP), a process controlled by interactions among members of the B-cell lymphoma-2 (Bcl-2) protein family. In parallel, the inhibitor of apoptosis (IAP) proteins provides an additional regulatory layer by restraining caspase activity downstream of mitochondrial signaling. Dysregulation of these apoptotic networks is a defining feature of numerous human diseases, including cancer, autoimmune disorders, neurodegeneration, and ischemic injury. Advances in understanding apoptotic control mechanisms have facilitated the development of targeted therapeutic strategies, such as BH3-mimetics and SMAC mimetics, aimed at modulating cell death susceptibility in disease-specific contexts. This review synthesizes current insights into the molecular architecture of apoptosis, highlighting key regulatory checkpoints, pathway integration, and emerging therapeutic opportunities.

**Keywords**: Mitochondrial outer membrane permeabilization (MOMP), Death receptors, BH3-mimetics, SMAC mimetics, Efferocytosis.

**How to cite this paper**

Saedi Marghmaleki, V., Azizi-Malekabad, H., 2026. Deciphering the Molecular Mechanisms of Apoptosis: Recent Advances in Controlled Cell Death Pathways. *Biospecies Research*, 1, pp. 24-34.

## Introduction

The term apoptosis was first introduced in 1972 by Kerr, Wyllie, and Currie to describe a distinct, genetically controlled mode of cell death characterized by unique morphological features and a non-inflammatory outcome (Kerr et al., 1972). This foundational work established apoptosis as a fundamentally different process from necrosis and laid the groundwork for subsequent investigations into its role in development, tissue maintenance, and disease. Apoptosis is now recognized as an evolutionarily conserved cellular program that enables multicellular organisms to eliminate superfluous, damaged, or potentially dangerous cells in a controlled manner.

The execution of apoptosis at the molecular level is driven by a sequential proteolytic cascade carried out by caspases. These enzymes are activated through two principal signaling pathways: the extrinsic pathway, initiated when ligands activate cell surface death receptors, and the intrinsic pathway, activated in response to internal stress signals like oxidative stress, growth factor deprivation, or DNA damage. Control of the intrinsic apoptotic pathway hinges on the Bcl-2 protein family, the master regulator of mitochondrial outer membrane permeabilization (MOMP). Concurrently, the Inhibitor of Apoptosis (IAP) proteins establish a crucial secondary checkpoint through direct caspase inhibition. Cellular fate is decided by the dynamic equilibrium between these pro-survival and pro-death factors (Kalkavan and Green, 2018, Singh et al., 2019).

A fundamental physiological function of apoptosis is to sculpt tissues during embryogenesis and to maintain tissue equilibrium in adults through the elimination of superfluous or impaired cells (Fuchs and Steller, 2015). In the immune system, apoptotic mechanisms are essential for eliminating virus-infected cells and for maintaining self-tolerance through the clonal deletion of autoreactive lymphocytes (Nagata, 2018).

The pathological relevance of apoptosis is underscored by the consequences of its dysregulation. Defective apoptosis is a defining feature of cancer, driving both tumor advancement and resistance to treatment. Conversely, neurodegenerative disorders and ischemic injury are often linked to the aberrant overactivation of apoptotic pathways (Carneiro and El-Deiry, 2020). As a result, the molecular machinery governing apoptosis has emerged as a major focus of therapeutic intervention, with strategies aimed at selectively restoring or restraining cell death depending on disease context.

## Forms of Programmed Cell Death

While apoptosis is the most widely studied form of regulated cell death (RCD), it is now understood to be one of several distinct pathways. The Nomenclature Committee on Cell Death (NCCD) has established rigorous morphological and biochemical criteria to classify different types of RCD (Galluzzi et al., 2018). The hallmark morphological changes of apoptosis encompass a sequence of events: the cell undergoes shrinkage, its chromatin condenses, the nucleus fragments, and the plasma membrane blebs, ultimately resulting in the production of apoptotic bodies. These bodies are swiftly phagocytosed by neighboring cells or professional phagocytes without eliciting an inflammatory response (D'arcy, 2019). Other major forms of RCD include necroptosis, a caspase-independent inflammatory death, and pyroptosis, an inflammatory form of death mediated by gasdermin proteins, often in response to pathogens (Galluzzi et al., 2018). This review will focus specifically on the molecular mechanisms of classical apoptosis.

## Apoptosis versus Necrosis: A Fundamental Dichotomy

A critical distinction in cell biology is that between apoptosis (a genetically regulated suicide program) and necrosis (an accidental death caused by severe damage). Necrosis has long been considered an unregulated, accidental process resulting from severe physicochemical insult or injury. The event is marked by cellular swelling (oncosis), the breaching of the plasma membrane, and efflux of intracellular material into the extracellular space, which invariably triggers a potent inflammatory response and can cause secondary tissue damage (Gong et al., 2019).

In stark contrast, apoptosis is an active, energy-dependent process that occurs under strict molecular control. The morphological hallmarks of apoptosis, as previously described, ensure the neat packaging of cellular contents for silent disposal (D'arcy, 2019). The display of "eat-me" signals, including phosphatidylserine on the cell surface's outer leaflet, allows for the efficient recognition and uptake of apoptotic cells by phagocytic cells. This efficient clearance mechanism is the primary reason apoptosis does not incite inflammation, preserving tissue integrity (Doran et al., 2020). This fundamental dichotomy underscores the vital role of apoptosis in maintaining metabolic and immune homeostasis (Fig.1).

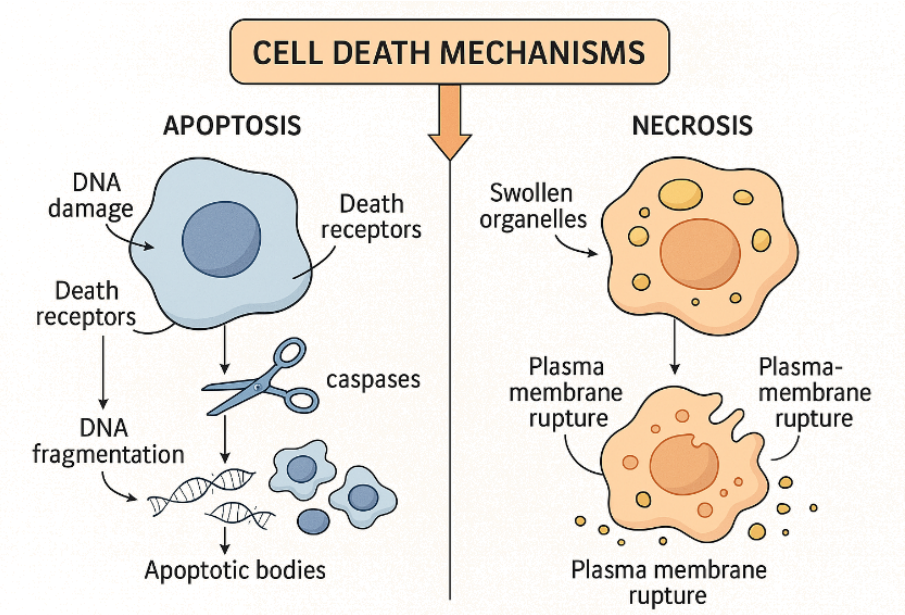


Figure 1: Difference between the stages of necrosis and programmed cell death.

This review provides a comprehensive synthesis of recent advances in elucidating the molecular mechanisms of apoptosis. Its objective is to critically analyze the core regulatory checkpoints, most notably the Bcl-2 protein family, caspases, and inhibitor of apoptosis (IAP) proteins, and delineate the intricate signaling cascades of the intrinsic (mitochondrial) and extrinsic (death receptor) pathways. A particular focus is placed on the mechanistic crosstalk between these pathways and the subsequent execution events at the mitochondrial and nuclear levels. Furthermore, this work evaluates the translational potential of modulating apoptosis, critically assessing emerging therapeutic strategies, such as BH3-mimetics and SMAC mimetics, alongside the persistent challenges in achieving selective targeting in pathologies like cancer and neurodegenerative diseases. The following sections systematically detail this molecular framework, concluding with a forward-looking analysis of the therapeutic landscape and unresolved questions in the field.

## The Core Molecular Machinery of Apoptosis

The genetic and molecular underpinnings of apoptosis were first elucidated through seminal studies in the nematode *Caenorhabditis elegans*, which identified key genes such as *"ced-3"* and *"ced-4"* that are vital for developmental cell death, and *"ced-9"* that acts as a survival regulator (Horvitz, 2003). The subsequent discovery that Bcl-2 is the mammalian homolog of CED-9 established an evolutionary conservation of the apoptotic machinery and provided a critical link to oncogenesis (Strasser and Vaux, 2018). The execution of apoptosis in mammals relies on two cores, interconnected signaling cascades. One is the extrinsic (death receptor) pathway, which extracellular ligand-receptor interactions activate. The other is the intrinsic (mitochondrial) pathway, mobilized by intracellular stressors like growth factor

deprivation, DNA damage, or oxidative stress (Singh et al., 2019). A third pathway, initiated by cytotoxic T-cells via granzyme B, directly activates the executioner phase of apoptosis (Cullen and Martin, 2015).

### The Bcl-2 Protein Family: Guardians of Mitochondrial Integrity

Mitochondrial outer membrane permeabilization (MOMP)—a critical step in the intrinsic apoptotic pathway—is regulated by the Bcl-2 protein family, which functions as its key regulatory determinant (Kalkavan and Green, 2018). Based on the number of Bcl-2 homology (BH) domains (up to four), the family is divided into three functional groups. The first group comprises anti-apoptotic proteins such as Bcl-2, Bcl-xL, and MCL-1. These proteins, equipped with all four BH domains, protect mitochondria by capturing and sequestering proteins that would otherwise trigger apoptosis. MOMP is directly mediated by the oligomeric pore-forming activity of pro-apoptotic effector proteins (e.g., BAX, BAK) following their activation. These proteins contain multiple BH domains.

Proteins belonging to the BH3-only class (e.g., BIM, BID, PUMA, BAD) monitor cellular stress. Their role in promoting MOMP involves two distinct actions: directly activating BAX/BAK or counteracting the inhibitory function of anti-apoptotic proteins (Chipuk et al., 2010). The cell's fate is determined by the complex interactions and stoichiometric balance between these factions, a concept described as the "rheostat" model (Kale et al., 2018). Notably, many viruses have evolved homologs of anti-apoptotic Bcl-2 proteins (e.g., vBcl-2 in Kaposi's sarcoma-associated herpesvirus) to subvert host cell death and promote viral persistence (Fig.2) (Kvansakul and Hinds, 2015).

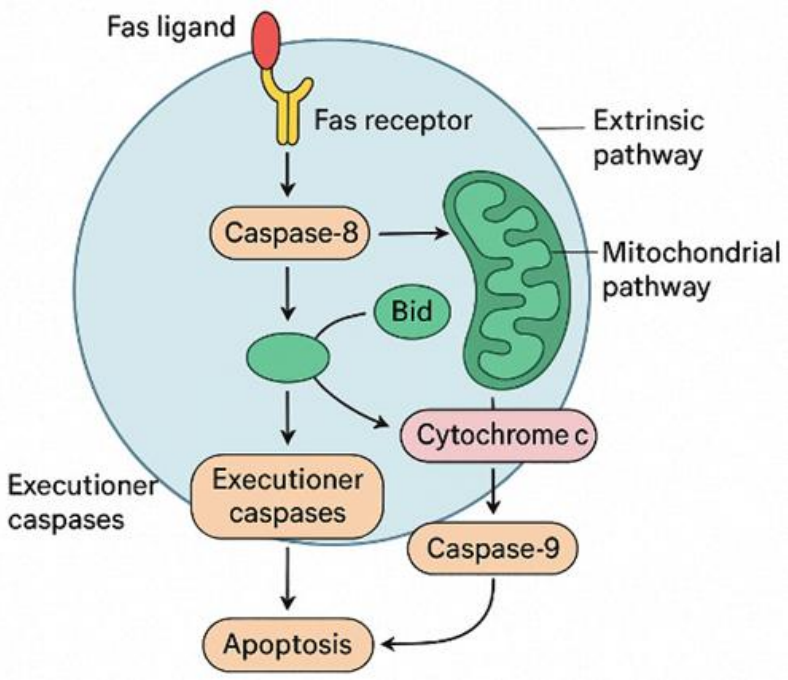


Figure 2. The receptor and mitochondrial pathways of programmed cell death.

### Caspases: The Orchestrators of Cellular Demolition

Caspases (cysteine-aspartic proteases) are the primary effectors of apoptosis, cleaving hundreds of cellular substrates after aspartic acid residues (Julien and Wells, 2017). They are synthesized as inactive zymogens (procaspases) consisting of a pro-domain, a large subunit, and a small subunit. Caspase activation follows a

proteolytic hierarchy, dividing them into two structural and functional classes (Julien and Wells, 2017). Initiator caspases (e.g., -8, -9, -10) feature long pro-domains that direct them to specific signaling platforms like the DISC or Apoptosome. Clustered at these sites, they autoactivate and then proteolytically ignite the downstream cascade (Bock and Tait, 2020).

Executioner caspases (e.g., -3, -6, -7) have short pro-domains. Once activated, they mediate the terminal phase of apoptosis by cleaving a wide array of cellular targets—including structural elements, DNA repair machinery, and regulatory proteins—to produce the defining morphological changes of cell death (Bock and Tait, 2020, McIlwain et al., 2013).

**Endogenous Caspase Inhibitors: The IAP Family**

To prevent inadvertent cell death, caspase activity is tightly regulated by endogenous inhibitors, most notably the Inhibitor of Apoptosis (IAP) proteins (Dubrez et al., 2013). Key mammalian IAPs include XIAP, cIAP1, and cIAP2. XIAP is a potent direct inhibitor of caspase-3, -7, and -9 via its Baculovirus IAP Repeat (BIR) domains (Gyrd-Hansen and Meier, 2010). Other IAPs, such as cIAP1/2, primarily function as regulators of inflammatory signaling via their RING domains, which confer E3 ubiquitin ligase activity. The mitochondrial protein SMAC/Diablo is released upon MOMP and counteracts IAP-mediated inhibition by binding to IAPs and displacing caspases, thereby promoting apoptosis (Lalaoui and Vaux, 2018).

**The p53 Tumor Suppressor: Integrating DNA Damage with Apoptosis**

The p53 protein is a critical tumor suppressor and a master regulator of the cellular response to stress, particularly DNA damage. Activation of p53 leads to one of two outcomes. It may enforce cell cycle arrest, creating a window for DNA repair. Alternatively, if the damage is beyond repair, it can activate the apoptotic pathway (Aubrey et al., 2018). It does so primarily by transcriptionally activating pro-apoptotic target genes, including the BH3-only proteins *PUMA and NOXA,* which directly engage the mitochondrial apoptotic pathway, and *BAX* (Kruiswijk et al., 2015). The critical role of p53 in tumor suppression is highlighted by the fact that many viruses, such as Human Papillomavirus (HPV) with its E6 oncoprotein, have evolved mechanisms to degrade or inactivate p53 to prevent apoptosis in infected cells (Kastenhuber and Lowe, 2017).

**The Role of Calcium Signaling**

Intracellular calcium ions ($Ca^{2+}$) act as important secondary messengers in apoptosis. Dysregulation of $Ca^{2+}$ homeostasis, often involving excessive release from the endoplasmic reticulum (ER), can promote apoptosis through multiple mechanisms. A rise in cytosolic $Ca^{2+}$ levels exert multiple pro-apoptotic effects. It can stimulate proteases such as calpains, alter the function of *Bcl-2* family proteins, and promote mitochondrial membrane permeabilization. This latter event results in cytochrome c release, thereby amplifying the death signal. (Kerkhofs et al., 2018).

**The Principal Pathways of Apoptotic Execution**

Initiation of the two primary apoptotic pathways relies on distinct triggers. Intracellular stressors activate the intrinsic (mitochondrial) pathway, whereas the extrinsic (death receptor) pathway is engaged by ligands outside the cell. Despite their different initiation mechanisms, both pathways ultimately converge to activate a cascade of executioner caspases, which orchestrate the systematic dismantling of the cell through the cleavage of hundreds of cellular substrates (Carneiro and El-Deiry, 2020).

**The Intrinsic (Mitochondrial) Pathway**

The intrinsic apoptotic pathway becomes engaged following significant intracellular distress, such as DNA damage, oxidative stress, lack of growth factors, or stress within the endoplasmic reticulum (ER). The Bcl-2 protein family acts as the central processor for these distress signals, with its control over mitochondrial outer membrane permeabilization (MOMP) determining the cell's fate (Kalkavan and Green, 2018). As outlined earlier, when pro-apoptotic signals dominate, the effector proteins BAX and BAK undergo oligomerization to create pores in the mitochondrial outer membrane. This crucial

step, MOMP, causes the efflux of key pro-apoptotic factors—including cytochrome c and SMAC/Diablo—from the space between mitochondrial membranes into the cell cytoplasm (Kalkavan and Green, 2018, Lalaoui and Vaux, 2018).

Once in the cytosol, cytochrome c interacts with Apaf-1, prompting this factor to assemble into a multi-subunit, wheel-shaped complex termed the apoptosome (Dorstyn et al., 2018). This apoptosome serves as a platform to recruit and activate the initiator protease procaspase-9. Active caspase-9 then propagates the death signal by proteolytically processing and turning on the downstream executioner caspases, primarily caspase-3 and -7 (Dorstyn et al., 2018). In a parallel pro-apoptotic mechanism, the released SMAC/Diablo protein works to counteract the inhibitory effects of IAPs on caspases, thereby further facilitating cell death (Lalaoui and Vaux, 2018).

**The Extrinsic (Death Receptor) Pathway**

Activation of the extrinsic apoptotic pathway commences when death ligands from the extracellular environment engage their matching death receptors on the cell surface. These receptors are part of the tumor necrosis factor (TNF) receptor family, with notable examples being CD95 (Fas), TRAIL-R1/DR4, TRAIL-R2/DR5, and TNFR1 (Jan, 2019). Following ligand-receptor engagement—such as the binding of FasL to CD95—the receptors assemble into trimers. This oligomerization allows them to bring together specific intracellular adapter proteins through interactions between homologous Death Domains (DDs). In the case of CD95, the primary adapter recruited is FADD (Fas-Associated protein with Death Domain). FADD contains an additional interaction module called a Death Effector Domain (DED). Via this DED, FADD binds to and recruits the inactive zymogen form of the initiator protease, procaspase-8 (and procaspase-10 in humans) (Ashkenazi and Salvesen, 2014). The resulting assembly of the receptor, FADD, and procaspase-8 forms a critical signaling hub known as the Death-Inducing Signaling Complex (DISC). It is within the confines of the DISC that procaspase-8 molecules are brought into proximity, leading to their autoactivation and the production of enzymatically active caspase-8 (Kesavardhana et al., 2020).

The initiation mechanism for TNF-R1 is more elaborate. Ligand binding to this receptor results in the recruitment of a different adapter protein, TRADD (TNF Receptor-Associated Death Domain). TRADD subsequently functions as a versatile platform. It can recruit FADD to direct the signal towards apoptosis, or it can assemble other proteins such as RIPK1 to channel the signal into activating the NF-κB pathway, which promotes inflammation (Van Opdenbosch and Lamkanfi, 2019).

**Pathway Integration and Cross-Talk**

The extrinsic and intrinsic apoptotic pathways function in a connected network, engaging in essential molecular dialogue to potentiate the cell death signal. A pivotal integrator of this cross-talk is the protein BID, a member of the Bcl-2 family. Caspase-8, activated within the DISC, proteolytically cleaves full-length BID residing in the cytosol. This cleavage generates a truncated, highly active fragment known as tBID. The tBID fragment subsequently migrates to the mitochondria. There, it directly stimulates the activation of the pro-apoptotic effector proteins BAX and BAK. This action effectively recruits the intrinsic apoptotic machinery, leading to a powerful amplification of caspase activity via the subsequent events of MOMP and apoptosome assembly (Delbridge et al., 2016). This integrative mechanism is especially vital in so-called Type II cells, where an effective apoptotic response depends on this reinforced mitochondrial feedback loop.

**Viral Modulation of Death Receptor Pathways**

Viruses have evolved sophisticated mechanisms to subvert death receptor-mediated apoptosis. A prominent example is the cellular and v-FLIP (viral-FLICE-inhibitory protein) proteins. Recruitment of c-FLIP to the DISC is facilitated by its structural mimicry of procaspase-8, a similarity conferred by the presence of homologous DED domains. However, it lacks catalytic activity. By binding

to FADD and procaspase-8, c-FLIP disrupts the formation of a functional DISC and inhibits caspase-8 activation (Guerrache and Micheau, 2024).

Several viruses encode v-FLIPs (e.g., K13 in HHV-8) to exploit this inhibitory mechanism. Other viral proteins, such as the adenovirus E1B-19K and the HIV Tat protein, can modulate the expression or function of death receptors and their ligands, thereby tipping the balance toward cell survival and viral persistence (Guerrache and Micheau, 2024).

## The Intrinsic Pathway: Mitochondrial Regulation and Nuclear Execution

### Mitochondrial Control of Apoptosis

In the intrinsic apoptotic pathway, mitochondria are cast in the role of the ultimate executioners, with the point of no return being mediated through mitochondrial outer membrane permeabilization (MOMP) (Kalkavan and Green, 2018). The principal mediators of this event are the pro-apoptotic Bcl-2 family proteins BAX and BAK. In viable cells, BAX is maintained in an inactive conformation primarily in the cytosol, whereas BAK is constitutively embedded within the mitochondrial outer membrane. Activation by specific "activator" BH3-only proteins triggers the translocation of BAX to mitochondria and induces extensive conformational changes in both effectors. These changes drive their homo-oligomerization and the formation of proteolipid pores, resulting in the compromise of mitochondrial membrane integrity (Meng et al., 2021, Czabotar et al., 2014).

MOMP causes the irreversible release of key pro-apoptotic factors from the mitochondrial intermembrane space into the cytosol. These include cytochrome c, which initiates apoptosome formation; SMAC/Diablo, which neutralizes the inhibitory function of IAP proteins; and the caspase-independent factors Apoptosis-Inducing Factor (AIF) and Endonuclease G, which are translocated to the nucleus to mediate chromatin condensation and DNA fragmentation, respectively (Lalaoui and Vaux, 2018, Dorstyn et al., 2018).

The assembled apoptosome serves as a platform for the recruitment and auto-activation of procaspase-9. According to the prevailing model, caspase-9 activation is achieved through proximity-induced dimerization within this complex, forming an active holoenzyme. This active holoenzyme is then responsible for the proteolytic cleavage and activation of the primary executioner caspases, caspase-3 and caspase-7 (Dorstyn et al., 2018).

### Nuclear Events in Apoptosis

The executioner caspases orchestrate the systematic dismantling of the nucleus, a hallmark of apoptosis. This process involves critical alterations in nucleocytoplasmic transport, where caspases play a leading role (Kopeina et al., 2018). Key nuclear events include the inactivation of DNA repair machinery via caspase-3-mediated cleavage of PARP-1, chromatin condensation facilitated by caspase-6-mediated cleavage of nuclear lamins, and DNA fragmentation. The subcellular relocation of caspases to the nucleus is a key regulatory step for these events (Prokhorova et al., 2018). DNA fragmentation is primarily mediated by CAD (Caspase-Activated DNase), which is liberated from its inhibitor ICAD upon cleavage by caspase-3, leading to the characteristic internucleosomal DNA ladder.

### Cytoskeletal Reorganization and Phagocytic Clearance

The structural integrity of the cell is dismantled through caspase-mediated cleavage of key cytoskeletal and adhesion proteins, including actin, vimentin, and cadherins (Julien and Wells, 2017). Consequently, cell-substrate adhesion is lost, the membrane undergoes blebbing, and apoptotic bodies are formed. A crucial phagocytic "eat-me" signal is generated by the translocation of phosphatidylserine to the outer plasma membrane leaflet. This externalization is enabled by scramblase activation and flippase inhibition, both of which are mediated by caspase activity (Segawa and Nagata, 2015).

The apoptotic process culminates in the prompt removal of the deceased cell. Following fragmentation into membrane-bound apoptotic bodies, these bodies are rapidly phagocytosed by adjacent cells or specialized phagocytes such as macrophages. This process, known as

efferocytosis, occurs without the release of pro-inflammatory cellular contents, thereby preventing an immune response and maintaining tissue homeostasis (Poon et al., 2014, Doran et al., 2020).

## Discussion

The molecular landscape of apoptosis, as detailed in this review, reveals an intricate and highly regulated system central to life and death decisions in metazoans. While the canonical pathways (intrinsic and extrinsic) and their core components (Bcl-2 family, caspases, IAPs) are well-established, recent research has shifted towards understanding their context-dependent regulation, crosstalk with other biological processes, and therapeutic exploitation amidst emerging challenges.

A critical comparison of the intrinsic and extrinsic pathways highlights their complementary roles and adaptive significance. The intrinsic pathway acts as a sensor for intracellular well-being, responding to metabolic stress, DNA damage, and oncogenic signals. In contrast, the extrinsic pathway serves as an executioner for immune surveillance and tissue remodeling. The discovery of the BID-mediated cross-talk bridged these pathways, illustrating an elegant fail-safe mechanism to ensure efficient elimination of compromised cells, particularly in cancer and viral infection (Kalkavan and Green, 2018, Singh et al., 2019). Recent findings challenge the simplicity of the "rheostat" model, suggesting that dynamic localization, post-translational modifications (e.g., phosphorylation, ubiquitination), and non-canonical interactions within the Bcl-2 family add layers of regulation that are cell-type and stimulus-specific (Kale et al., 2018).

Therapeutic targeting of apoptosis, particularly in oncology, has seen both remarkable successes and sobering challenges. The clinical success of venetoclax (ABT-199), a specific Bcl-2 inhibitor, in hematological malignancies validates the concept of "reactivating" apoptosis (Carneiro and El-Deiry, 2020). However, resistance frequently emerges through upregulation of other anti-apoptotic proteins like MCL-1 or Bcl-xL, highlighting the need for combination therapies or pan-Bcl-2 inhibitors. Similarly, SMAC mimetics showed promise in preclinical models by antagonizing IAPs, but their efficacy in solid tumors has been limited, partly due to compensatory activation of NF-κB signaling (Lalaoui and Vaux, 2018). A major contemporary challenge is the selective induction of apoptosis in cancer cells while sparing normal tissues. Strategies exploiting synthetic lethality (e.g., combining PARP inhibitors with Bcl-2 inhibition in BRCA-mutant cancers) or targeting apoptotic priming represent promising avenues informed by recent mechanistic studies (Singh et al., 2019).

Furthermore, apoptosis does not occur in isolation. Its interplay with other forms of regulated cell death (RCD), such as necroptosis and ferroptosis, forms a complex network where inhibition of one pathway can shunt cell death to another. This has profound implications for therapy; for instance, caspase inhibition in some contexts can lead to necroptosis, an inflammatory death that might enhance anti-tumor immunity (Galluzzi et al., 2018). Recent experimental studies using CRISPR screens and chemical biology are mapping these dependencies, offering blueprints for rational combination therapies. Another emerging frontier is the role of apoptosis in shaping the tumor immune microenvironment. Immunogenic cell death (ICD), a variant of apoptosis accompanied by the release of danger signals, can stimulate anti-tumor immunity, suggesting that coupling apoptosis inducers with immunotherapies could yield synergistic effects (Carneiro and El-Deiry, 2020).

In conclusion, while the core mechanics of apoptosis are deciphered, the field is now grappling with its complexity in vivo. Future progress will depend on integrating structural biology insights with systems-level approaches in relevant disease models to overcome drug resistance, improve specificity, and harness the immunogenic potential of apoptotic cell death.

## Conclusion and Future Perspectives

In conclusion, the molecular deciphering of apoptosis has provided unparalleled insights into a fundamental

biological process with direct relevance to human health and disease. The intricate balance within the apoptotic machinery, governed by the Bcl-2 family rheostat, the caspase cascade, and IAP-mediated inhibition, presents a double-edged sword for therapeutic intervention. The successful clinical development of BH3-mimetics like venetoclax (a Bcl-2 inhibitor) for hematological malignancies validates the strategy of reactivating apoptosis in cancer (Kale et al., 2018). Concurrently, efforts to develop caspase inhibitors and IAP mimetics aim to protect neurons in stroke and neurodegenerative conditions.

Looking forward, future research must address several key challenges to fully harness the therapeutic potential of apoptosis modulation. These include improving the specificity of agents to minimize on-target toxicity, developing effective drug delivery systems to target tissues or tumor microenvironments, and devising strategies to overcome inherent and acquired resistance to apoptosis-inducing drugs. Additionally, the growing understanding of how apoptotic cell death shapes the immunogenic landscape—for instance, through the release of damage-associated molecular patterns (DAMPs) in certain contexts—opens new frontiers for rational combination therapies, pairing apoptosis inducers with immunomodulatory agents (Carneiro and El-Deiry, 2020).

Future perspectives should also focus on several emerging areas: First, the systems-level analysis of apoptotic networks in patient-derived samples will be crucial for identifying predictive biomarkers of response and resistance. Second, exploring the role of non-canonical apoptosis and its initiators (e.g., caspase-2, -4, -5) in specific pathological contexts may reveal novel targets. Third, advancing the chemical biology toolbox—such as with proteolysis-targeting chimeras (PROTACs) to degrade anti-apoptotic proteins—offers a promising strategy to achieve deeper and more sustained inhibition. Finally, understanding the temporal and spatial control of apoptosis *in vivo*, perhaps through advanced imaging techniques, will be key to translating mechanistic knowledge into precise therapies. As our molecular understanding continues to deepen, so too will our capacity to precisely manipulate this critical pathway for therapeutic benefit across a wide spectrum of human diseases.

**Acknowledgment**

The authors wish to acknowledge the collective body of scholarly work that served as the cornerstone for this review. We are also indebted to our colleagues for the stimulating dialogue that helped refine the concepts presented herein.

**Conflicts of interest**

There are no conflicts of interest.

**References:**

Ashkenazi, A. and Salvesen, G., 2014. Regulated cell death: signaling and mechanisms. *Annual review of cell and developmental biology*, *30*, pp.337-356.

Aubrey, B.J., Kelly, G.L., Janic, A., Herold, M.J. and Strasser, A., 2018. How does p53 induce apoptosis and how does this relate to p53-mediated tumour suppression?. *Cell death & differentiation*, *25*(1), pp.104-113.

Bock, F.J. and Tait, S.W., 2020. Mitochondria as multifaceted regulators of cell death. *Nature reviews Molecular cell biology*, *21*(2), pp.85-100.

Carneiro, B.A. and El-Deiry, W.S., 2020. Targeting apoptosis in cancer therapy. *Nature reviews Clinical oncology*, *17*(7), pp.395-417.

Chipuk, J.E., Moldoveanu, T., Llambi, F., Parsons, M.J. and Green, D.R., 2010. The BCL-2 family reunion. *Molecular cell*, *37*(3), pp.299-310.

Cullen, S.P. and Martin, S.J., 2015, March. Fas and TRAIL 'death receptors' as initiators of inflammation: Implications for cancer. In *Seminars in cell & developmental biology* (Vol. 39, pp. 26-34). Academic Press.

Czabotar, P.E., Lessene, G., Strasser, A. and Adams, J.M., 2014. Control of apoptosis by the BCL-2 protein family: implications for physiology and therapy. *Nature reviews Molecular cell biology*, *15*(1), pp.49-63.D'ARCY, M. S. 2019. Cell death: a review of

the major forms of apoptosis, necrosis and autophagy. *Cell biology international,* 43, 582–592.

Delbridge, A.R., Grabow, S., Strasser, A. and Vaux, D.L., 2016. Thirty years of BCL-2: translating cell death discoveries into novel cancer therapies. *Nature Reviews Cancer*, *16*(2), pp.99-109.

Doran, A.C., Yurdagul Jr, A. and Tabas, I., 2020. Efferocytosis in health and disease. *Nature Reviews Immunology*, *20*(4), pp.254-267.

Dorstyn, L., Akey, C.W. and Kumar, S., 2018. New insights into apoptosome structure and function. *Cell Death & Differentiation*, *25*(7), pp.1194-1208.

Dubrez, L., Berthelet, J. and Glorian, V., 2013. IAP proteins as targets for drug development in oncology. *OncoTargets and therapy*, pp.1285-1304.

Fuchs, Y. and Steller, H., 2015. Live to die another way: modes of programmed cell death and the signals emanating from dying cells. *Nature reviews Molecular cell biology*, *16*(6), pp.329-344.

Galluzzi, L., Vitale, I., Aaronson, S.A., Abrams, J.M., Adam, D., Agostinis, P., Alnemri, E.S., Altucci, L., Amelio, I., Andrews, D.W. and Annicchiarico-Petruzzelli, M., 2018. Molecular mechanisms of cell death: recommendations of the Nomenclature Committee on Cell Death 2018. *Cell Death & Differentiation*, *25*(3), pp.486-541.

Gong, Y., Fan, Z., Luo, G., Yang, C., Huang, Q., Fan, K., Cheng, H., Jin, K., Ni, Q., Yu, X. and Liu, C., 2019. The role of necroptosis in cancer biology and therapy. *Molecular cancer*, *18*(1), p.100.

Guerrache, A. and Micheau, O., 2024. TNF-related apoptosis-inducing ligand: non-apoptotic signalling. *Cells*, *13*(6), p.521.

Gyrd-Hansen, M. and Meier, P., 2010. IAPs: from caspase inhibitors to modulators of NF-κB, inflammation and cancer. *Nature Reviews Cancer*, *10*(8), pp.561-574.

Horvitz, H.R., 2003. Nobel lecture: Worms, life and death. *Bioscience reports*, *23*(5), pp.239-303.

Jan, R., 2019. Understanding apoptosis and apoptotic pathways targeted cancer therapeutics. *Advanced pharmaceutical bulletin*, *9*(2), p.205.

Julien, O. and Wells, J.A., 2017. Caspases and their substrates. *Cell Death & Differentiation*, *24*(8), pp.1380-1389.

Kale, J., Osterlund, E.J. and Andrews, D.W., 2018. BCL-2 family proteins: changing partners in the dance towards death. *Cell Death & Differentiation*, *25*(1), pp.65-80.

Kalkavan, H. and Green, D.R., 2018. MOMP, cell suicide as a BCL-2 family business. *Cell Death & Differentiation*, *25*(1), pp.46-55.

Kastenhuber, E.R. and Lowe, S.W., 2017. Putting p53 in context. *Cell*, *170*(6), pp.1062-1078.

Kerkhofs, M., Bittremieux, M., Morciano, G., Giorgi, C., Pinton, P., Parys, J.B. and Bultynck, G., 2018. Emerging molecular mechanisms in chemotherapy: Ca2+ signaling at the mitochondria-associated endoplasmic reticulum membranes. *Cell death & disease*, *9*(3), p.334.

Kerr, J.F., Wyllie, A.H. and Currie, A.R., 1972. Apoptosis: a basic biological phenomenon with wideranging implications in tissue kinetics. *British journal of cancer*, *26*(4), pp.239-257.

Kesavardhana, S., Malireddi, R.S. and Kanneganti, T.D., 2020. Caspases in cell death, inflammation, and pyroptosis. *Annual review of immunology*, *38*(1), pp.567-595.

Kopeina, G.S., Prokhorova, E.A., Lavrik, I.N. and Zhivotovsky, B., 2018. Alterations in the nucleocytoplasmic transport in apoptosis: Caspases lead the way. *Cell Proliferation*, *51*(5), p.e12467.

Kruiswijk, F., Labuschagne, C.F. and Vousden, K.H., 2015. p53 in survival, death and metabolic health: a lifeguard with a licence to kill. *Nature reviews Molecular cell biology*, *16*(7), pp.393-405.

Kvansakul, M. and Hinds, M.G., 2015. The Bcl-2 family: structures, interactions and targets for drug discovery. *Apoptosis*, *20*(2), pp.136-150.

Lalaoui, N. and Vaux, D.L., 2018. Recent advances in understanding inhibitor of apoptosis proteins. *F1000Research*, *7*, pp.F1000-Faculty.

McIlwain, D.R., Berger, T. and Mak, T.W., 2013. Caspase functions in cell death and disease. *Cold Spring Harbor perspectives in biology*, *5*(4), p.a008656.

Meng, Y., Sandow, J.J., Czabotar, P.E. and Murphy, J.M., 2021. The regulation of necroptosis by post-translational modifications. *Cell Death & Differentiation*, *28*(3), pp.861-883.

Nagata, S., 2018. Apoptosis and clearance of apoptotic cells. *Annual review of immunology*, *36*(1), pp.489-517.

Poon, I.K., Lucas, C.D., Rossi, A.G. and Ravichandran, K.S., 2014. Apoptotic cell clearance: basic biology and therapeutic potential. *Nature Reviews Immunology*, *14*(3), pp.166-180.

Prokhorova, E.A., Kopeina, G.S., Lavrik, I.N. and Zhivotovsky, B., 2018. Apoptosis regulation by subcellular relocation of caspases. *Scientific reports*, *8*(1), p.12199.

Segawa, K. and Nagata, S., 2015. An apoptotic 'eat me'signal: phosphatidylserine exposure. *Trends in cell biology*, *25*(11), pp.639-650.

Singh, R., Letai, A. and Sarosiek, K., 2019. Regulation of apoptosis in health and disease: the balancing act of BCL-2 family proteins. *Nature reviews Molecular cell biology*, *20*(3), pp.175-193.

Strasser, A. and Vaux, D.L., 2018. Viewing BCL2 and cell death control from an evolutionary perspective. *Cell Death & Differentiation*, *25*(1), pp.13-20.

Van Opdenbosch, N. and Lamkanfi, M., 2019. Caspases in cell death, inflammation, and disease. *Immunity*, *50*(6), pp.1352-1364.

University of Jiroft

**Biospecies Research**

Journal homepage: bsr.ujiroft.ac.ir

Iranian Biology Society

# Interaction effect of thiamine (Vit B1) and 24-epibrassinolide on rapeseed (*Brassica napus*) growth improvement and change of some physiological parameters content under cadmium stress

Shima Sanjari[1], Hossein Mozafari[2*], Batool Keramat[3], Nazi Nadernejad[4]

https://doi.org/10.22034/bsr.2026.563894.1005

[1]*PhD Graduate, Department of Biology, Shahid Bahonar University of Kerman, Iran; shimasanjari2300@gmail.com ORCID: 0000-0002-9109-2566*

[2]*Assistant Professor, Department of Ecology, Institute of Science and High Technology and Environmental Sciences, Graduate University of Advanced Technology, Kerman, Iran; h.mozafari@kgut.ac.ir, Mozafari.hossein@gmail.com ORCID: 0000-0001-7642-6145*

[3]*Associate Professor, Department of Biology, Shahid Bahonar University of Kerman, Iran; keramatbatool@gmail.com ORCID: 0000-0001-7642-6145*

[4]*Assistant Professor, Department of Biology, Shahid Bahonar University of Kerman, Iran; nnadernejad@uk.ac.ir ORCID: 0000-0001-7642-6145*

## ARTICLEINFO

**Article Type**

Original Article

**Article History**

Received: 03 December 2025

Accepted: 30 January 2026

Published: 15 February 2026



***Corresponding author**

Mozafari.hossein@gmail.com

## ABSTRACT

The heavy metal cadmium is an environmental pollutant that causes various toxicities in living organisms, especially plants. The organic substances thiamine and 24-epibrassinolide are known as plant growth regulators that cause different growth and physiological responses in plants. In this study, the induction of possible resistance-inducing effects by the application of thiamine (Vit B1) and epibrassinolide (EBL) treatment on the reduction of cadmium toxicity in rapeseed was investigated. Rapeseed plants were grown in a greenhouse environment under standard conditions for 4 weeks. After this period, the effects of experimental treatments including concentrations of thiamine (0, 100, and 200 µM), epibrassinolide (0, 0.02, and 0.5 µM), and cadmium (0, 250, and 500 µM) were tested on plants every other day for 7 days. The experiment and treatments were performed in a completely randomized design with 3 replications on the plants. The resulting data were statistically analyzed using ANOVA and Duncan's multiple range test at a significance level of 5% using SPSS 18.0 software. The results of this study showed that cadmium stress reduced plant height parameters, fresh and dry weights of shoots and roots, and reduced the content of photosynthetic pigments and sugars in the leaves of stressed plants compared to the control. On the other hand, the increase in the content of phenolic compounds, anthocyanins, and flavonoids under cadmium stress conditions and in treatment with thiamine and epibrassinolide indicates the activation of the phenylpropanoid pathway under these conditions and the role of these compounds in quenching oxygen free radicals. A decrease in ascorbate and proline levels was observed in plants treated with thiamine, epibrassinolide, and cadmium compared to plants exposed to cadmium stress alone. The results obtained indicate that the interaction of 24-epibrassinolide at a concentration of 0.02µM with thiamine at a concentration of 200 µM can play a positive role in eliminating the damage caused by cadmium stress.

**Keywords:** Anthocyanin, flavonoids, heavy metal, environmental pollutant, phenolic compounds

**How to cite this paper**

Sanjari, SH., Mozafari, H., Keramat, B., Nadernejad, N., 2026. Interaction effect of thiamine (Vit B1) and 24-epibrassinolide on rapeseed (Brassica napus) growth improvement and change of some biochemical parameters content under cadmium stress. *Biospecies Research*, 1, pp. 35-56.

## Introduction

Environmental stresses such as cold, heat, salinity, cadmium, radiation, chemicals and pollutants, heavy metals, ozone are among the most important factors reducing plant yield and growth in the world (Gallego et al., 2012; Gill & Tuteja, 2010). Cadmium stress causes the production of reactive oxygen species, damage to cell membranes, inhibition of electron transfer, reduction of photosynthetic pigments, sugars and total protein (Zhang et al., 2014; Gill et al., 2011). By storing and increasing the content of soluble sugars and amino acids, plants can tolerate or adapt to various stresses by carefully controlling the entry and exit of ions, activating the inhibitory system, and eliminating reactive oxygen species (Li et al., 2012; Farid et al., 2013). The problem of heavy metal pollution has become a serious problem with increasing industrialization and disruption of natural biogeochemical cycles. Heavy metals are naturally present in soil as trace elements. The main source of heavy metal emissions into the environment is human activities, which may cause significant damage to ecosystems. Heavy metal pollution affects the production rate and quality of agricultural products, the quality of drinking water, and the health and lives of animals and humans. Heavy metal pollution is one of the biggest environmental problems today and is toxic to animals and humans due to DNA damage, carcinogenic effects, and mutagenicity (Bajguz & Hayat, 2009).

Plant toxicity is mostly due to contamination by metals such as arsenic, cadmium, chromium, and lead, which usually have very low toxicity thresholds (Kartal et al., 2009). These elements are not essential for humans and may enter the food chain through eating contaminated food products. However, contamination of the food chain with heavy metals often depends on the plant species, the behavior and reaction of plants in the way they absorb and accumulate metals, the type and amount of metal, and the way they are consumed and used in plant products (Liu et al., 2015). Cadmium is not only not essential for biological activities, but is also considered a toxic element for most organisms, with its toxicity being 2 to 20 times higher than other heavy metals, including copper, zinc, nickel, and silver (Singh & Prasad, 2014).

The first visible signs of cadmium toxicity in plants are yellowing and tabularization of leaves in the aerial organs (Gallego et al., 2012). Retardation in plant growth has been reported as a symptom of cadmium toxicity. Reports have shown that cadmium affects cell division and growth, overall plant growth, cell division in the meristematic region, and regulation of plant growth and development (Kohli et al., 2017; Singh & Prasad, 2014). Cadmium has been shown to reduce photosynthesis, transpiration, and respiration. Cadmium levels above the threshold limit cause shortening of the branch axis and increased yellowing of old leaves in plants (Farid et al., 2013; Ahmad et al., 2012). Cadmium toxicity leads to inhibition of DNA, RNA, and protein synthesis, as well as inhibition of enzyme including the inhibition of metal-dependent enzymes and the induction of oxidative stress. (Ali et al., 2015; Fariduddin et al., 2014). Adverse environmental conditions, especially metal pollution, can lead to disruption of metabolic and cellular functions in plants, which causes plants to evolve a complex set of mechanisms to maintain optimal metal levels (Fariduddin et al., 2014; Hacham et al., 2011). Cadmium-induced oxidative stress is either in the form of ROS production or by reducing the concentration of both enzymatic and non-enzymatic antioxidants. Plants have evolved enzymatic and non-enzymatic defense systems to overcome the harmful effects of ROS.

Catalase is a class of iron-containing proteins and is activated in plant and animal cells when the amount of H2O2 in the environment is high (Gallego et al., 2012; Gill & Tuteja, 2010). There are two groups of non-enzymatic antioxidants: 1- Fat-soluble antioxidants such as α-tocopherol, carotenoids and xanthophylls; 2- Water-soluble antioxidants such as glutathione, ascorbate and phenolic compounds (Yusuf et al., 2017).

Today, more than 70 compounds with similar structure and action have been extracted from plant

sources, which have been named as a new group of plant hormones called brassinosteroids. Brassinosteroids are poly hydroxylated plant steroid hormones that play a role in promoting plant growth and development. They also play a role in the response mechanism of plants to biotic and abiotic stresses (Kapoor et al., 2014; Petrov & Van Breusegem, 2012). In general, brassinosteroids are able to regulate the uptake of ions into plant cells and can be used to reduce the accumulation of heavy metals, as they can reduce metal uptake by roots and can also stimulate the synthesis of some ligands such as phytochelatins. They also increase the activity of some antioxidant enzymes that enhance ROS detoxification during heavy metal stress (Vardhini & Anjum, 2015; Gill & Tuteja, 2010). Therefore, external application of brassinosteroids leads to improved growth and metabolic activity in plants under heavy metal stress (Hacham et al., 2011).

Thiamine is an important antioxidant in plants. The cofactor form of thiamine, thiamine pyrophosphate, is the most abundant vitamin B1 in plants. It has been suggested that thiamine plays an indirect role as an antioxidant in plants by providing NADH and NADPH to counteract oxidative stress. Thiamine has been reported to reduce the effects of environmental stresses. External application of thiamine counteracts the detrimental effects of salinity on growth. It also promotes resistance to fungal, bacterial and viral infections in various plants including rice, Arabidopsis and grapes (Hacham et al., 2011; Gill et al., 2011).

In one study, it was shown that in Arabidopsis seedlings exposed to high light stress, low temperature, osmotic stress, salinity, or paraquat, the levels of thiamine, thiamine monophosphate, and thiamine pyrophosphate increased. This increase was a result of increased transcription levels of thiamine biosynthesis genes (Gill & Tuteja, 2010). In another study, increased expression of genes involved in the thiamine diphosphate biosynthesis pathway was observed in Arabidopsis seedlings exposed to Cd or salinity stress (Stolfa et al., 2015).

On the other hand, thiamine in maize and sunflower plants increases the resistance of plants to salinity. Thus, ion leakage, which is increased by salinity, is reduced when thiamine is applied (Li et al., 2012; Olubunmi & Olorunsola, 2010). Therefore, it seems necessary to use appropriate solutions that can reduce the destructive effects of cadmium stress on plant growth, bio chemicals and primary products. In many studies, brassinosteroids or vitamins have been used to alleviate the harmful effects of environmental stresses. In this study, to investigate the interaction between 24-epibrassinolide and thiamine (vit B1) in reducing the toxic effects of cadmium metal on physiological and biochemical processes effective in developing resistance to cadmium stress, different concentrations of 24-epibrassinolide and thiamine were treated in rapeseed plants under different levels of cadmium. And the effects of EBL and thiamine on various stress coping mechanisms such as activation of the phenyl propanoid pathway and antioxidant defense mechanism were investigated.

## Materials and methods

### Research design and treatment groups:

The plant studied in this research was rapeseed Brassica napus L, cultivar Hyola 401, the seeds of which were obtained from Pakan Bazr Company, Isfahan, Iran. The reason for choosing this plant is because of its economic value, and also because it has unsaturated fatty acids and no cholesterol, which plays an effective role in reducing cardiovascular diseases. Rapeseed seeds were disinfected with 0.5% sodium hypochlorite for one minute and then washed twice with distilled water. Then the soaked seeds were transferred to pots. For each treatment, 3 pots were considered as 3 replications. One seed was planted in each pot as a sample. After cultivation, the pots were placed in a greenhouse under 16:8 light/dark conditions with 75% humidity and a day/night temperature of 20/25°C. In order to provide the plant with the necessary nutrients, the pots were irrigated with Hoagland's nutrient solution at a dilution of 1/2 for 4 weeks. The above nutrient solution was prepared with a pH of 5.7, and then the pH of the solution was adjusted to 6.25 ± 0.25 using hydrochloric acid and 1 mM sodium hydroxide for better treatment effects. The composition of

Hoagland's solution is shown in Table 1-2 (He et al., 2016). Plants were used for treatment after 4 weeks of growth. In this study, after about 4 weeks of growth, plants were treated with cadmium chloride 0, 250, and 500 mM, 24-epibrassinolide 0, 0.02, and 0.5 mM, and thiamine 0, 100, and 200 mM. These treatments were prepared in a base solution of distilled water. The control plants were irrigated with distilled water without the treatments. Treatment was applied for 7 days every other day with the treatment code given in the table. Treatments were performed in a completely randomized design with 3 replications. At the end, samples were collected, washed with distilled water, and immediately frozen with liquid nitrogen and stored at -80°C for subsequent measurements (Farid et al., 2013; Kaznina & Titov, 2014).

Table 1: Composition and concentration of treatments (factor codes 1-27) included EBL (epibrassinolide), Thiamine (Vit. B1) and cadmium stress (Cd) used in the study, which were applied to plants in a completely randomized design.

| | Factor code | | | | | | | | | | | | |
|---|---|---|---|---|---|---|---|---|---|---|---|---|---|
| | 1 | 2 | 3 | 4 | 5 | 6 | 7 | 8 | 9 | 10 | 11 | 12 | 13 |
| EBL(µM) | 0 | 0 | 0 | 0.02 | 0.02 | 0.02 | 0.5 | 0.5 | 0.5 | 0 | 0 | 0 | 0.02 |
| Thiamine (µM) | 0 | 0 | 0 | 0 | 0 | 0 | 0 | 0 | 0 | 100 | 100 | 100 | 100 |
| Cd (µM) | 0 | 250 | 500 | 0 | 250 | 500 | 0 | 250 | 500 | 0 | 250 | 500 | 0 |

| | Factor code | | | | | | | | | | | | | |
|---|---|---|---|---|---|---|---|---|---|---|---|---|---|---|
| | 14 | 15 | 16 | 17 | 18 | 19 | 20 | 21 | 22 | 23 | 24 | 25 | 26 | 27 |
| EBL(µM) | 0.02 | 0.02 | 0.5 | 0.5 | 0.5 | 0 | 0 | 0 | 0.02 | 0.02 | 0.02 | 0.5 | 0.5 | 0.5 |
| Thiamine (µM) | 100 | 100 | 100 | 100 | 100 | 200 | 200 | 200 | 200 | 200 | 200 | 200 | 200 | 200 |
| Cd (µM) | 250 | 500 | 0 | 250 | 500 | 0 | 250 | 500 | 0 | 250 | 500 | 0 | 250 | 500 |

Measurement of growth parameters: The fresh weight of roots and shoots in fresh rapeseed samples was measured using a scale with an accuracy of 0.01 grams and the results were recorded in grams. In order to determination the length of the shoot and root, a 1 mm ruler was used, after cutting the collar area of the plant and separating the root from the shoot, and the basis for measuring the root length is the main root (Kaznina & Titov, 2014). The relative content of leaf water: In order to measure the relative water content, the last developed leaves of the plants were selected and separated. As soon as it was separated, it was placed in ice. In the laboratory, the weight of the leaves was measured with a scale. Then the samples were placed in distilled water at laboratory temperature for 24 hours. After 24 hours, Turgor's weight of the leaves was measured. Then the same leaves were placed in aluminum foil and placed in an oven at 72°C for 24 hours. After 24 hours, the dried samples were taken out from inside the foil and their weight was measured by an accurate scale. The relative content of leaf water was measured according to the method of Ritchie et al., 1990 (Hacham et al., 2011).

Measurement of leaf ion leakage percentage: To measure cell membrane leakage, ion leakage was measured by the method (Farid et al., 2013). For this aim, after washing with deionized water, 0.2 grams of fresh plant tissue was placed in a test tube with a screw cap, and 10 cc of distilled water was added to it, and it was kept in the laboratory environment after 2 hours. The initial electrical conductivity of the solution (EC1) was

measured by EC meter Metrohm co. Then the tubes are transferred to the autoclave for 20 minutes to heat and release the rest of the ions. After cooling in the laboratory environment, the secondary electrical conductivity (EC2) of the solution is measured again. Finally, the amount of ionic leakage of the desired tissue is calculated through the opposite formula and in terms of percentage (Posmyk et al., 2009; Farid et al., 2013).

Figure 1: 14-day-old rapeseed (Brassica napus L.) plants, grown and growing in 12 cm plastic pots filled with perlite growing medium, ready for treatment in this study with 27 treatments specified in a factorial experiment. The treatments contained different amounts of thiamine (Vit. B1), epibrassinolide (EBL) and cadmium stress (Cd). The treatments contained different amounts of thiamine, epibrassinolide and cadmium stress. The pots were regularly irrigated with Hoagland's basic solution with or without treatment until the end of the plant cultivation period in this study.

Measurement of photosynthetic pigments: Photosynthetic pigments were measured according to Lichtenthaler's 1987 method. At first, 0.2 grams of fresh plant tissue was weighed using a digital scale in the laboratory, and each leaf was ground in a Chinese mortar with 15 cc of 80% acetone, and centrifuged for 15 minutes at 9000 rpm at 4 degrees. The supernatant solution was poured into the cell, then their absorbance was read at wavelengths of 646.8, 663.20, and 470 nm with a spectrophotometer Biowave.

The concentration of pigments was calculated using the following relations and in terms of milligrams per gram of fresh weight of the plant (He et al., 2016). Soluble carbohydrates: The Fales (1951) method was used to measure soluble carbohydrates. 200 microliters of each sample were poured into a test tube and 5 ml of anthrone reagent was added to it. After mixing, it was placed in a 90°C water bath for 17 minutes to form a color, and after cooling, the absorbance of the samples was read at 625 nm. The concentration of each sample was calculated in

mg/g wet weight using a standard curve (Oklestkova et al., 2015).

Proline of roots and shoots: The Bates (1973) method was used to measure proline. 2 ml of the supernatant was mixed with 2 ml of ninhydrin reagent and 2 ml of pure acetic acid and placed in a hot water bath at 100°C for one hour. Then, the tubes containing the mixture were immediately cooled in an ice bath. The absorbance of the upper colored layer containing toluene and proline was determined at 520 nm, and the proline standard curve was used to calculate the proline content, and the results were calculated in milligrams per gram of wet weight (Gill et al., 2011).

Total phenolic compounds: The content of total phenolic compounds was determined using the method of Sonald and Laima (1999) (Faizan et al., 2011). Total flavonoids: Total flavonoids were measured by the aluminum chloride calorimetric method of Zhishen et al. (1999) (Kapoor et al., 2011). Determination of anthocyanin content: The Wagner (1979) method was used to measure the anthocyanin content of leaves (Tran et al., 2013). Total Protein content: The Bradford (1976) method was used to measure protein content. For this purpose, 0.1 ml of protein extract and 5 ml of Biuret reagent were added to test tubes and vortexed rapidly. After two minutes and before one hour, their absorbance was read with a spectrophotometer at a wavelength of 595 nm (Stolfa et al., 2015).

**Statistical Analysis**

The data obtained from the experiment were statistically analyzed in the form of a completely random design and in the form of a factorial experiment and 3 repetitions using SPSS IBM version 20 statistical software. The averages of growth parameters were compared using Duncan's multi-range test at the 5% level. The graphs of the mentioned parameters were drawn using Excel 2019 software. However, in this study, 3 independent factors were used in the form of 16 treatment codes with 4 repetitions to affect rapeseed plants of Hyola 401 variety. The raw data were entered into the statistical software after practical measurements. Data normalization and variance homogenization were performed. The coefficient of variation (CV) was checked according to the used experimental design.

**Results**

After normalizing the data and controlling the CV of obtained data, the overall average of the test error rate and the ANOVA table were calculated for all measured parameters; which is shown in Table 2. The analysis of variance table showed that 27 codes and treatment groups had a significant effect on the change of all measured parameters. It can also be said that the B1 and EP in the treatments had a significant effect on the improvement of the growth and biochemical parameters in plants under stress (Table 2).

The occurrence of Cd stress compared to the control led to a decrease in shoot length. In this way, Cd stress in the form of 250 µM of CdCl2 caused a 34% decrease in root length and a 45% decrease in shoot length compared to the control plants without Cd stress. According to Figure 3, in conditions without Cd stress, the application of both EP and B1 at a level of 5% had a significant effect on root length compared to the control. The results showed that in the conditions of applying Cd stress, the interaction of B1 and EP led to a significant increase in shoot and root length and growth more than the control (Figure 2, 3).


Figure 2: Effect of some experimental treatments containing thiamine and brassinolide on the visual and morphological growth of rapeseed plants of Hyola401 cultivar under cadmium stress. Treatment codes on each image are stated according to the treatment table in the Materials and Methods section. Cd; Cadmium, E; Epibrassinolide, B; Thiamine

Table2: Analysis of variance table of data obtained from measuring growth and biochemical parameters between treatment factors in this study at a significant level of 5% and with 3 replications and 27 treatments.

| parameter | Mean Square | df | F | Sig. | |
|---|---|---|---|---|---|
| chla | 2619.007 | 26 | 1010.731 | 42830.525 | .000 |
| chlb | 697.047 | 26 | 26.810 | 540.649 | .000 |
| chlT | 6051.953 | 26 | 232.767 | 5165.665 | .000 |
| cart | 599.917 | 26 | 23.074 | 10505.744 | .000 |
| Shoot FW | .663 | 26 | .026 | 8003.680 | .000 |
| Root FW | 215.01 | 26 | 8.426 | 4229.268 | .000 |
| Shoot DW | .663 | 26 | .0126 | 8003.680 | .000 |
| Root DW | 119.012 | 26 | 8.4226 | 4229.268 | .000 |
| phenols | 213.088 | 26 | 7.4202 | 5229.268 | .000 |

| parameter | Mean Square | df | F | Sig. | |
|---|---|---|---|---|---|
| Shoot lenght | 3619.007 | 26 | 5010.731 | 3230.525 | .004 |
| Root lenght | 697.047 | 26 | 216.810 | 540.649 | .000 |
| RWC | 6051.953 | 26 | 232.767 | 5165.665 | .000 |
| Ion leakage | 599.917 | 26 | 23.074 | 1575.744 | .0010 |
| Leaf proteins | .663 | 26 | .026 | 8003.680 | .000 |
| sugars | 315.01 | 26 | 8.426 | 4229.268 | .000 |
| Total proteins | .463 | 26 | .026 | 8403.680 | .000 |
| flavonoids | 4019.012 | 26 | 8.426 | 40229.268 | .000 |
| Anthocyanin | 17 9.062 | 26 | 8.426 | 5228.268 | .001 |
| proline | 119.012 | 26 | 8.426 | 4249.268 | .004 |

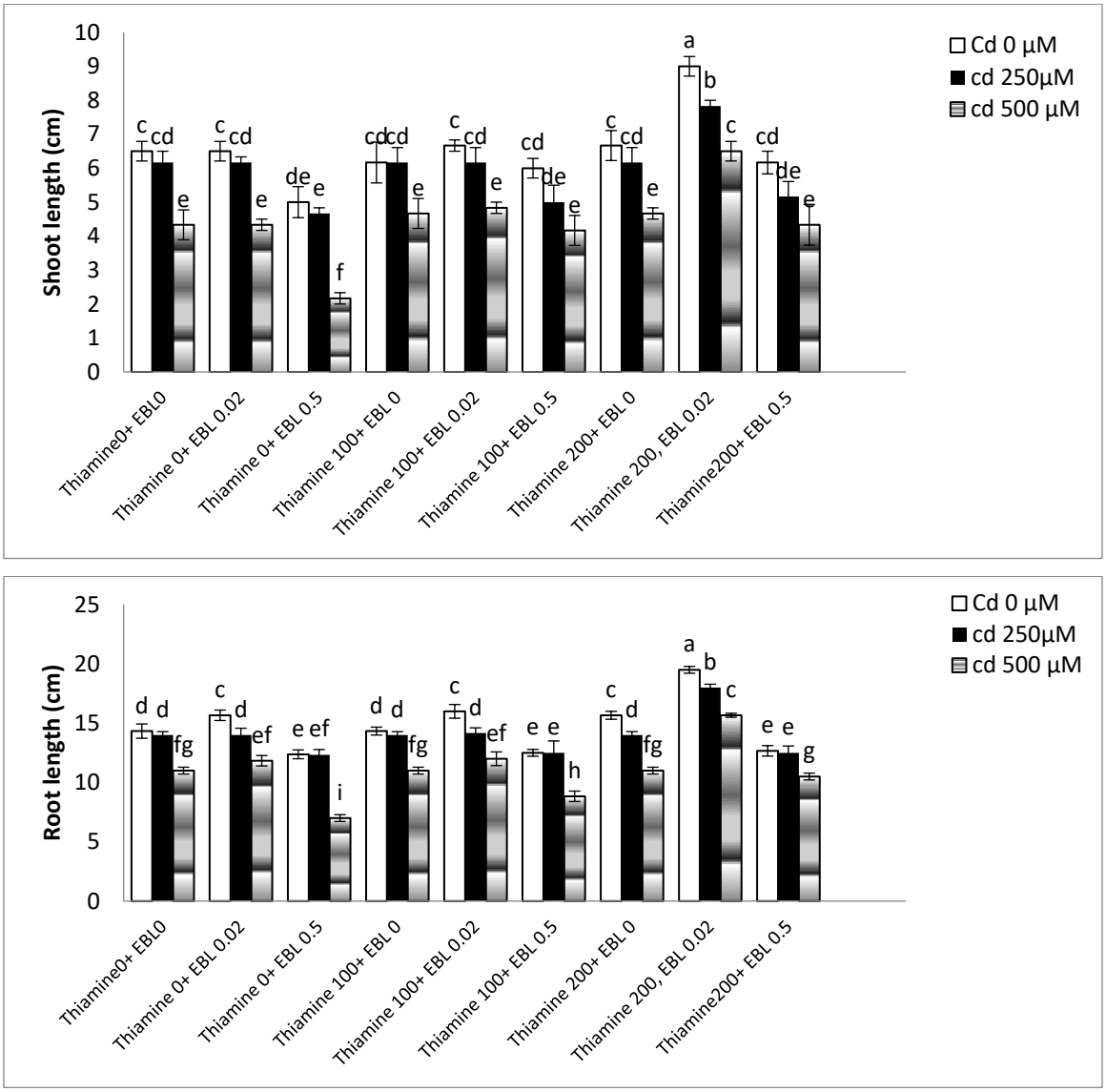


Fig. 3: Effect of different concentrations of cadmium, epibrassinolide and thiamine on the shoot and root length of rapeseed (n = 3). All means have at least one letter in common and are not statistically significantly different (I = SE, P ≤ 0.05).

The results of measuring shoot length in canola plants treated with cadmium are presented in Fig. 3. Cadmium stress caused a reduction in shoot length compared to control plants, which was only significant at a cadmium level of 500 µM with a 34% reduction. Application of 0.02 µM epibrassinolide and 200 µM thiamine to rapeseed plants under 250 and 500 µM cadmium levels increased shoot length by 27% and 50% compared to the corresponding stress levels, respectively (Fig. 3). Also, in the conditions of Cd stress, the application of B1 and EP improved the longitudinal growth of the shoot by 34% and the longitudinal growth of the root by 50% compare to what. Therefore, it can be said that the longitudinal growth of root and shoot under Cd stress conditions has given a better response to the combined treatment of B1 and EP. However, all the treatments containing B1 and EP had positive and improving effects in the conditions of Cd stress and dehydration.

The separate application of B1 and EP under Cd 250 stress conditions had a less significant effect on shoot length. For example, the use of B1 and EP led to a 13% improvement in shoot length growth, and the use of only B1 and EP led to a 20% improvement in the same parameter compared to stress conditions. The separate

application of B1 and EP together had a negative effect of 50% on the longitudinal shoot growth of rapeseed plants under stress, while the interaction of theses B1 and EP treatments with B1 and EP was very effective. The use of B1 and EP separately under Cd stress conditions led to a significant increase in root length by 27 and 29% compared to plants under stress. The separate use of B1 and EP in the aerial organs also improved the root length by 27% compared to the stress conditions. However, our results showed that the separate application of the three types of B1 and EP used in this research was more significant on the longitudinal growth of roots compared to aerial organs, but the mutual effect of these three types of B1 and EP was quite significant according to the interaction table, and especially the combined effect of B1 and EP had the greatest effect on improving the longitudinal growth of rapeseed plants under the influence of Cd stress (Figures 3).

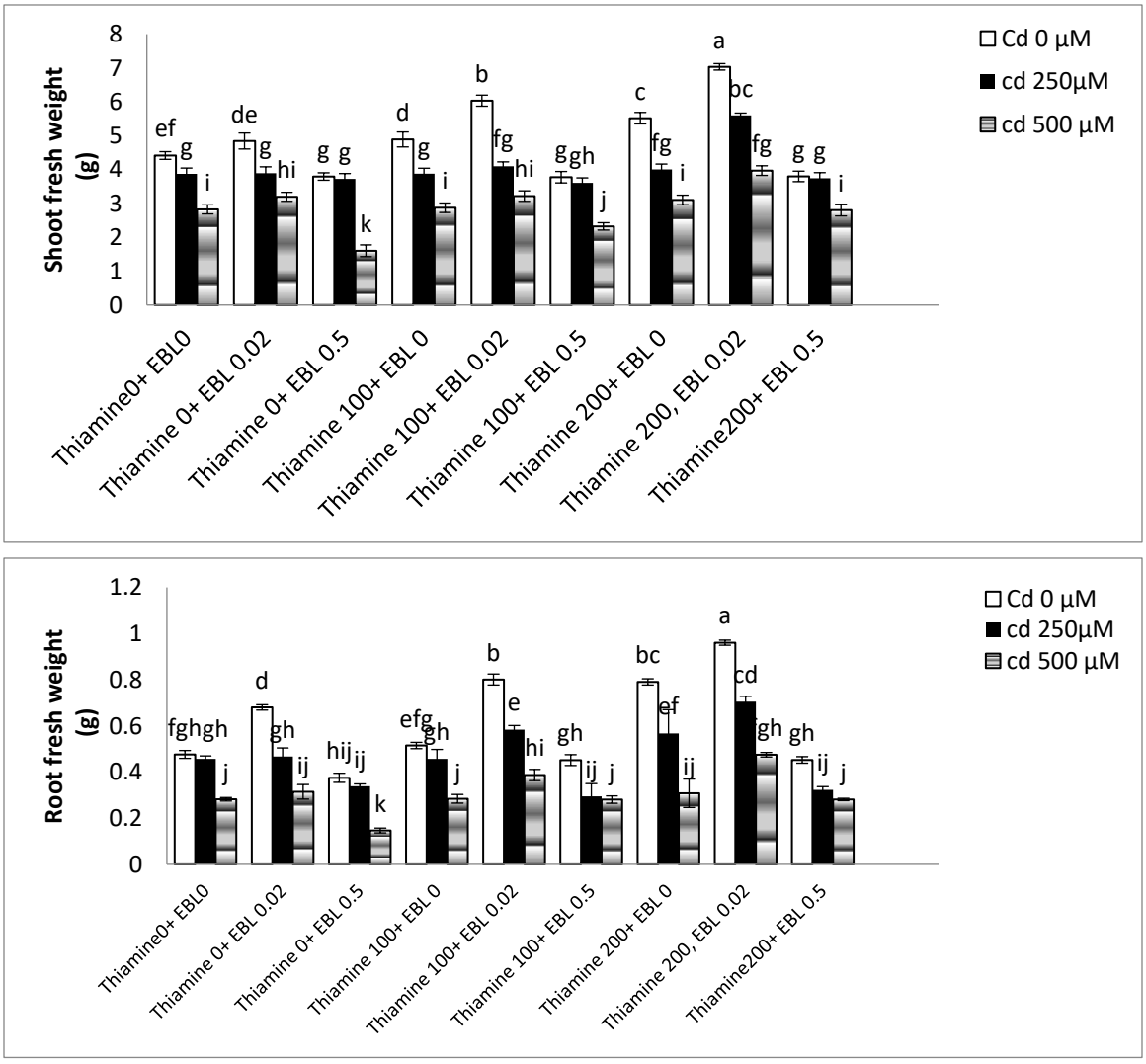


Fig. 4: Effect of different concentrations of cadmium, epibrassinolide and thiamine on shoot and root fresh weight of rapeseed shoots (n = 3). All means have at least one common letter and are not statistically significantly different (I = SE, P ≤ 0.05).

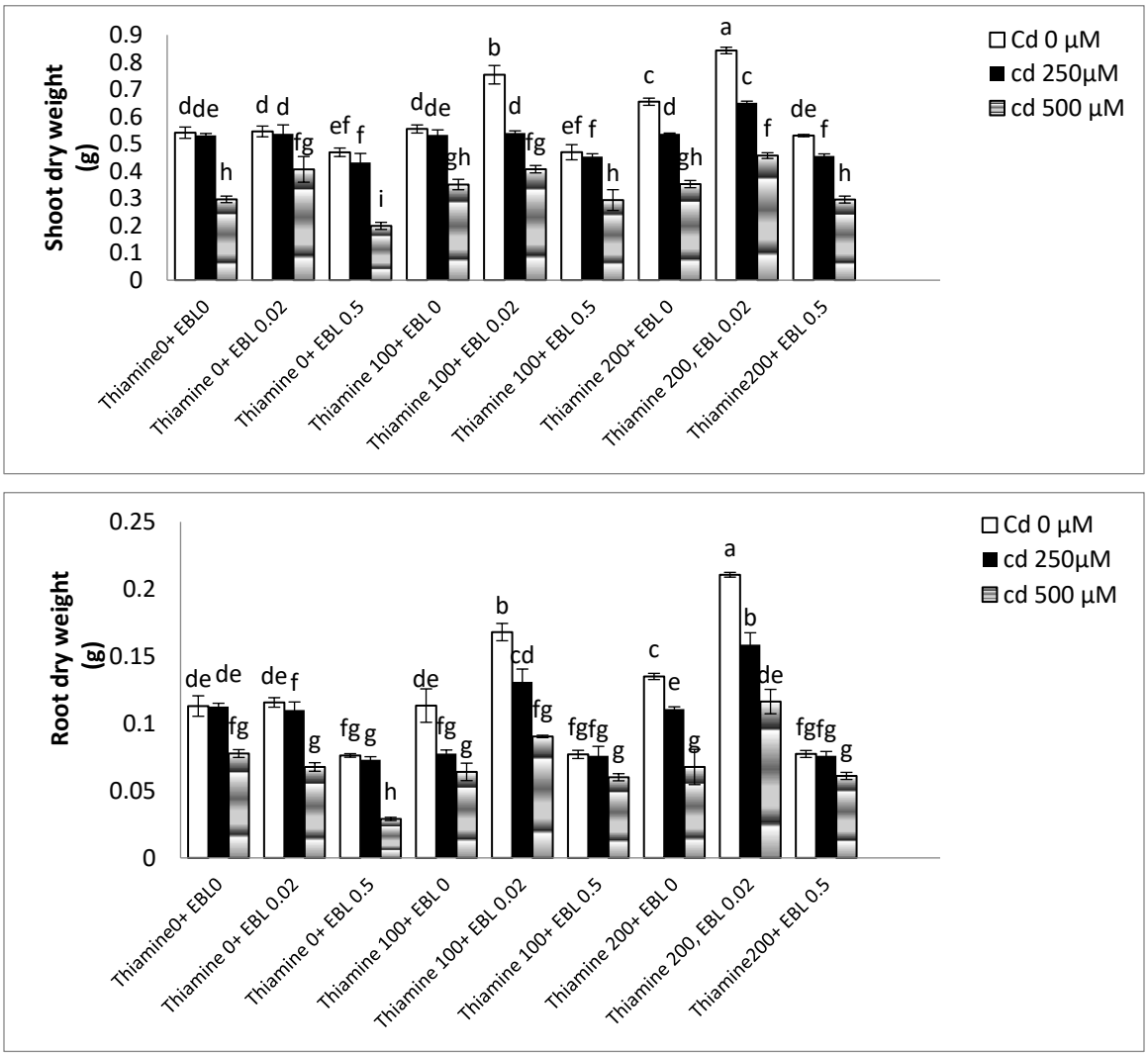


Fig. 5: Effect of different concentrations of cadmium, epibrassinolide and thiamine on shoot and root dry weight of rapeseed shoots (n = 3). All means have at least one common letter and are not statistically significantly different (I = SE, P ≤ 0.05).

Data from measuring the fresh weight of canola plants showed that 250 and 500 µM cadmium stress caused a 12% and 36% reduction in fresh weight of the shoots compared to the control. A significant increase in fresh weight of the shoots with a 44% increase was observed in plants treated with 200 µM thiamine and 0.02 µM epibrassinolide that received 250 µM cadmium stress compared to the stress alone (Fig 4). Cd stress alone without the use of B1 and EP caused a 36% decrease in shoot weight compared to the control. The use of B1 and EP in most cases caused an increase in weight. Only when both B1 and EP were used together, the fresh weight of aerial parts did not increase significantly compared to the control and only a 20% significant increase was observed. The combined use of both B1 and EP led to a significant improvement in shoot weight by 88% compared to plants under Cd stress (Fig 4). However, the separate or combined application of B1 and EP improved the root wet weight in dry conditions, but the effect was less than the shoot weight parameter, and the best effect was related to the 50% increase in root wet weight, which was obtained from the B1 and EP. It was used together with B1 and EP under 250 Cd stress conditions (Fig 4).

In general, the separate or combined application of B1 and EP improved the leaf area up to 92% of the control value or even more, and the increase in leaf area was related to the combined application of B1 and EP. For example, the combined application of 50 mg/L of each of B1 and EP caused the leaf area to be close to control plants under Cd stress conditions. This issue was also observed

for the combined application of B1 and EP (Fig. 4). The effect of the treatments had a significant and statistical effect on the change of dry weight (DW) of the plant. In this way, the stress of low water caused a 51% reduction in the dry weight of the stem of the plants under stress than the control plants, and the application of B1 and EP along with iron improved the dry weight of the lost stem and brought it to the level of the control plants) Figure 5). Cd stress led to a significant decrease in the dry weight of aerial parts in aerial parts of rapeseed plants by 51% compared to control plants (Fig. 5). While these decreases in root dry weight were about 24%. The combined or separate use of B1 and EP also led to an improvement in stem fresh weight, especially in aerial parts, compared to environmental stress conditions of dehydration in this research. The application of B1 and EP together, this B1 and EP led to an increase in the amount of dry weight in aerial organs compared to stress. The use of both B1 and EP separately and together with iron in the form of B1 and EP in both root and stem organs of stressed plants was significant at the level of 5% (Fig. 5). It can be said that the leaf surface data shows that in stress conditions, the use of B1 and EP improved the leaf surface better and more favorably than in stress-free conditions, so that in stress-free conditions, the application of B1 and EP significantly reduced the leaf area by 47% compared to the control. In the stress conditions, the amount of leaf surface increased and improved under the effect of treatments containing B1 and EP, which was previously stated (data not shown).

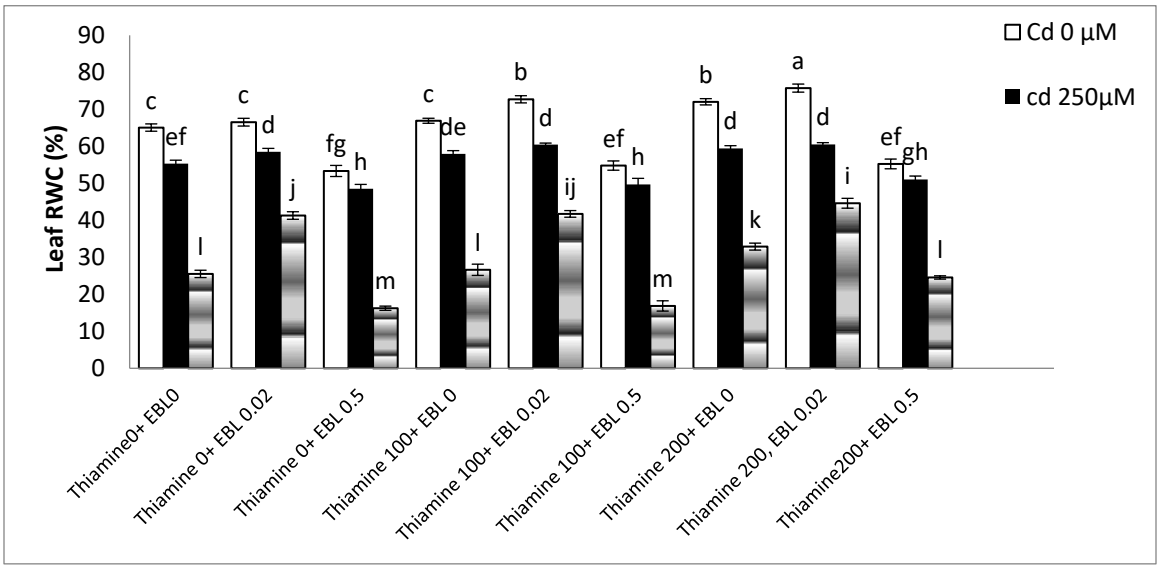


Fig. 6: Effect of different concentrations of cadmium, epibrassinolide and thiamine on the relative water content (RWC) of rapeseed leaves (n = 3). All means have at least one common letter and are not statistically significantly different (P ≤ 0.05I = SE).

Measurement of the relative water content of canola leaves showed that cadmium stress caused a significant decrease in relative leaf water content compared to control plants, the highest reduction being related to the 500 µM cadmium treatment with a 66% reduction. In plants stressed with 250 and 500 µM cadmium, simultaneous application of 200 µM thiamine and 0.02 µM epibrassinolide showed a significant increase in leaf relative water content by 10% and 75% compared to the stress levels alone. Similar changes were also obtained for the 100 µM thiamine and 0.02 µM epibrassinolide treatments (Fig 6). In the conditions of Cd stress in rapeseed plants, the application of B1 and EP increased the relative water content by 1.23 times compared to stressed plants. The greatest increase in relative water content is related to the combined use of both B1 and EP. But the combined use of B1 and EP significantly increased the relative water content by 78% compared to the second treatment code, which is the separate application of Cd stress (Fig. 6).

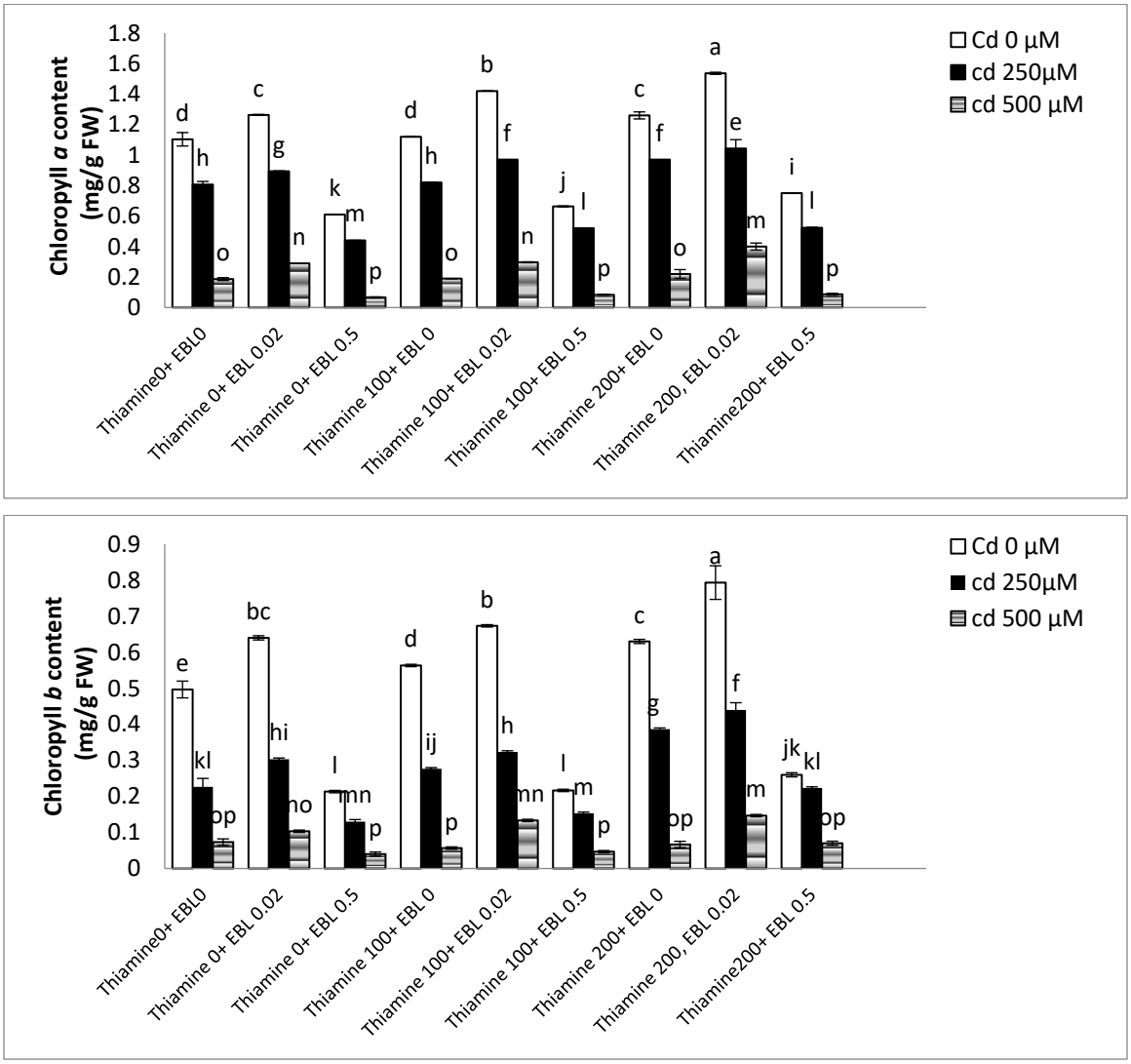


Fig. 7: Effect of different concentrations of cadmium, epibrassinolide and thiamine on the chla and chlb content in rapeseed leaves (n = 3). All means have at least one common letter and are not statistically significantly different (P ≤ 0.05I = SE).

As seen in the graphs, 250 and 500 micromolar cadmium stress caused a significant decrease in chlorophyll a content by 27% and 83% compared to the control. A significant increase in chlorophyll a content was observed under simultaneous treatment with 200 µM thiamine and 0.02 µM epibrassinolide in plants under 250 µM cadmium stress with a 29% increase compared to the application of cadmium alone. The analysis of variance table shows that the experimental treatments generally had a significant effect on the amount of chlorophyll a, and Cd stress alone reduced chlorophyll a in the leaves of rapeseed plants by 38%. The slope of the bars shows that the application of B1 and EP without the other B1 and EP improved and increased the amount of chlorophyll a in this treatment. Although the mutual effect of B1 and EP on the improvement of chlorophyll a under Cd was significant, but the increase of this main leaf pigment in separate treatments of B1 and EP in conditions containing a period of Cd stress in rapeseed plants was significant and impressive (Fig. 7). The results regarding chlorophyll b content also showed a significant decrease in the content of this pigment under both cadmium levels compared to the control. This decrease was especially observed under 500 µM stress with a decrease of 85%. The

10-day irrigation period in this research reduced the amount of chlorophyll b in the leaves of rapeseed plants by 38% compared to the control. The application of B1 and EP combined with B1 and EP significantly improved the content of chlorophyll b to 63% of the control value. The combined use of all B1 and EP levels significantly increased the amount of this type of chlorophyll compared to stress conditions (Fig. 7).

The highest amount of total chlorophyll in the leaves of the plants under 16 treatments used in this treatment was related to the B1 and EP alone, which significantly increased the amount of total chlorophyll compared to the control without stress. However, the application of both B1 and EP elicitors under stress conditions had the greatest effect on improving total leaf chlorophyll content compared to plants under cadmium stress, as cadmium stress caused a significant 34% decrease in total chlorophyll content compared to control canola plants without cadmium stress. However, the application of both B1 and EP elicitors under stress conditions had the greatest effect on improving total leaf chlorophyll content compared to plants under cadmium stress (Fig. 8). Considering that the amount of leaf carotenoids of rapeseed plants increased by 60% compared to the control under Cd stress conditions. But the use of B1 and EP in this leaf parameter was quite clear and obvious. The separate or combined effect of B1 and EP was decreasing and the amount of carotenoids returned to the control level. The greatest effect of reducing B1 and EP was related to the separate treatment of B1 and EP with a concentration of 50 mg/liter in the form of a 75% reduction in the amount of this auxiliary leaf pigment (Figure 8).

A decrease in leaf ion leakage was observed during the combined treatment of 200 µM thiamine and 0.02 µM epibrassinolide in control and stress conditions. The highest amount of ion leakage was observed in the treatment of 0.5 µM epibrassinolide and 500 µM cadmium with a 22% increase compared to the 500 µM stress. The above graph showed that cadmium stress significantly increased the release of ions and soluble salts in rapeseed plants compared to the control group. So that two concentrations of 250 and 500 µM cadmium significantly increased the ion leakage of leaves of treated plants compared to control plants. A decrease in leaf ion leakage was observed during the combined treatment of 200 µM thiamine and 0.02 µM epibrassinolide in control and stress conditions. The highest amount of ion leakage was observed in the treatment of 0.5 µM epibrassinolide and 500 µM cadmium with a 22% increase compared to the 500 µM stress (Fig 9). In the conditions of Cd stress without the application of B1 and EP, the percentage of ion leakage increased by 2.78 times than the control plants. The use of B1 and EP without the B1 and EP significantly reduced the amount of ion leakage in leaves under Cd stress. However, the results of this research on rapeseed showed that the use of B1 and EP decreased more than the separate use of ion leakage. In the treatment code 16 according to the treatment table, this contained all B1 and, the amount of ion leakage decreased by 4.58 times compared to the Cd stress conditions in rapeseed plants (Fig. 9). The numbers 0 and 50 under the horizontal axis of the graph represent the concentrations of 0 and 50 mg/L of each type of B1 and EP used.

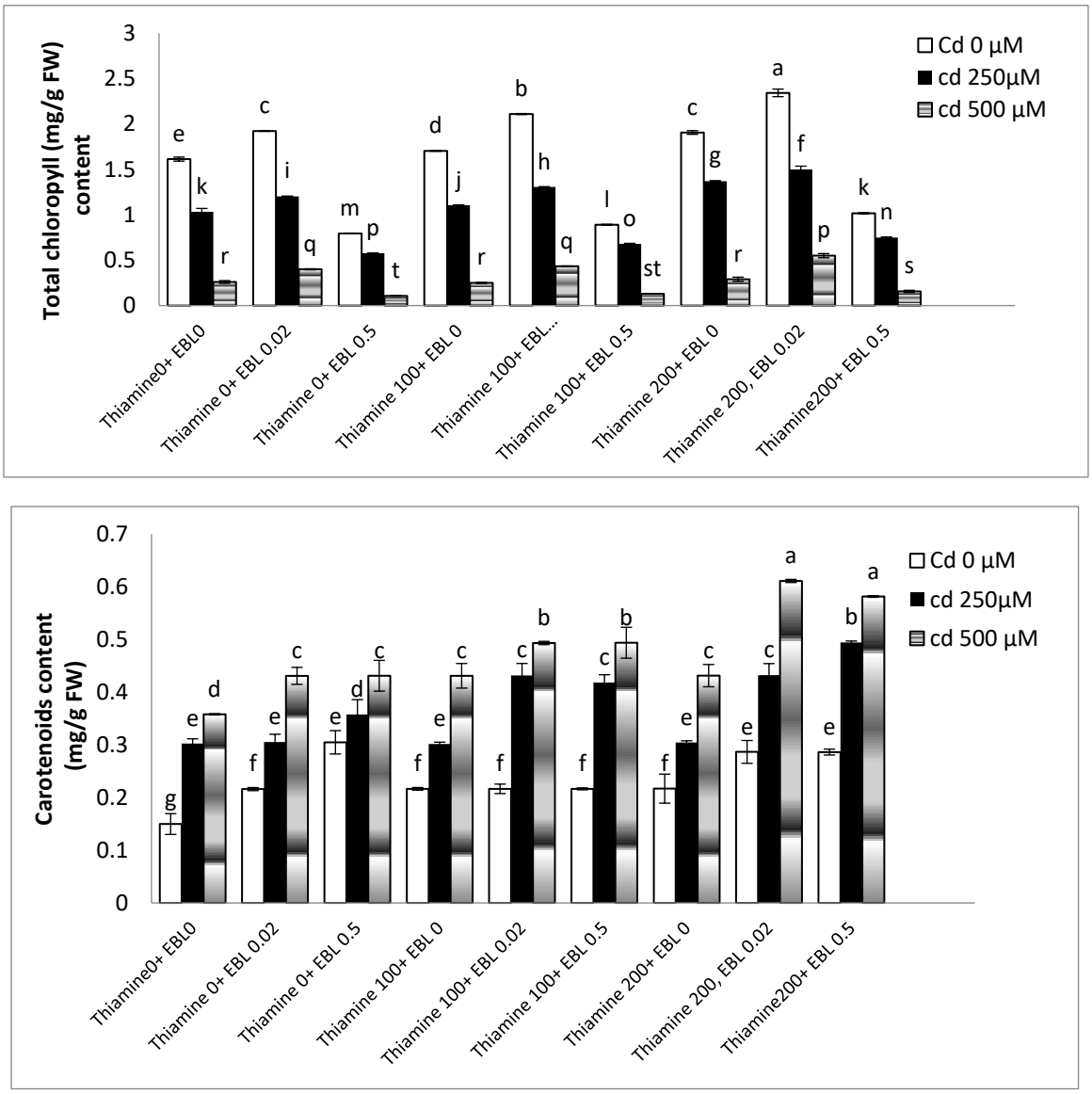


Fig. 8: Effect of different concentrations of cadmium, epibrassinolide and thiamine on the chlT and carotenoids content in rapeseed leaves (n = 3). All means have at least one common letter and are not statistically significantly different (P ≤ 0.05I = SE).

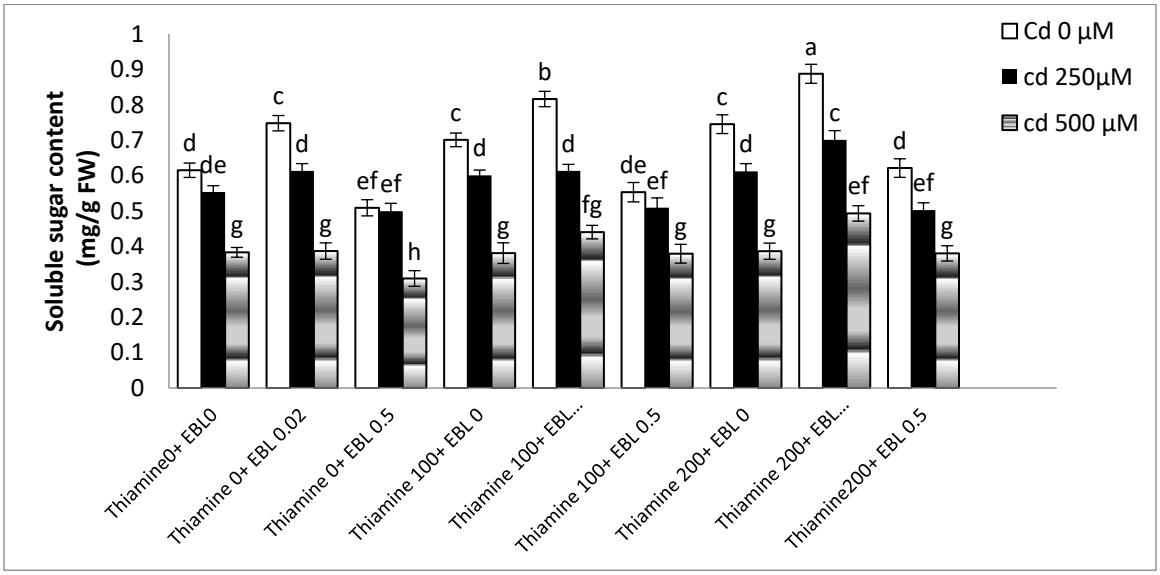

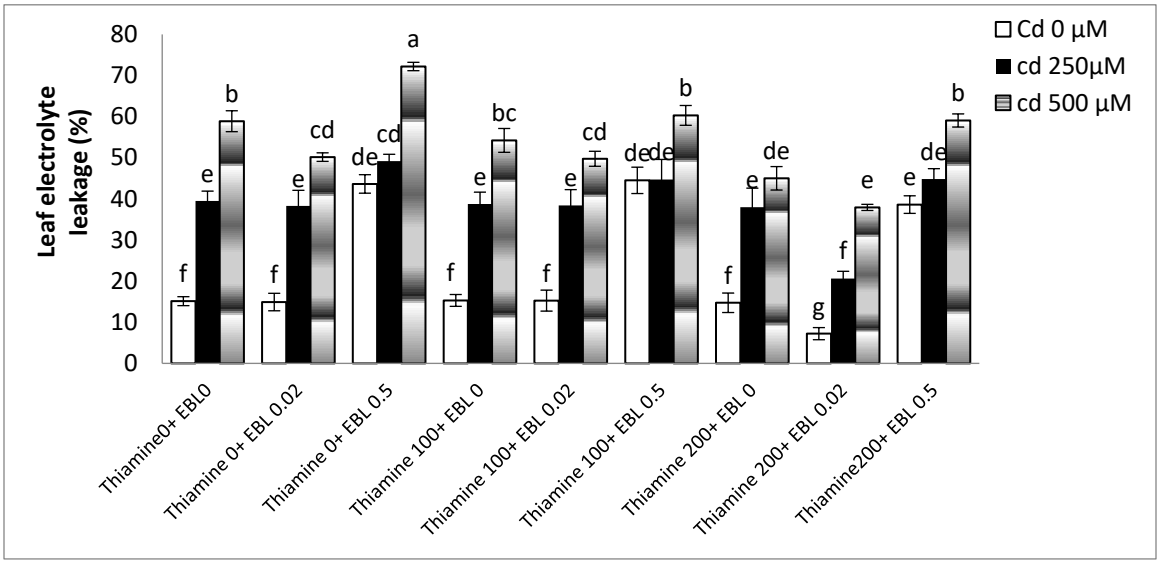


Fig. 9: Effect of different concentrations of cadmium, epibrassinolide and thiamine on the soluble sugar content and electrolyte leakage (%) in rapeseed leaves (n = 3). All means have at least one common letter and are not statistically significantly different (P ≤ 0.05I = SE).

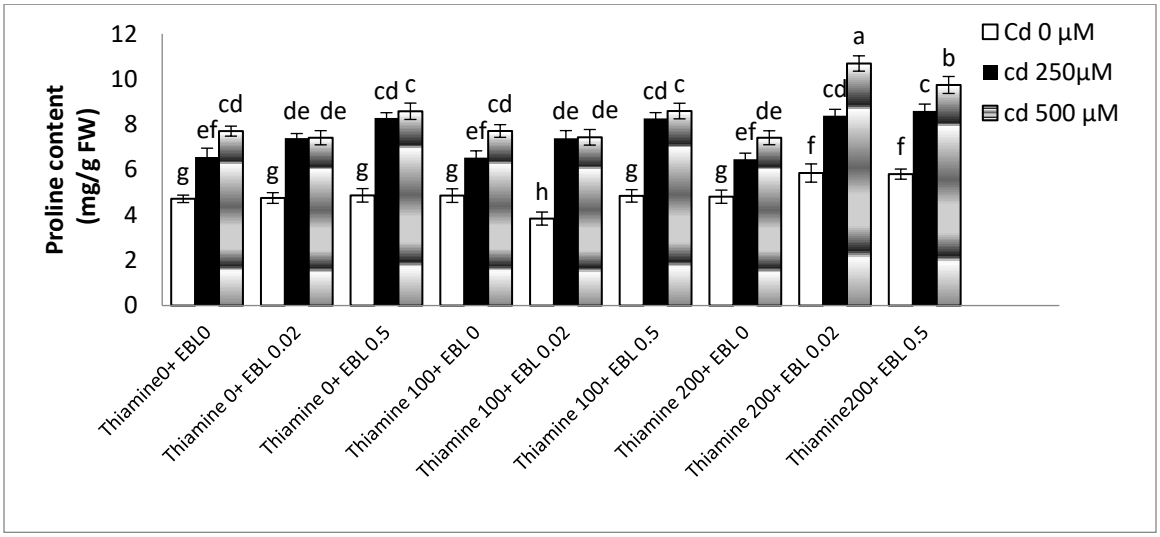


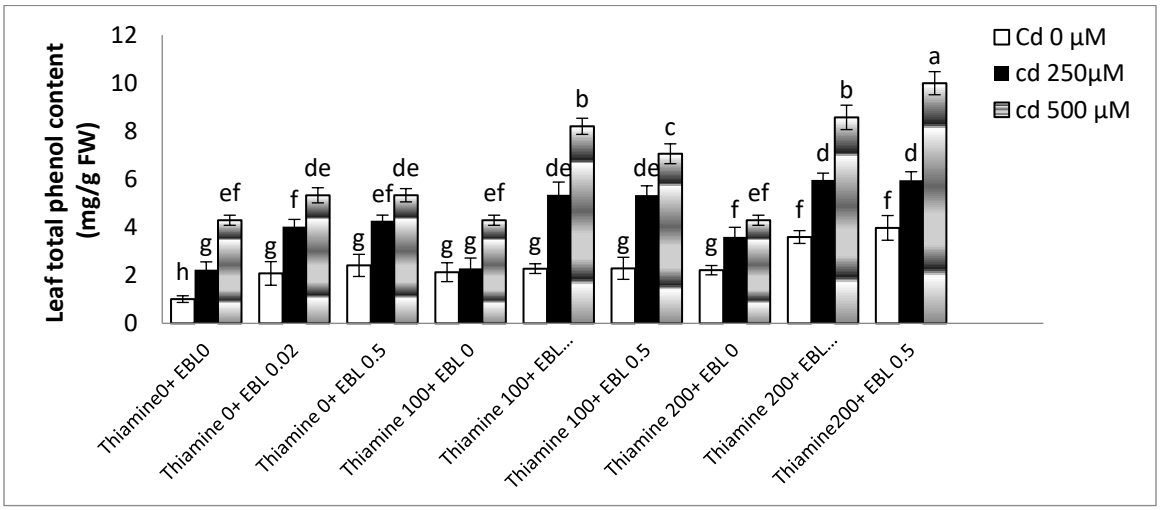

Fig. 10: Effect of different concentrations of cadmium, epibrassinolide and thiamine on the proline content and total phenol in rapeseed leaves (n = 3). All means have at least one common letter and are not statistically significantly different (P ≤ 0.05I = SE).

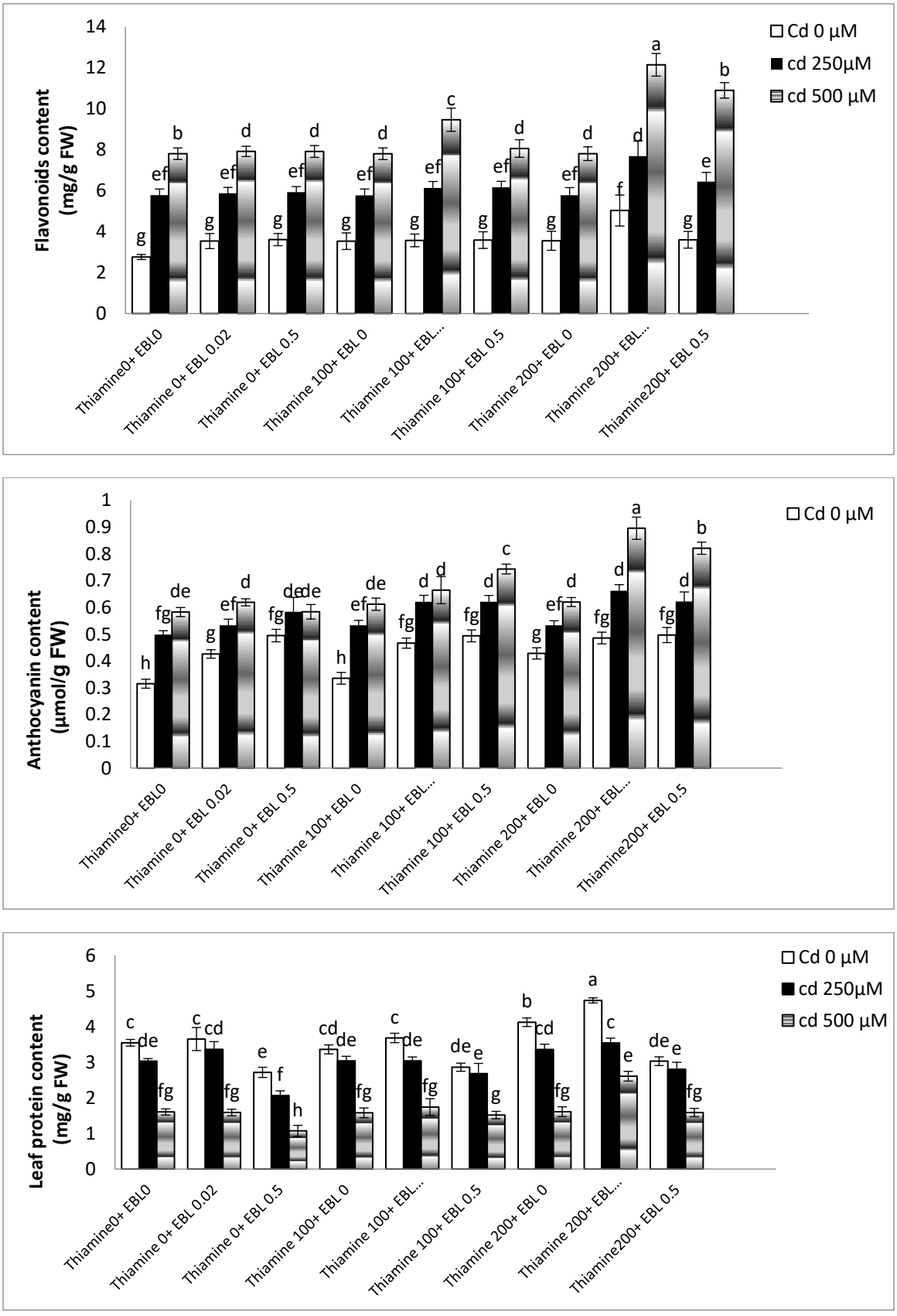

Fig. 11: Effect of different concentrations of cadmium, epibrassinolide and thiamine on the flavonoids, anthocyanin and total proteins content in rapeseed leaves (n = 3). All means have at least one common letter and are not statistically significantly different (P ≤ 0.05I = SE).

In other parameters such as the content of phenols, proline, flavonoids, anthocyanins, and total protein, the effect of using elicitors in reducing the effects of cadmium stress is also clearly seen (Figs 10 and 11).

**Discussion**

The general response of higher plants to heavy metal toxicity is growth inhibition and reduced biomass production. Inhibition of both cell elongation and division by heavy metals can lead to some reduction in plant biomass production. In higher plants, roots are the first organ in contact with toxic metal ions, and their growth and cell division are significantly impaired at high metal concentrations. Cadmium-induced growth inhibition has been reported in several species including wheat (Kaznina & Titov, 2014), licorice (Kartal et al., 2009), fava bean (Kohli et al., 2012), safflower (Gallego et al., 2012), and beans (Naz et al., 2013). In this study, a decrease in growth parameters (stem and root length, fresh and dry weight of stem and root) was observed under cadmium stress compared to control plants. This decrease was significant at high cadmium concentrations (Figures 3, 4, 5, 6, 7 and 8). Growth inhibition by cadmium could also be due to the effect of this metal on the rate of photosynthesis, destruction or inhibition of chlorophyll biosynthesis. Also, the reduction of root and shoot growth by cadmium may be partly due to irreversible inhibition of the proton pump, which is responsible for the process of cell elongation (Li et al., 2012; Wan et al., 2012). In addition, cadmium stress affects plant growth by interfering with metabolic processes such as water and nutrient uptake and photosynthesis (Kohli et al., 2017; Rezvani et al., 2012). Studies have shown that the ability of brassinosteroids to reduce the toxic effects of heavy metals is due to their effects on the electrical properties, permeability, structure, and stability of cell membranes (Gubrelay et al., 2013).

Therefore, the application of brassinosteroids enhances plant growth. Induction of cell proliferation by brassinosteroids is associated with proton efflux and hyperpolarization of the cell membrane, which significantly stimulates and accelerates cell growth (Gill et al., 2011). Brassinosteroids increase cell division by increasing the transcription levels of genes encoding the Cyclin-D3 protein. Cyclin-D3 is a regulatory protein in the cell cycle. External treatment of plants with brassinosteroids under stress conditions causes a wide range of responses in plant tissues (Olubunmi & Olorunsola, 2010). For example, brassinosteroids induce nucleic acid and protein synthesis, regulate gene expression, and increase photosynthesis. The collective effects of all these cellular events induce plant growth. Improvement of plant growth by application of brassinosteroids under heavy metal stress has been reported in various plants including: Arabidopsis thaliana (Korenkov et al., 2007), rice (Zhu, 2016), Indian mustard (Liu et al., 2015; Singh et al., 2016), sunflower (Kaznina & Titov, 2014) and tomato (Hacham et al., 2011; Dias et al., 2013). In addition, brassinosteroids treatment induced significant changes in cell wall carbohydrates including cellulose and hemicellulose biosynthesis, confirming the potential contribution of brassinosteroids to plant growth under stress conditions (Petrov & Van Breusegem, 2012). External application of thiamine has been reported to increase all growth parameters in plant species, indicating its role in maintaining plant growth (Duman & Ozturk, 2010; Dobrikova et al., 2014).

Plant roots are the main sites of metal uptake, and the concentration of metals in the roots is positively correlated with the amount of metal present in the environment. In most plants, after exposure to cadmium, it has been observed that the concentration of cadmium in the roots is higher than in the shoots (Kao, 2014; Takahashi et al., 2011). To prevent the uptake and accumulation of high concentrations of free heavy metal

ions, plants have developed multiple mechanisms to maintain and regulate cellular metal homeostasis (Szekeres & Bishop 2008; Janicka-Russak ee al., 2008). The higher accumulation of cadmium in roots than in shoots may be a defense strategy for the plant that protects the aerial parts of the plant from metal damage, which it does by sequestering a higher concentration of metal in the root vacuole (Domagalska et al., 2007; Jaleel et al., 2009).

Cd limitation in root tissue may be due to efficient binding and sequestration to the vacuole by glutathione and phytochelatin or by immobilization of cadmium by the cell wall and extracellular carbohydrates. It has been reported that cadmium accumulation in the roots and shoots of tomato seedlings increased with increasing cadmium concentration in the environment, so that in plants treated with a low dose of cadmium (3 mg/kg soil), cadmium accumulation in the roots was 3.8 times higher than in the shoots (Alia et al., 2015; Clouse & Sasse, 1998).

## Conclusion

According to the above reports, it can be concluded that the increase in growth parameters by epibrassinolide and thiamine treatments is attributed to their ability to regulate cell division and cell elongation activities in plants under cadmium stress. The highest growth parameters were obtained by simultaneous treatment of 0.02 µM EBL and 200 µM thiamine compared to control and stress conditions in rapeseed plants. Relative moisture content in leaves is a measure of plant water status, which reflects metabolic activity in plant tissues. The accumulation of heavy metals in the roots causes the transfer of water and dissolved substances from the roots to the aerial parts to stop, causing the aerial parts to suffer from drought stress. In the research conducted, based on the measurement and statistical comparison of various parameters, including growth and biochemical parameters, in rapeseed plants under different treatments containing thiamine, 24-epibrassinolide, and cadmium, it can be stated that the interaction effect of thiamine and epibrassinolide was observed compared to their separate effects on better growth and greater resistance of rapeseed to cadmium stress, and this interaction effect was significant. However, combined treatments of thiamine and epibrassinolide significantly increased and improved parameters such as longitudinal growth, fresh and dry weight, and relative leaf water content in rapeseed plants under cadmium stress levels. Regarding biochemical parameters, the interaction effect of thiamine and epibrassinolide on improving parameters of photosynthetic pigments, soluble sugars, and protein was well observed.

## Acknowledgments

This research is part of the Phd student thesis project (first author) in Department of Biology, Shahid Bahonar University of Kerman, Kerman, Iran. The authors of the MS are grateful to the university authorities for their support.

## References

Ahmad, P., Ozturk, M., Gucel, S., 2012. Oxidative damage and antioxidants induced by heavy metal stress in two cultivars of mustard (Brassica juncea L.) plants. *Fresenius Environmental Bulletin* 21, 2953-61.

Ali, B., Deng, X., Hu, X., Gill, R.A., Ali, S., Wang, S., Zhou, W., 2015. Deteriorative Effects of Cadmium Stress on Antioxidant System and Cellular Structure in Germinating Seeds of Brassica napus L. *Journal of Agricultural Science and Technology* 17(1), 63-74.

Alia, N., Sardar, K., Said, M., Salma, K., Sadia, A., Sadaf, S., Toqeer, A., Miklas, S., 2015. Toxicity and bioaccumulation of heavy metals in spinach (Spinacia oleracea) grown in a controlled environment. *International journal of environmental research and public health* 12(7), 7400-16.

Bajguz, A., Piotrowska-Niczyporuk, A., 2014. Interactive effect of brassinosteroids and cytokinins on growth, chlorophyll, monosaccharide and protein content in the green alga Chlorella vulgaris (Trebouxiophyceae). *Plant physiology and biochemistry* 80, 176-183.

Bajguz, A., Hayat, S., 2009. Effects of brassinosteroids on the plant responses to environmental stresses. *Plant Physiology and Biochemistry* 47(1), 1-8.

Clouse, S.D., Sasse, J.M., 1998. Brassinosteroids: essential regulators of plant growth and development. *Annual review of plant biology* 49(1), 427-451.

Dias, M.C., Monteiro, C., Pereira, J.M., Correia, C., 2013. Cadmium toxicity affects photosynthesis and plant growth at different levels. *Acta physiologiae plantarum* 35(4), 1281-89.

Dobrikova, A.G., Vladkova, R.S., Rashkov, G.D., Todinova, S.J. Krumova, S.B., Apostolova., E.L., 2014. Effects of exogenous 24-epibrassinolide on the photosynthetic membranes under non-stress conditions. *Plant physiology and biochemistry* 80, 75-82.

Domagalska M.A., Schomburg, F.M., Amasino, R.M., Vierstra, R.D., Nagy, F., Davis, S.J., 2007. Attenuation of brassinosteroid signaling enhances FLC expression and delays flowering. *Development* 134(15), 2841-50.

Duman, F. Ozturk, F., 2010. Nickel accumulation and its effect on biomass, protein content and antioxidative enzymes in roots and leaves of watercress (Nasturtium officinale). *Journal of Environmental Sciences* 22(4), 526-532.

Faizan, S., Kausar, S., Perveen, R., 2011. Varietal differences for cadmium-induced seedling mortality, foliar toxicity symptoms, plant growth, proline and nitrate reductase activity in chickpea (Cicer arietinum L.). *Biologic Medications* 3(2), 196-206.

Farid, M., Shakoor, M.B., Ehsan, S., Ali, S., 2013. Morphological, physiological and biochemical responses of different plant species to Cd stress. *International Journal of Chemical and Biochemical Sciences* 3(2013), 53-60.

Fariduddin, Q., Yusuf, M., Ahmad, I., Ahmad, A., 2014. Brassinosteroids and their role in response of plants to abiotic stresses. *Biologia Plantarum* 58(1), 9-17.

Gallego, S.M., Pena, L.B., Barcia, R.A., Azpilicueta, C.E., 2012. Unravelling cadmium toxicity and tolerance in plants: insight into regulatory mechanisms. *Environmental and Experimental Botany* 83, 33-46.

Gill, S.S. Tuteja, N., 2010. Reactive oxygen species and antioxidant machinery in abiotic stress tolerance in crop plants. *Plant physiology and biochemistry* 48(12), 909-930.

Gill, S.S., Tutej, N., 2011. Cadmium stress in crop plants by nutrients management: morphological, physiological and biochemical aspects. *Plant Stress* 5(1), 1-23.

Gubrelay, U., Agnihotri, R.K., Sharma, R.K., 2013. Effect of heavy metal Cd on some physiological and biochemical parameters of Barley (Hordeum vulgare L.). *International Journal of Agriculture and Crop Sciences* 5(22), 2743.

Hacham, Y., Holland, N., Butterfield, C., Ubeda-Tomas, S., 2011. Brassinosteroid perception in the epidermis controls root meristem size. *Development* 138(5), 839-848.

He, J., Wang, Y., Ding, H., Ge., C., 2016. Epibrassinolide confers zinc stress tolerance by regulating antioxidant enzyme responses, osmolytes, and hormonal balance in Solanum melongena seedlings. *Brazilian Journal of Botany* 39(1), 295-303.

Jaleel, C.A., Riadh, K., Gopi, R., Manivannan, P., Ines, J., Al-Juburi, H.J., Chang-Xing, Z., 2009. Antioxidant defense responses: physiological plasticity in higher plants under abiotic constraints. *Acta Physiologiae Plantarum* 31(3), 427-436.

Janicka-Russak, M., Kabała, K., Burzyński, M., Kłobus, G., 2008. Response of plasma membrane $H^+$-ATPase to heavy metal stress in Cucumis sativu s roots. *Journal of Experimental Botany* 59(13), 3721-28.

Kao, C.H., 2014. Cadmium Stress in Rice Plants. *Influence of Essential Elements* 11(3), 113-118.

Kapoor, D., Kaur, S., Bhardwaj, R., 2014. Physiological and biochemical changes in Brassica juncea plants under Cd-induced stress. *BioMed research international*10, 14-19.

Kartal, G., Temel, A., Arican, E., Gozukirmizi, N., 2009. Effects of brassinosteroids on barley root growth, antioxidant system and cell division. *Plant Growth Regulation* 58(3), 261-267.

Kaznina, N., Titov, A., 2014. The influence of cadmium on physiological processes and productivity of Poaceae plants. *Biology Bulletin Reviews* 4(4), 335-348.

Kohli, S.K., Handa, N., Sharma, A., Gautam, V., Arora, S., Bhardwaj, R., Alyemeni, M.N., Wijaya, L., 2017. Combined effect of 24-epibrassinolide and salicylic acid mitigates lead (Pb) toxicity by modulating various metabolites in Brassica juncea L. seedlings. *Protoplasma* 5, 1-14.

Korenkov, V., Hirschi, K., Crutchfield, J.D., Wagner, G.J., 2007. Enhancing tonoplast Cd/H antiport activity increases Cd, Zn, and Mn tolerance, and impacts root/shoot Cd partitioning in Nicotiana tabacum L. *Planta* 226(6), 1379-87.

Li, X., Zhao, M., Guo, L., Huang, L., 2012. Effect of cadmium on photosynthetic pigments, lipid peroxidation, antioxidants, and artemisinin in hydroponically grown Artemisia annua. *Journal of Environmental Sciences* 24(8), 1511-18.

Liu, S., Yang, R., Pan, Y., Ma, M., Pan, J., Zhao, Y., 2015. Nitric oxide contributes to minerals absorption, proton pumps and hormone equilibrium under cadmium excess in Trifolium repens L. plants. *Ecotoxicology and environmental safety* 119, 35-46.

Naz, A.A., Sardar Khan, S.K. Muhammad Qasim, M.Q., Salma Khalid., S.K., 2013. Metals toxicity and its bioaccumulation in purslane seedlings grown in controlled environment. *Natural Science* 5(5), 573-575.

Oklestkova, J., Rárová, L., Kvasnica, M., Strnad., M., 2015. Brassinosteroids: synthesis and biological activities. *Phytochemistry reviews* 14(6), 1053-72.

Olubunmi, F.E., Olorunsola, O.E., 2010. Evaluation of the status of heavy metal pollution of sediment of Agbabu bitumen deposit area, Nigeria. *European Journal of Scientific Research* 41(3), 373-382.

Petrov, V.D., Van Breusegem, F., 2012. Hydrogen peroxide: a central hub for information flow in plant cells. *AoB plants, Oxford Academic*.

Posmyk, M., Kontek, R., Janas, K., 2009. Antioxidant enzymes activity and phenolic compounds content in red cabbage seedlings exposed to copper stress. *Ecotoxicology and Environmental Safety* 72(2), 596-602.

Rezvani, M., Zaefarian, F., Miransari, M., Nematzadeh., G.A., 2012. Uptake and translocation of cadmium and nutrients by Aeluropus littoralis. *Archives of Agronomy and Soil Science* 58(12), 1413-25.

Singh, S. Prasad, S.M., 2017. Effects of 28-homobrassinoloid on key physiological attributes of Solanum lycopersicum seedlings under cadmium stress: Photosynthesis and nitrogen metabolism. *Plant Growth Regulation* 1(82), 161-173.

Singh, S. Prasad, S.M., 2014. Growth, photosynthesis and oxidative responses of Solanum melongena L. seedlings to cadmium stress: mechanism of toxicity amelioration by kinetin. *Scientia Horticulturae* 176, 1-10.

Singh, S., Parihar, P., Singh, R., Singh, V.P., 2016. Heavy metal tolerance in plants: role of transcriptomics, proteomics, metabolomics, and ionomics. *Frontiers in plant science* 6, 1143-45.

Stolfa, I., Pfeiffer, T.Z., Spoljaric, D., Teklic, T., Loncaric, Z., 2015.Heavy metal-induced oxidative stress in plants: response of the antioxidative system, in Reactive Oxygen Species and Oxidative Damage in Plants Under Stress, *Springer*, 127-163.

Szekeres, M. Bishop, G.J., 2008. Integration of brassinosteroid biosynthesis and signaling. *Annual Plant Reviews. Plant Hormone Signaling* 24, 67-68.

Takahashi, R., Y., Ishimaru, Y., Senoura, T., Shimo, H., Ishikawa, S., Arao, T., Nakanishi, H., 2011. The OsNRAMP1 iron transporter is involved in Cd accumulation in rice. *Journal of experimental botany* 62(14), 4843-50.

Tran, T.A. Popova, L.P., 2013. Functions and toxicity of cadmium in plants: recent advances and future prospects. *Turkish Journal of Botany* 37(1), 1-13.

Vardhini, B.V., Anjum, N.A., 2015. Brassinosteroids make plant life easier under abiotic stresses mainly by modulating major components of antioxidant defense system. *Frontiers in Environmental Science* 2, 67-72.

Wan, Y., Luo, S., Chen, J., Xiao, X., Chen, L., Zeng, G., Liu, C., He, Y., 2012. Effect of endophyte-infection on growth parameters and Cd-induced phytotoxicity of

Cd-hyperaccumulator Solanum nigrum L. *Chemosphere* 89(6), 743-750.

Yusuf, M., Khan, T.A., 2017. Brassinosteroids: Physiological Roles and its Signalling in Plants, in Stress Signaling in Plants: Genomics and Proteomics Perspective, 2nd. *Springer*, 241-260.

Zhang, F., Wan, X., Zheng, Y., Sun, L., Chen, Q., Zhu, X., Guo, Y.L., Liu, M., 2014. Effects of nitrogen on the activity of antioxidant enzymes and gene expression in leaves of Populus plants subjected to cadmium stress. *Journal of plant interactions* 9(1), 599-609.

Zhu, J.K., 2016. Abiotic stress signaling and responses in plants. *Cell* 167(2), 313-324.

University of Jiroft

**Biospecies Research**

Journal homepage: bsr.ujiroft.ac.ir

Iranian Biology Society

# Integrated weed management in rice: practical strategies for enhancing yield and production sustainability in Iranian paddy fields

Behrooz Khalil Tahmasebi[1*], Rahman Khakzad[2], Mohammad Roozkhosh[3]

https://doi.org/ 10.22034/bsr.2026.563581.1006

[1]*South of Kerman Agricultural and Natural Resources Research and Education Center, Agricultural Research, Education and Extension Organization (AREEO), Jiroft, Iran.*

[2]*Department of Agrotechnology, Faculty of Agriculture, University of Mohaghegh Ardabili, Iran*

[3]*Department of Agrotechnology, Faculty of Agriculture, Ferdowsi University of Mashhad, Mashhad, Iran.*

**ARTICLE INFO**

**Article Type**

Review Article

**Article History**

Received: 03 December 2025

Accepted: 30 January 2026

Published: 15 February 2026



***Corresponding author**

Bhroz.weedscience@gmail.com

**ABSTRACT**

Weeds are the most significant constraint on rice production in Iran, capable of causing yield losses of up to 90% under severe infestation. while herbicide application remains the predominant control method, its indiscriminate and repeated use has led to herbicide resistance in key species such as *Echinochloa crus-galli* and *Cyperus* spp. This practice has also resulted in surface water pollution, increased production costs, and environmental degradation. This article presents integrated weed management (IWM) as a sustainable, economical, and environmentally sound alternative for farmers. The IWM framework is built on five practical pillars: management of the soil seed bank through false seedbed preparation, deep plowing, and rice straw mulching; cultivation of competitive rice varieties with strong vigor and allopathic potential; increased planting density and optimized square planting patterns for rapid canopy closure; smart water management via alternate wetting and drying (AWD) irrigation to reduce water use by 20–30%; and implementation of a structured five-year herbicide rotation program incorporating varied modes of action to delay resistance evolution. The integrated application of these strategies reduces reliance on herbicides, increases yield, protects environmental health, improves farmer profitability, and ensures the long-term sustainability of rice production systems.

**Keywords**: Tillage, No-till farming, Competition, Integrated management, Transplanting

**How to cite this paper**

Khalil Tahmasebi, B., Khakzad, R., Roozkhosh, M., 2026. Integrated Weed Management in Rice: Practical Strategies for Enhancing Yield and Production Sustainability in Iranian Paddy Fields. *Biospecies Research*, 1, pp. 57-69.

## Introduction

Rice, a strategic crop and staple food for more than half of the world's population, plays a vital role in global food security. In Iran, rice holds significant economic and social importance, with an annual cultivation area exceeding 790,000 ha$^{-1}$ (Anynomus, 2023). However, the average rice yield in Iran (4.3 to 4.7 tons/ ha$^{-1}$) remains considerably lower than its potential yield (over 6 tons per hectare). Among the factors contributing to this gap, weeds are recognized as the primary limiting factor, accounting for a substantial portion of this disparity

(Kraehmer et al., 2016). Research indicates that weeds can reduce rice yields by 30 to 90%, and in some cases, may even lead to complete crop loss. Invasive species such as *Echinochloa crus-galli* (L.) P.Beauv. (barnyard grass) and Cyperus spp. (nutsedge), which are among the most problematic weeds in Iranian rice fields, cause significant damage not only through competition for resources (light, water, and nutrients) but also through the release of allelopathic compounds and by acting as hosts for pests and diseases (Chauhan et al., 2011). While chemical control using herbicides is a common weed management method, their indiscriminate use has led to serious consequences. These include the emergence of herbicide resistance in various weed species, shifts in weed population composition, increased production costs, contamination of surface water, and adverse effects on non-target organisms. Furthermore, changing climatic patterns and successive droughts have limited access to sufficient water resources for traditional weed control methods, such as continuous flooding (Khalil Tahmasebi et al., 2024). These challenges underscore the growing need to transition toward alternative and sustainable solutions. Among them, weeds pose the most threat as they are direct natural enemies to rice plants in the field. weeds pose the most threat as they are direct natural enemies to rice plants in the field. The herbicides are effective but their curious use is suggested due to their adverse effects on human health problems and the emergence of herbicide resistant weed strains (Kaur et al., 2024) . This article provides a comprehensive review and proposes practical integrated weed management strategies for Iranian rice fields. These strategies-encompassing seed bank management, competitive and allelopathic cultivars, optimized planting, water management, crop rotation, and rational herbicide use—aim to reduce chemical reliance. By protecting the environment, they support increased yields and sustainable farmer livelihoods. Within this framework, preventive management and farm hygiene are emphasized as the primary and most effective defense, focusing on stopping the introduction, establishment, and spread of weeds.

**A**). The use of healthy, certified seeds free from weed seeds is one of the most fundamental preventive methods, as contaminated seeds are a primary source for introducing new weed species into the field (Shahmoradi et al., 2023).

**B). Irrigation management** also plays a critical role; precise control of water inflow and outflow from the field, along with the installation of appropriate filters at water inlets, can effectively block the transport of weed seeds from adjacent areas (Bagheri et al., 2021).

**C). Thoroughly cleaning agricultural implements and machinery before entering a field**, especially when moving from infested areas, is essential to prevent the mechanical transmission of seeds.

**D). Managing field borders and irrigation canals is another crucial preventive focus**, as these areas can act as primary sources of infestation. Controlling weeds in these zones prevents seeds from entering the main field (Rahmani & Ghorbani, 2021).

E). **Management of plant residues and organic amendments** must be considered. Animal manures should be properly composted to avoid introducing weed seeds, and appropriate handling of crop residues helps prevent the augmentation of the weed seed bank (Mousavi et al., 2023). Understanding the concept of the soil weed seed bank – as a reservoir of viable weed seeds – is vital for appreciating the necessity of these preventive measures. This bank is formed through the accumulation of seeds from various species over time and is responsible for replenishing more than 90% of the annual weed population. A single weed plant can produce thousands of seeds capable of persisting for future years. the longevity of these seeds varies from two to over five years depending on the species and environmental conditions, highlighting the persistent, long-term challenge of weed control (Davis, 2023). Even a single period of inadequate control can, due to the persistence of seeds in this bank, lead to increased field infestation in the long term.

**Strategies for Depleting the Weed Seed Bank**

Various methods have been proposed to reduce the weed seed bank in soil:

A) **Preventing Seed Production:** Timely weed control before flowering to minimize seed set (Buhler et al., 1997).

B) **Anaerobic/Aerobic Tillage Rotation:** Alternating between flooded (anaerobic) and dry (aerobic) conditions, particularly effective for species dependent on aerobic conditions, such as weedy rice *Echinochloa crus-galli* (L.) P.Beauv. (Chauhan and Johnson, 2011).

C) **Occasional Deep Plowing:** Periodic deep tillage to bury seeds into deeper soil layers, thereby removing them from the germination zone (Mohler, 2011).

D) **Adoption of Reduced or No-Tillage Systems:** These systems offer a strategic advantage, as weed seeds remaining on the soil surface are exposed to depletion factors such as predation by soil organisms and decay induced by unfavorable environmental conditions (Westerman et al., 2003).

E) **Crop Rotation:** Implementing rotations with crops like wheat and canola, which establish under different germination and growth conditions compared to rice, can disrupt the life cycle of rice-associated weeds (Liebman and Dyck, 1993).

F) **Use of Mulch or Rice Straw:** Applying mulch or rice straw suppresses seed germination by limiting light penetration and moderating soil temperature fluctuations (Teasdale and Mohler, 2000).

G) **Physical Effects:** A layer of residue significantly delays and reduces weed emergence by preventing light from reaching the soil surface (essential for germination of many weed species), dampening diurnal temperature fluctuations, and creating a physical barrier that impedes seedling emergence.

H) **Chemical Effects (Allelopathy):** Plant residues may release specific chemical compounds (e.g., allelochemicals or microbial decomposition products) that can inhibit the germination and growth of weeds (Jabran, 2015).

I) **False Seedbed Technique:** This involves stimulating weed germination through light irrigation or rainfall before sowing the main crop. The emerged weed seedlings are then eliminated using non-selective herbicides (e.g., glyphosate) or shallow tillage (e.g., disking) before crop establishment. This method leads to a significant reduction in the weed seed bank and initial field infestation (Bond and Grundy, 2001).

## 1. The Role of Rice Cultivars in Weed Management: Competitive and Allelopathic Approaches

The selection of rice cultivars possessing desirable competitive and allelopathic traits has gained attention as a complementary strategy within integrated weed management systems. By reducing reliance on chemical herbicides, these cultivars offer the potential to realize more sustainable agricultural systems.

### Cultivars with Superior Competitive Traits

Studies indicate that rice cultivars characterized by strong seedling vigor, particularly in upland and direct-seeded systems, exhibit a highly competitive ability for suppressing weeds. Research has demonstrated a significant positive correlation between traits such as culm length and seedling vigor index with this competitive ability (Kanbar et al., 2006). The most critical of these traits include rapid canopy establishment, high tillering capacity, substantial initial biomass production, and the development of a high leaf area index.

### The Role of Allelopathy in Rice Cultivars for Weed Management

Rice, a vital global cereal crop, possesses a remarkable natural ability known as "allelopathy" for managing weeds (Khawar, 2017). This defense mechanism, which functions through the release of chemical compounds from intact roots, inhibits the growth of major weeds such as barnyard grass (*E. crus-*

*galli*). Compounds like phenolics and momilactones not only exert an effect on weeds (Kong et al., 2011) but also enhance the activity of beneficial soil microorganisms (Khawar, 2017). Research indicates that allelopathy contributes approximately 34% to the overall competitive ability of rice. This potential has been widely confirmed worldwide; for instance, studies in Australia, India, Korea, Iran, and Sri Lanka have identified cultivars capable of reducing weed growth by 50 to 90 percent (Table 1). In Iran, for example, studies demonstrated that the cultivars Dinorado, Domsiah, and Dalar exhibited the highest allelopathic potential, respectively (Modarres Sanavy et al., 2015). The concurrent optimization of this trait with other competitive characteristics is key to developing cultivars with superior weed-suppressing ability for sustainable agriculture (Ranagalage and Wattalagala, 2015; Sadat Asilan et al., 2013).

**Table 1.** Rice varieties or genotypes with reported allelopathic activity from different regions of the world.

| Allelopathic Rice Variety/Genotype | Target Weed Species | Country | Reference |
|---|---|---|---|
| STG06L-35-061 | *Echinochloa crus-galli* (L.) P.Beauv. | USA | Gealy et al. (2013b) |
| Tuna Bria, Hungary No. 1 | *Damasonium minus (R.Br.) Buchenau* | Australia | Seal and Pratley (2010) |
| Amaroo, Giza 176, Ratna, Takanishiki, Italpatna | *Echinochloa crus-galli (L.) P.Beauv.* | Australia | Seal and Pratley (2010) |
| PI312777, Hagan-1 | *E. crus-galli*, *Echinochloa colona* (L.) Link, *Cyperus difformis* L. | China | Kong et al. (2011) |
| Hagan-3 | *E. crus-galli*, *Echinochloa prostrate*, *Cyperus difformis* L. | China | Kong et al. (2011) |
| Jianliangyou 527, Ziyashui 417, Zhongzu 14, Ganxin 203, Zhongzhao 22 | *Lactuca sativa* L. | China | Ma et al. (2014) |
| PI312777 | *E. crus-galli* | China | Fang et al. (2015) |
| IAC165, Taichung Native 1 | *E. crus-galli* | China, Philippines | Bi et al. (2007) |
| Kouketsumochi | *E. crus-galli* | China | Guo et al. (2009) |
| Jangahnbyeo | Not Specified | Republic of Korea | Chung et al. (2006) |
| Donganbyeobongji, Daengbyeo | *E. crus-galli* | Republic of Korea | Chung et al. (2006) |
| Daechangjeong, Kasarwala, Mundara, Damagang, Daegado | *E. crus-galli* | Republic of Korea | Chung et al. (2006) |
| Nowindari, Baekna, Baekkwanguk | *Bulbostylis junciformis* (Kunth) C.B.Clarke Roxb., *Eleocharis kuroguwai* Ohwi, *Echinochloa crus-galli*, *Pontederia vaginalis* Burm.f.(Burm.f.) C. Presl | Republic of Korea | Chung et al. (2006) |
| Sathi, AC1423, PI312777 | *E. crus-galli*, *Monochoria vaginalis* (Burm.f.) C.Presl | Republic of Korea | Lee et al. (2005) |

| | | | |
|---|---|---|---|
| AC1423, Taichung Native 1, Tang Gan, Sathi | *E. crus-galli* | Republic of Korea | Lee et al. (2005) |
| Sathi | *E. crus-galli* | Republic of Korea | Junaedi et al. (2007) |
| Taichung Native 1 | *Echinochloa* spp., *Trianthema portulacastrum* L. | Republic of Korea, Taiwan | Kim et al. (2005) |
| Super Basmati | Wheat (*Triticum aestivum* L.), Berseem Clover (*Trifolium alexandrinum* L.), Oat (*Avena sativa* L.), Barley (*Hordeum vulgare* L.), Mung Bean, *Vigna radiata* (L.) R.Wilczek | Pakistan | Javaid et al. (2009) |
| BR17 | *Echinochloa* spp. | Bangladesh | Salam et al. (2009) |
| Karthik Shail | *Echinochloa* spp., *Lolium multiflorum* Lam., *Digitaria sanguinalis* (L.) Scop. | Bangladesh | Kato-Noguchi et al. (2011) |
| BR26, WITA3, WITA12, BRRI, Dular | *Spinacia oleracea* L. | Bangladesh | Kabir et al. (2010) |
| Goria, Birun, Karthiksail, Boteshwar | *Echinochloa* spp. | Bangladesh | Masum et al. (2016) |
| Ld356, Ld368, Ld365, Ld408 | *E. crus-galli* | Sri Lanka | Ranagalag and Wattagala (2015) |
| Bw400, Ld355, Ld368, Bw364 | *E. crus-galli* | Sri Lanka | Ranagalag and Wattagala (2015 |
| HKR126, IR64, Jaya, Haryana Basmati-1 | *Phalaris minor* Retz. | India | Junaedi et al. (2007) |
| Sorkheh, Anbarboo, Yousen, Dasht, Dular, Neda, Dinorado | *E. crus-galli* | Iran | Berendji et al. (2008) |
| Dinorado, Neda | *Sagittaria platyphylla* (Engelm.) J.G. Sm. | Iran | Berendji et al. (2011) |
| Giza179 | *E. crus-galli* | Egypt | El Shamey et al. (2015) |

## 2. The Role of Planting Density and Row Spacing in Weed Management of Rice

### 2–1. Importance of Planting Density:

Planting density serves as a strategic tool for weed management in rice fields. Increased plant density accelerates canopy closure, thereby reducing light availability for light-dependent weeds such as *E. crus-galli* (barnyard grass). Research indicates that enhancing planting density can suppress weed biomass by up to 59% while simultaneously increasing crop yield significantly (Chauhan et al., 2011). This approach is particularly effective in low-input and organic systems, which often face challenges with herbicide resistance. However, determining the optimal density that balances effective weed control with the prevention of intraspecific competition is essential for each specific cultivar and region. For high-yielding cultivars like "Hashemi" and "Gilaneh," a density of 30–35 plants per square meter is recommended. In contrast, for short-statured and high-tillering cultivars such as Sepidrood, a higher density of approximately 40–45 plants per square meter have demonstrated greater efficacy in suppressing weeds.

### 2-2. The Role of Planting Pattern

Linear or square planting patterns (with spacings of $20 \times 20$ cm or $25 \times 25$ cm), compared to scattered planting, lead to a more uniform distribution of plants and faster canopy closure. Furthermore, the critical period for weed control is shorter in narrower rows (15 cm) than in wider rows (30 cm), which facilitates weed management (Chauhan et al., 2011). Another study also indicated that weeds in 20 cm rows, compared to 30 cm rows, exhibit lower aerial biomass and seed production (Chauhan et al., 2011).

## 3. Effect of Planting Date on Weed Establishment

Planting time is one of the most critical factors determining the severity of weed infestation and the yield of rice.

### 3–1. Delayed Planting

Research in Guilan Province has demonstrated that delaying rice transplanting from mid-May to early June leads to a 40–60% reduction in the density of barnyardgrass (*E. crus-galli*). This is attributed to the fact that the seeds of this weed exhibit higher germination rates under the higher temperatures and longer days of June. Consequently, with delayed planting, the rice crop loses the opportunity for early growth and canopy development, which would otherwise suppress weeds. However, it is important to note that excessive delay (e.g., beyond June 10) may result in reduced rice yield due to a shorter growing season and increased damage from pests and diseases (Mahdavi-Damghani et al., 2020).

### 3–2. Early Planting

Early planting (early May) generally allows rice to pass through its sensitive growth stages without facing intense competition from weeds. A study conducted in Mazandaran Province indicated that planting rice on April 30 led to a 25% reduction in the density of purple nutsedge (*Cyperus rotundus*) and increased rice yield by 1.2 tons per hectare compared to planting on May 26 (Yousefi et al., 2021).

### 3–3. Regional Examples

In Guilan, the optimal planting window for the 'Hashemi' cultivar is typically reported to be between May 5 and May 20. In Mazandaran, earlier planting (early May) for cultivars such as 'Shiroodi' and 'Khazar' has yielded better results in reducing weed competition. Conversely, in Khuzestan (for summer rice cultivation), delayed planting has been associated with an increased density of barnyardgrass.

## 4. Water Management and Its Role in Weed Control

Water management serves as a key ecological tool for controlling weeds in Iran's paddy fields, which are predominantly cultivated under flooded conditions. Research indicates that maintaining a continuous flood depth of 5 to 7 cm can reduce the density of major weeds such as barnyardgrass (*Echinochloa crus-galli* (L.) P.Beauv. and purple nutsedge (*Cyperus rotundus* L.) by up to 75% and 62%, respectively (Abdollahi et al., 2023). However, due to water resource limitations, intermittent flooding systems, which achieve 20-30% water savings, are being adopted. It should be noted that if mismanaged, this alternative system can lead to an increase in weed density. The impact of water management varies among different weed species; for instance, barnyardgrass growth can be 2 to 3 times greater under intermittent flooding conditions, while semi-aquatic species like purple nutsedge can survive even under continuous flooding (Norouzi & Mirzakhani, 2022).

## 5. Crop Rotation and Cover Crops in Weed Management

### 5-1. Importance of Crop Rotation

Crop rotation is considered one of the most effective methods for the ecological management of weeds in rice paddy systems. By altering the cultivated crop, the germination patterns and growth cycles of weeds are disrupted, thereby reducing competitive pressure on the rice crop. In northern Iran, a rice-wheat rotation has been demonstrated to reduce the density of

barnyardgrass and purple nutsedge by 40-50% in the subsequent year (Chauhan et al., 2011). The primary reason for this reduction is the alteration of soil conditions and the alternation between flooded and dry periods, which are incompatible with the life cycles of these specific weeds. Overall, combining crop rotation with integrated nutrient management effectively reduced both weed density and biomass through various mechanisms inherent to the system. The incorporation of an offseason green manure crop, especially in conventional systems, proved effective for weed control. Furthermore, including sunhemp within organic fertilization regimes significantly lowered grass weed biomass, playing a key role in altering weed community composition (Wickramasinghe et al., 2023). In Iranian rice cultivation systems, crop rotation has been recognized as a classic and effective strategy for breaking the life cycle of rice-specific weeds (such as barnyardgrass and sprangletop). Research indicates that replacing rice with crops such as winter cereals (wheat and barley), forage plants (clover), or row crops (corn and soybean) within a rotation system significantly reduces weed density and diversity. This reduction is attributed to changes in soil moisture, planting timing, and ecological competition (Ranjbar et al., 2019).

### 5-2. Utilization of Cover Crops

In addition to preventing soil erosion, cover crops play a significant role in competing with weeds and reducing the weed seed bank. Common species include beans (*Phaseolus vulgaris* L.), clover (*Trifolium pratense* L.), and rye (*Secale cereale* L.). Soil coverage by these plants reduces light penetration, inhibits the germination of barnyardgrass and ryegrass seeds, and enhances the activity of soil microorganisms, which contribute to seed decay. Cover crops play a key role by covering the ground with a substantial amount of biomass. This suppresses weeds through competition and, upon termination, contributes to nutrient release for the subsequent crop (Didon et al., 2014). The use of cover crops, such as clover (Trifolium spp.), and common vetch (Vicia sativa L.) during fallow periods or between main rice cultivations is being increasingly adopted as an integrated weed management strategy in northern and some western regions of Iran. Field studies have confirmed that soil coverage with these plants suppresses weed germination and growth through competition for light, water, and nutrients, as well as through the release of allelochemicals (Karimi & Mousavi, 2020).

## 6. The Role of Chemical Management in Rice Weed Control

Herbicides are considered a key component within integrated weed management systems for rice. The rational and scientific use of these compounds, alongside other management practices, can provide effective control against weed populations. Selecting an appropriate herbicide should be based on the dominant weed species, the growth stage of the crop, climatic conditions, and the type of cropping system (Khakzad et al., 2016). Herbicide application must be accompanied by adherence to resistance management principles. Rotating herbicides with different modes of action and using herbicide mixtures can prevent the emergence and spread of resistant biotypes. Correct timing of herbicide application is also particularly crucial, as application during the early growth stages of weeds is generally more effective. The development of selective herbicides with suitable spectra of control and reduced environmental impact is among the recent research achievements in this field. The use of new formulations with higher efficacy and lower active ingredient usage can be more economical while simultaneously reducing the environmental pollution load. Furthermore, the adoption of precise herbicide application methods utilizing modern technologies can prevent the unnecessary dispersion of these compounds.

Table 2. List of Recommended Herbicides and Their Weed Control Spectrum for Rice Fields in Iran (Zand et al., 2019)

| Common Name | Trade Name | Site of Action | Formulation | Application Rate per Hectare | Application Timing and Weed Control Spectrum |
|---|---|---|---|---|---|
| Oxadiazon | Ronstar | PPO Inhibitor | 12% SL | 4-3.5 L | Pre-emergence, before 2-leaf stage of barnyardgrass (*Echinochloa crus-galli*), smartweed (*Persicaria* spp.), arrowhead (*Sagittaria* spp.), water plantain (*Alisma* spp.), and annual sedge (*Cyperus* spp.). |
| Molinate | Ordram | Fatty Acid Inhibitor | 72% EC | 5-6 L | 5 to 12 days after transplanting; controls barnyardgrass. |
| Bentazone* | Basagran | PSII Inhibitor | 48% SL | 3-5 L | 3 to 5 weeks after transplanting; controls arrowhead, water plantain, duckweed (*Lemna minor* L.), false pimpernel (*Lindernia* spp.), ammania (*Ammania* spp.), toothcup (*Rotala* spp.), hygrophila (*Hygrophila* spp.), false foxglove (*Adenosma* spp.), common rush (*Juncus bufonius* L.), goosegrass (*Eleusine indica (L.) Gaertn* ., small-flowered nutsedge, annual sedge, and water clover (*Marsilea* spp.). |
| Thiobencarb | Saturn | Fatty Acid Inhibitor | 50% EC | 5-6 L | Before 2-leaf stage of barnyardgrass (barnyardgrass, common rush, goosegrass). |
| Bispyribac-sodium* | Nominee | ALS Inhibitor | 10% SC | 250 mL | 2 to 5-leaf stage of weeds: barnyardgrass, arrowhead, water plantain, Ludwigia spp., false pimpernel, ammania, toothcup, false foxglove, barnyardgrass, small-flowered nutsedge, annual sedge, perennial sedge, sprangletop (*Leptochloa* spp.), and purple nutsedge. |
| Bispyribac-sodium* | Clean Weed | ALS Inhibitor | 40% SC | 250 mL | 2 to 5-leaf stage of weeds: barnyardgrass, arrowhead, water plantain, Ludwigia spp., false pimpernel, ammania, toothcup, false foxgun, barnyardgrass, small-flowered nutsedge, annual sedge, perennial sedge, sprangletop, and purple nutsedge. |
| Bensulfuron-methyl* | Londax | ALS Inhibitor | 60% DF | 50-75 g | 7 to 12 days after transplanting; controls arrowhead, monochoria (*Monochoria* spp.), water plantain, Ludwigia spp., duckweed, false pimpernel, ammania, toothcup, rotala, hygrophila, false foxglove, common rush, goosegrass, small-flowered nutsedge, perennial sedge, alkali weed (*Aloecuris* spp.), sprangletop, purple nutsedge, water clover, salvinia (*Salvinia* spp.), and azolla (*Azolla* spp.). |
| Cyhalofop-butyl** | Stet | ALS Inhibitor | 20% WG | 100-150 g | 7 to 12 days after transplanting; controls arrowhead, monochoria, water plantain, Ludwigia spp., duckweed, false pimpernel, ammania, toothcup, rotala, hygrophila, and false foxglove. |
| Pretilachlor* | Rifit | Fatty Acid Inhibitor | 50% EC | 2 L | 5 to 7 days after transplanting; barnyardgrass at 2-leaf stage, arrowhead, water plantain, common rush, goosegrass, small-flowered nutsedge, and annual sedge. |

| | | | | | |
|---|---|---|---|---|---|
| Anilofos + Ethoxysulfuron** | Sun Rice Plus | Cell Division Inhibitor + ALS Inhibitor | 31.5% SC | 3 L | 4 to 7 days after transplanting; controls arrowhead, duckweed, false pimpernel, ammania, toothcup, rotala, hygrophila, and false foxglove. |
| 2,4-D + MCPA | U46 Kombi-fluid | Synthetic Auxin | 72% SL | 1.5 L | Late tillering to first node stage; controls arrowhead, monochoria, water plantain, Ludwigia spp., duckweed, false pimpernel, ammania, toothcup, rotala, hygrophila, and false foxglove. |
| Oxadiargyl** | Topstar | PPO Inhibitor | 80% WG / 30% EC | 125-150 g / 3-3.5 L | Pre-emergence up to 7 days after transplanting; controls arrowhead, barnyardgrass, and annual sedge. |
| Penoxsulam | Rizal | ALS Inhibitor | 40% SC | 150 mL | 3 to 7 days after transplanting; controls arrowhead, water plantain, Ludwigia spp., false pimpernel, ammania, toothcup, false foxglove, barnyardgrass, small-flowered nutsedge, annual sedge, perennial sedge, sprangletop, purple nutsedge, water clover, salvinia, and azolla. |
| Ethoxysulfuron + Triafamone* | Council | ALS Inhibitor | 30.6% WG | 100-150 g | Before 2-leaf stage of weeds: arrowhead, water plantain, Ludwigia spp., false pimpernel, ammania, toothcup, false foxglove, barnyardgrass, common rush, small-flowered nutsedge, annual sedge, perennial sedge, sprangletop, purple nutsedge, water clover, salvinia, and azolla. |
| Flucetosulfuron* | Ziclor | ALS Inhibitor | 10% WG | 300 g | Before 2-leaf stage of weeds: barnyardgrass, arrowhead, water plantain, Ludwigia spp., false pimpernel, ammania, toothcup, false foxglove, barnyardgrass, small-flowered nutsedge, annual sedge, perennial sedge, sprangletop, purple nutsedge, water clover, salvinia, and azolla. |

* Demonstrates better efficacy in simultaneously controlling all three major weed groups (grasses, sedges, broadleaves). ** Obsolete internationally.

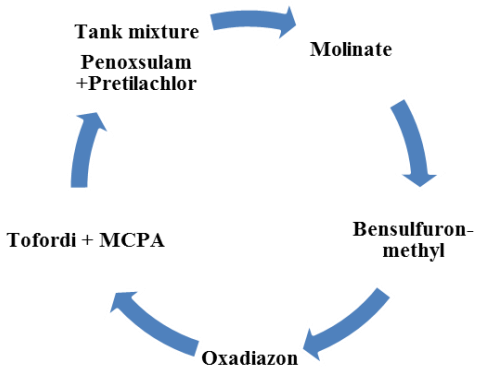


Figure 1. **A multi-faceted, cyclical framework for managing and delaying herbicide resistance in weeds in rice crops.** This model emphasizes the strategic application of herbicides (chemical control) as its foundation, with the primary aim of reducing selection pressure for resistance.

## 7. Integrated Management

In conclusion, integrating herbicides with other management methods -such as competitive cultivars, cultural practices, and biological control-can greatly support the development of sustainable rice production systems. This integrated weed management strategy provides effective control while simultaneously reducing herbicide reliance and minimizing environmental impact (Table 3).

Table 3. Management and damage reduction strategies for weeds in rice cultivation

| Strategy Category | Specific Method | Mechanism of Action | Considerations & Applications |
|---|---|---|---|
| Reducing the Seed Bank | Enhancing Seed Predation by Soil Organisms | Increases seed mortality of weeds through consumption by insects, earthworms, rodents, and birds. | Avoid burning crop residues and field borders; pile residues to create shelter and food for predators; use cover crops in rotation. |
| | False Seedbed Technique | Stimulates weed seed germination with light irrigation, followed by their destruction before sowing the main crop. | Use of non-selective herbicides (e.g., glyphosate) or shallow tillage; highly effective for photoblastic species like crabgrass and goosefoot; requires sufficient time interval between cultivation cycles. |
| Tillage and Residue Management | No-Till/Reduced-Till System | Maintains a greater proportion of weed seeds on the soil surface, exposing them to mortality factors (predation, decay). | Results in slower germination and weaker growth of weeds; suitable for species like ryegrass; requires effective residue management. |
| | Deep Moldboard Plowing | Buries a large volume of the weed seed bank at depths greater than 10 cm (exceeding emergence depth). | An emergency strategy when the surface seed bank is highly enriched; studies indicate performing this once every 5 years can control problems with weeds like green foxtail. |
| | Use of Plant Residue Mulch (Straw) | Physically and chemically suppresses weed seed germination and growth. | Creates a physical barrier, prevents light penetration, reduces fluctuations in temperature and moisture, and releases allelopathic compounds; requires specific seeders (e.g., turbo) for planting under heavy residue conditions. |
| Use of Competitive Varieties | Varieties with Superior Morphological Traits | Competes for light, water, and nutrients through rapid canopy closure and shading. | Varieties with strong seedling vigor, rapid early growth, high tillering capacity, high Leaf Area Index (LAI), and droopy leaves; highly effective in dryland and direct-seeded systems. |
| | Allelopathic Varieties | Release inhibitory chemical compounds from roots that suppress the germination and growth of adjacent weeds. | Can contribute up to 34% to the overall competitive ability of rice; still primarily in the research phase and requires further development for practical application. |
| | Varieties Tolerant to Anaerobic/Waterlogged Conditions | Enables the creation of waterlogged conditions to suppress non-tolerant weeds. | Allows for flooding immediately after planting in direct-seeded systems; currently, limited varieties are available (under research at IRRI). |
| Planting Management | Increasing Seeding Rate | Enhances crop competitiveness by establishing a denser plant population and promoting faster canopy closure. | Reduces space and resources available for weeds; studies show increasing the seeding rate from 25 to 100 kg/ha reduced weed biomass by 47-59%. |
| | Reducing Row Spacing | Promotes faster closure of inter-row spaces, reducing light penetration to the soil surface. | Shortens the critical period for weed control; studies indicate 20 cm row spacing resulted in lower weed incidence compared to 30 cm spacing. |

**conclusion**

In conclusion, achieving sustainable and productive rice cultivation in Iranian paddy fields necessitates a paradigm shift from over-reliance on herbicides to a sophisticated, multi-component Integrated Weed Management (IWM) strategy. This holistic approach synergistically combines preventive sanitation, strategic seed bank depletion through tillage and false seedbeds, the deployment of competitive and allelopathic cultivars, optimized planting density and geometry, smart water management via Alternate Wetting and Drying, and structured crop rotations. When underpinned by a disciplined, science-based herbicide rotation program, this integrated framework effectively suppresses weed populations, delays resistance evolution, enhances yield potential, conserves vital water resources, and safeguards environmental and economic sustainability for future generations.

**Refference**

Abdollahi, M., Rezvani Moghaddam, P., Soleimani, R. 2023. Evaluation of the effect of different paddy irrigation regimes on weed growth and density (Case study: Gilan Province). *Iranian Journal of Weed Research*, 15(3), 27-45.

Anynomus, 2023. Volume 1: Crop Products. Ministry of Jihad-e-Agriculture, Deputy of Planning and Economics. *Information and Communication Technology Center*. Tehran, Iran. 126 pp.

Bagheri, R., Nasiri Mahalati, M., & Koocheki, A. 2021. Weed seed dispersal through irrigation water: A review. *Journal of Applied Research in Water and Wastewater,* 8(1), 45-52.

Berendji, S., Asghari, J. B., & Matin, A. A. (2008). Allelopathic potential of rice (*Oryza sativa*) varieties on seedling growth of barnyardgrass (Echinochloa crus-galli). *Journal of Plant Interactions, 3*, 175–180.

Berenji, S., Asghari, J., Matin, A. A., & Samizadeh, H. (2011). Screening for Iranian rice allelopathic varieties by HPLC and bioassays. *Allelopathy Journal, 27*.

Bi, H. H., Zeng, R. S., Su, L. M., An, M., & Luo, S. M. (2007). Rice allelopathy induced by methyl jasmonate and methyl salicylate. *Journal of Chemical Ecology, 33*, 1089–1103.

Bond, W., Grundy, A. C. 2001. Non-chemical weed management in organic farming systems. *Weed Research,* 41(5), 383–405

Buhler, D. D., Hartzler, R. G., & Forcella, F. (1997). Implications of weed seedbank dynamics to weed management. *Weed Science*, 45(3), 329–336.

Chauhan, B.S., Singh, V.P., Kumar, A., Johnson, D.E. 2011. Relations of rice seeding rates to crop and weed growth in aerobic rice. *Field Crops Research*, 121(1): 105–115.

Chung, I. M., Kim, J. T., & Kim, S.-H. 2006. Evaluation of allelopathic potential and quantification of momilactone A, B from rice hull extracts and assessment of inhibitory bioactivity on paddy field weeds. *Journal of Agricultural and Food Chemistry*, 54, 2527–2536.

Davis, A. S. (2023). Weed seed persistence and management in agroecosystems. *Weed Science, 71*(3), 245-254.

Didon, U.M., Kolseth, A.K., Widmark, D. and Persson, P., 2014. Cover crop residues—effects on germination and early growth of annual weeds. *Weed science*, *62*(2), pp.294-302.

El Shamey, E., El Sayed, M., & El Gamal, W. (2015). Genetical analysis for allelopathic activity in some rice varieties. *Egyptian Journal of Plant Breeding, 19*, 125–137.Fang, C., Li, Y., Li, C., Li, B., Ren, Y., Zheng, H., et al. (2015). Identification and comparative analysis of microRNAs in barnyardgrass (Echinochloa crus-galli) in response to rice allelopathy. *Plant, Cell & Environment, 38*, 1368–1381.

Gealy, D., Moldenhauer, K., & Duke, S. (2013b). Root distribution and potential interactions between

allelopathic rice, sprangletop (Leptochloa spp.), and barnyardgrass (*Echinochloa crus-galli*) based on 13C isotope discrimination analysis. *Journal of Chemical Ecology, 39*, 186–203.

Guo, Y., Ahmad, N., Shin, D., & Kim, K.-U. (2009). Allelopathic effects of rice cultivars on barnyardgrass growth to reduce the herbicide dose. *Allelopathy Journal, 24*.

Jabran, K., Mahajan, G., Sardana, V., & Chauhan, B. S. 2015. Allelopathy for weed control in agricultural systems. *Crop Protection,* 72, 57–65.

Jabran, K., Mahajan, G., Sardana, V., Chauhan, B. S. 2015. Allelopathy for weed control in agricultural systems. *Crop Protection*, 72, 57–65. https://doi.org/10.1016/j.cropro.2015.03.004

Javaid, A., Ahmad, S., Javaid, A., Shad, N., & Jabeen, K. (2009). Screening of mungbean cultivars under rice allelopathic stress for best agronomic and symbiotic traits. *Allelopathy Journal, 24*, 331–339.

Junaedi, A., Jung, W.-S., Chung, I.-M., & Kim, K.-H. (2007). Differentially expressed genes of potentially allelopathic rice in response against barnyardgrass. *Journal of Crop Science and Biotechnology, 10*, 231–236.

Kabir, A., Karim, S., Begum, M., & Juraimi, A. S. (2010). Allelopathic potential of rice varieties against spinach (Spinacia oleracea). *International Journal of Agriculture and Biology, 12*, 809–815.

Kanbar, A., Janamatti, M., Sudheer, E., Vinod, M.S., Shashidhar, H.E. 2006. Mapping qtls underlying seedling vigour traits in rice (*Oryza sativa* L.). *Current Science*, 90(1): 24–26.

Karimi, P., & Mosavi, S. A. 2020. Evaluation of the effect of cover crops on weed control and rice yield under Mazandaran climatic conditions. *Journal of Agricultural Science and Technology*, 24(1), 112-125.

Kato-Noguchi, H., Salam, M. A., & Suenaga, K. (2011). Isolation and identification of potent allelopathic substances in a traditional Bangladeshi rice cultivar Kartikshail. *Plant Protection Science, 14*, 128–134.

Kaur, R., Choudhary, D., Bali, S., Bandral, S.S., Singh, V., Ahmad, M.A. 2024. Pesticides: An alarming detrimental to health and environment. *Science of the Total Environment*, 915, 170113. Available from: https:// doi.org/10.1016/j.scitotenv.2024.170113

Khakzad. R., Valiolahpor. R., Alebrahim. M. T. 2016. Assessment of Performance the Recorded Herbicides in Rice (*Oryza sativa*) to Control Weed Species in Raton. *Iranaian Plan Protection Research, 30*, 494-504.

Khalil Tahmasebi. B., Zand. E., Yousefi. A., Babaei. S., Sadeghpour. A. 2024. Surveillance and mapping of tribenuron-methyl-resistant weeds in wheat fields. *Scientific Reports*, 14:28626. https://doi.org/10.1038/s41598-024-75308-1

Khawar, J., 2017. Manipulation of Allelopathic Crops for Weed Control. Springer Briefs in Plant Science Part of: SpringerBriefs in Plant Science, ISBN 978-3-319-53185-4 ISBN 978-3-319-53186-1 (eBook), March 2, 2017

Kim, S., Madrid, A., Park, S., Yang, S., & Olofsdotter, M. (2005). Evaluation of rice allelopathy in hydroponics. *Weed Research, 45*, 74–79.

Kong, C. H., Chen, X. H., Hu, F., Zhang, S. Z. 2011. Breeding of commercially acceptable allelopathic rice cultivars in China. *Pest Management Science*, 67, 1100–1106.

Kraehmer, H., Jabran, K., Mennan, H., Chauhan, B. S. 2016. Global distribution of rice weeds- a review. *Crop Protection*, 80, 73–86.

Lee, S.-B., Ku, Y. C., Seong, K. Y., Song, D. Y., Seo, K. I., Shin, J. C. 2005. Evaluation method of weed suppression by rice plant. *Korean Journal of Medicinal Crop Science*, 50, 79–83 .

Liebman, M., Dyck, E. 1993. Crop rotation and intercropping strategies for weed management. *Ecological Applications, 3*(1), 92–122.

Ma, Y., Zhang, M., Li, Y., Shui, J., & Zhou, Y. (2014). Allelopathy of rice (Oryza sativa L.) root exudates and its relations with Orobanche cumana Wallr. and Orobanche minor Sm. germination. *Journal of Plant Interactions, 9*, 722–730.

Mahdavi-Damghani, A., Mojaddam, M., Shamsabad, H. R. M. 2020. Effects of transplanting date on growth, yield components and weed control of rice (Hashemi

cultivar) in north of Iran. *Journal of Crop Production and Processing*, 10 (1), 15-28.

Masum, S. M., Hossain, M. A., Akamine, H., Sakagami, J. I., & Bhowmik, P. C. (2016). Allelopathic potential of indigenous Bangladeshi rice varieties. *Weed Biology and Management, 16*, 119–131.

Modarres Sanavy, S. A. M., Delfieh, M., Ghahary, S. (2015). Evaluation of allelopathic effects of Iranian rice cultivars (*Oryza sativa* L.) on growth factors of barnyard grass (*Echinochloa crus-galli* L.). *Journal of Agricultural Science*, 7 (10), 227–236. https://doi.org/10.5539/jas.v7n10p227.

Mohler, C. L. 2001. Mechanical management of weeds. In M. Liebman, C. L. Mohler, C. P. Staver (Eds.), *Ecological management of agricultural weeds* (pp. 139–209). Cambridge University Press.

Mousavi, S. R., Eskandari, H., & Rahimian Mashhadi, H. 2023. Effects of organic amendment management on weed seed bank dynamics in paddy fields. *Journal of Plant Protection Research, 63*(1), 88-97.

Norouzi, A., Mirzakhani, K. 2022. Ecological weed control in rice cultivation through optimal water management. *Journal of Water and Soil Science, 26*(4), 907-923.

Rahmani, B., & Ghorbani, N. 2021. The role of border and irrigation ditch management in reducing weed infestation in rice fields. *Iranian Journal of Weed Science,* 17(2), 135-150.

Ranagalage, A., Wathugala, D. 2015. Allelopathic potential of improved rice (*Oryza sativa* L.) varieties against Echinochloa crus-galli L. *Allelopathy Journal*, 36(1), 37–47.

Ranjbar, H., Ghadami, M., Shirani, S. 2019. The effect of crop rotation on reducing weed populations in rice fields of Guilan Province. *Iranian Journal of Weed Research*, 10(2), 45-58.

Sadat Asilan, K., Modarres Sanavy, S. A. M., Ghahary, S., Moradi Ghahderijan, M., & Panahi, M. 2013. The evaluation allelopathic effects of Iranian rice (Oryza sativa L.) cultivars on growth factors of barnyard grass (Echinochloa crus-galli L.). *Environmental Sciences Journal*, 12 (4), 145-158.

Seal, A., Pratley, J. 2010. The specificity of allelopathy in rice (*Oryza sativa*). *Weed Research*, 50, 303–311.

Shahmoradi, M., Koocheki, A., Nasiri Mahalati, M., Gholami, J. 2023. Evaluation of rice seed quality in terms of weed seed contamination in Guilan province. *Iranian Journal of Seed Research,* 10(2), 1-15

Teasdale, J. R., Mohler, C. L. 2000. The quantitative relationship between weed emergence and the physical properties of mulches. *Weed Science,* 48(3), 385–392.

Westerman, P. R., Wes, J. S., Kropff, M. J., & van der Werf, W. 2003. Annual losses of weed seeds due to predation in organic cereal fields. *Journal of Applied Ecology,* 40(5), 824–836.

Wickramasinghe, D., Devasinghe, U., Suriyagoda, LD., Egodawatta, C., Benaragama, DI., 2023. Weed dynamics under diverse nutrient management and crop rotation practices in the dry zone of Sri Lanka. *Front Agron*. 2023; 5:1211755. https://doi.org/10.3389/ fagro. 1211755.

Yousefi, A., Rahimi, M. R., Pour, S. A. 2021. Optimizing planting date and rice density to suppress weed growth and enhance crop productivity. *Weed Technology*, 35 (5), 798-805.

Zand, A., Nezamabadi, N., Baghestani, M.A., Shimi, P., Mosavi, S.K., 2019. Guidelines for Chemical Control of Weeds in Iran. *Mashhad University Jihad Publications*. 216 pp.

University of Jiroft

**Biospecies Research**

Journal homepage: bsr.ujiroft.ac.ir

Iranian Biology Society

# Comparative characterization of extracellular vesicles isolated from Aloe vera leaf peel and gel using ultracentrifugation and PEG precipitation

Abdollah Ramzani Ghara[1*], Fereshteh Ezzati Ghadi[2], Seyed Hamzeh Hosseini[3]

https://doi.org/10.22034/bsr.2026.568098.1011

[1]*Department of Biology, Faculty of Science, University of Jiroft, Jiroft, Iran. a.ramzani@ujiroft.ac.ir, ORCID: 0000-0002-8051-7143*

[2]*Department of Biology, Faculty of Science, University of Jiroft, Jiroft, Iran. f.ezzati@ujiroft.ac.ir, ORCID: 0000-0003-0776-7338*

[3]*Department of Biology, Faculty of Science, University of Jiroft, Jiroft, Iran. hamze@ujiroft.ac.ir*

**ARTICLE INFO**

**Article Type**
Original Article

**Article History**
Received: 22 December 2025
Accepted: 07 February 2026
Published: 15 February 2026



***Corresponding author**
a.ramzani@ujiroft.ac.ir

**ABSTRACT**

This study aimed to evaluate different isolation methods, including ultracentrifugation (UC) and polyethylene glycol (PEG)-based precipitation of extracellular vesicles (EVs) from Aloe vera and investigate their yield, purity, and physicochemical properties. Plant-derived extracellular vesicles (PDEVs) have attracted increasing attention as natural nanocarriers for biomedical, nutraceutical, and food-related applications. In this study, EVs were isolated from Aloe vera leaf peel and gel using UC and PEG methods. The EVs were characterized by nanoparticle tracking analysis (NTA), NanoDrop protein quantification, and zeta potential measurements. Aloe vera gel-derived EVs using the UC method showed higher particle concentrations, more consistent size distributions, and lower protein contamination compared with peel and gel PEG-derived samples. The PEG isolation markedly increased apparent protein concentration, especially in the gel, indicating co-precipitation of non-vesicular plant components and polymer-associated artifacts. Zeta potential analysis further revealed significant surface charge variation on PEG-derived vesicles, both in peel and gel, particularly after high-speed centrifugation. In conclusion, these results demonstrate that UC provides superior purity and physicochemical stability of Aloe vera EVs, while PEG precipitation inflates protein yield and alters vesicle surface properties. The present study highlights the importance of the isolation method, which affects its potential applications.

**Keywords**: Aloe vera, Extracellular vesicle, Polyethylene glycol, Zeta potential

**How to cite this paper**

Ramzani Ghara, A., Ezzati Ghadi, F., Hosseini, S.H., 2026. Comparative characterization of extracellular vesicles isolated from Aloe vera leaf peel and gel using ultracentrifugation and PEG precipitation. *Biospecies Research*, 1, pp. 70-79.

## Introduction

Extracellular vesicles (EVs) are nanoscale lipid bilayer-enclosed particles secreted by virtually all living cells (Abdal Dayem et al., 2025). EVs are included: apoptotic bodies, microvesicles, and exosomes. EVs play essential roles in intracellular communication by transferring proteins, lipids, nucleic acids, and other bioactive

molecules (Battistelli & Falcieri, 2021). Although EVs have been extensively studied in mammalian systems, recent research has revealed that plants also produce extracellular vesicles, often referred to as plant-derived nanovesicles (PDNVs) (Mu et al., 2023). PDNVs are cost-effective, sustainable, non-toxic, non-immunogenic, and suitable for therapeutic application. In contrast, mammalian EVs, such as Human cell-derived EVs, revealed batch-to-batch variability, high costs, and safety concerns (Fawzy et al., 2025, Ruf et al. 2022) suggested that the biogenesis mechanisms of EVs from plants and mammals are structurally similar, and also their intercellular communication is functionally analogous (Ruf et al., 2022). Plant-derived EVs exhibit unique stability compared to animal and bacterial-derived EVs due to their lipid composition and bioactive compounds (Langellotto et al., 2024). PDNVs are increasingly recognized for their potential in therapeutics, agriculture, and nutrition. Plant-derived nanovesicles are enriched with biologically active compounds like microRNAs, enzymes, lipids, and secondary metabolites, which can modulate physiological and biochemical processes in recipient organisms. PDNVs isolated from fruits, vegetables, and medicinal plants have shown anti-inflammatory, antioxidant, and immunomodulatory properties (Lo et al., 2024). Plant-derived nanovesicles protect sensitive molecules from enzymatic degradation, allowing more efficient delivery to target cells. Plant exosomes are considered safer for human consumption than their animal-derived counterparts, making them attractive candidates for drug delivery and nutraceutical applications (Rawat et al., 2025).

Aloe vera, a succulent plant widely used in traditional medicine and skincare, is a particularly auspicious source of plant nanovesicles. The leaves of Aloe vera contain a rich array of bioactive molecules, including polysaccharides (Matei et al., 2025), proteins (Mitra et al., 2023), phenolic compounds, and antioxidants (Solaberrieta et al., 2022). Studies have reported that Aloe vera showed therapeutic effects in wound healing, anti-inflammatory activity, and immunomodulation (Naini et al., 2021). A study indicated that nanovesicles isolated from Aloe vera can retain bioactive compounds, potentially enhancing their stability, bioavailability, and cellular uptake compared to crude plant extracts (Kim et al., 2021). Nanovesicles derived from Aloe vera have demonstrated potential to modulate cellular pathways associated with inflammation and oxidative stress, supporting their application in nutraceutical and biomedical properties (Ramírez et al., 2024; Choi et al., 2023).

Despite their growing importance, the field of plant exosomes is still in its infancy. A significant challenge in plant EV research is the lack of standardized isolation techniques. EVs isolation from plant sources, including affinity-based methods, differential centrifugation, density gradient centrifugation, filtration method, polymer-based precipitation, and size-exclusion chromatography. Differential centrifugation and polymer-based precipitation using polyethylene glycol are the most commonly used methods for EVs isolation from plant sources. Variations in isolation procedures can lead to differences in yield, purity, and the functional integrity of the nanovesicles, complicating their characterization and downstream applications. Understanding how different isolation methods affect the biophysical properties of plant-derived nanovesicles is crucial for both basic research and applied purposes. Comparative studies are essential for determining optimal protocols that maximize vesicle recovery while preserving their native structure and bioactivity. The present study aims to investigate different isolation methods, including UC and PEG-based precipitation of EVs across different tissue sources of Aloe vera to evaluate the impact of isolation techniques on EV yield, purity, and physicochemical properties.

## Materials and Methods

### Chemicals and reagents

All chemicals used in the present study were purchased from Merck & Co., Inc.

### Isolation of Aloe vera gel and peel

Fresh Aloe vera plants were obtained from a local market and thoroughly washed three times with sterile distilled water to remove surface contaminants. Leaves were sterilized by 70% ethanol and allowed to dry for a few seconds. Leaves were separated into inner gel and outer peel (rind) using a sterile knife. Gel (44g) and peel (62g) tissues were processed independently in all subsequent steps under a sterile laminar flow hood (Heraguard™). All equipment and reagents used in this study were sterilized. Each tissue was mixed with 1X standard fresh-chilled phosphate-buffered saline (pH: 7.4) at a weight-to-volume ratio of 1:3 and incubated at room temperature for one hour to facilitate the release of soluble components. The mixtures were then homogenized using a blender (Ninja 1200W) until a uniform suspension was obtained.

Gel homogenates were centrifuged (Eppendorf 5415R) first at 300 × g for 3 min, then 500 × g for 10 min, and finally 2000 × g for 20 min at 4 ºC. The supernatant after each centrifugation step was collected and used for the next centrifugation step. For peel samples, centrifugation was carried out three times. At first, centrifugation was carried out at 1000 × g for 10 min, and the supernatant was collected. The second step of centrifugation was at 3000 × g for 30 min. Finally, 10000 × g for 60 min, the supernatant was collected after each step. The final supernatants in peel-derived samples were passed through a 0.45 μm filter (Whatman uniflo) to remove large particles.

### Ultracentrifugation-based isolation of Aloe vera EVs from gel and peel

Clarified supernatants obtained from gel or peel homogenates were subjected to high-speed centrifugation according to established EV isolation protocols (Shen et al., 2025). The supernatants were centrifuged (Beckman Coulter Optima™ L-90k) at 150000 × g twice, and the resulting pellets were collected and resuspended in PBS, stored at -4 ºC for short-term use before characterization.

### PEG-based precipitation of Aloe vera EVs from gel and peel

For polyethylene glycol (PEG)-based isolation, a twofold concentrated PEG stock solution (8% w/v PEG 6000 in 1 M NaCl) was prepared and mixed with clarified supernatants at a 1:1 volume ratio (Kim & Park, 2022). Mixtures were incubated at 4 ºC for 16 hours to allow EV precipitation. Samples were centrifuged at 1500 × g for 30 min, then at 10000 × g for 60 min to collect PEG-precipitated EVs. The pellets were gently washed with PBS to remove residual PEG, then resuspended in PBS. The preparations were designated as PEG-isolated Aloe vera EVs and stored at -4 ºC for short-term use before characterization.

### Protein quantification by NanoDrop

Total protein concentration of EVs preparations was measured using a NanoDrop spectrophotometer (Thermoscientific NanoDrop one C microvolume UV-Vis spectrophotometer w/cuvette). Protein content was estimated by measuring absorbance at 280 nm. A260/280 ratios were recorded to assess sample purity and potential nucleic acid contamination.

### Nanoparticle tracking analysis

Particle size and distribution, and concentration of Aloe vera EVs were determined by nanoparticle tracking analysis (NTA) using a Particle Metrix system (Nanoparticle tracking NS300). The EV preparations were appropriately diluted in PBS before measurement. All samples were recorded at a camera level (CL) of 15, except for selected gel-derived PEG samples evaluated at a camera level (CL) of 12 due to signal saturation.

### Zeta potential and pH measurement

Zeta potential measurements were performed (using Zeta potential Malven Zetasizer zs) to assess the surface charge and colloidal stability of Aloe vera EVs. Measurements were conducted on multiple preparations for each isolation method and tissue source. Also, the pH

of the EV suspensions was recorded concurrently to evaluate the chemical environment of the samples.

### Statistical analysis

All data are presented as mean ± standard deviation (SD). Statistical analyses among groups were performed using One-Way Analysis of Variance (ANOVA). P-values less than 0.05 were considered statistically significant.

## Result

### NanoDrop Protein Quantification

Protein concentration and absorbance ratios measured by NanoDrop are summarized in Table 1. Apparent differences were observed between isolation methods and tissue sources. EVs isolated by UC exhibited substantially lower protein concentrations compared with PEG-isolated samples for both peel and gel. In peel samples from Aloe vera, UC yielded a protein concentration of 0.713 ± 0.001 mg/ml, PEG precipitation significantly increased ($p < 0.05$) apparent protein levels to 2.543 ± 0.00 mg/ml ($1500 \times g$) and further to 3.313 ± 0.00 mg/ml ($10000 \times g$). Gel-derived EVs showed a similar trend, with UC samples containing 2.359 ± 0.00 mg/ml protein compared to 4.321 ± 0.00 mg/ml and 5.427 ± 0.00 mg/ml, which significantly increased ($p < 0.05$) for PEG isolates collected at $1500 \times g$ and $10000 \times g$, respectively.

Measurements of A260/280 ratios showed UC-isolated EVs displayed significantly lower ratios ($p < 0.05$), particularly in peel samples (0.90 ± 0.01) compared to gel samples (1.38 ± 0.01). PEG-derived samples, in comparison, showed significantly elevated A260/280 ratios ($p < 0.05$), especially in gel EVs isolated at $10000 \times g$ (1.79 ± 0.01).

Table 1. NanoDrop protein concentration and purity ratios

| Sample | Isolation | Centrifugation (g) | Protein concentration (mg/ml) | A280 | A260/280 |
|---|---|---|---|---|---|
| Peel | UC | 150000 | 0.713 ±0.001* | 0.71±0.001 | 0.90± 0.01* |
| Peel | PEG | 1500 | 2.543 ±0.000 * | 2.54±0.000* | 1.26± 0.01* |
| Peel | PEG | 10000 | 3.313±0.000* | 3.31±0.000* | 1.40± 0.01* |
| Gel | UC | 150000 | 2.359±0.000 | 2.36±0.000 | 1.38± 0.01 |
| Gel | PEG | 1500 | 4.321±0.000* | 4.32±0.000* | 1.50± 0.01* |
| Gel | PEG | 10000 | 5.427±0.000* | 5.42±0.000* | 1.79± 0.01* |

All data are presented as mean ± standard deviation (SD).

Statistical comparisons among groups were performed using One-way ANOVA. * $p < 0.05$ was considered statistically significant.

### Nanoparticle tracking analysis (NTA)

Particle size distribution and concentration data obtained by NTA are presented in Table 2. Gel-derived UC EVs exhibited the highest ($p < 0.05$) particle concentration ($4.97 \times 10^{11}$ ± 0.01 particles/ml) with a mean size of 125.8 nm. In contrast, peel-derived UC EVs showed a significantly smaller mean size (85 nm) and a concentration of $1.63 \times 10^{11}$ particles/ml.

PEG precipitation for peel-derived EVs resulted in $4.71 \times 10^{9}$ ± 0.01 particles/ml at $1500 \times g$ and decreased to $2.80 \times 10^{10}$ ± 0.01 particles/ml at $10000 \times g$. Gel-derived PEG EVs showed $1.53 \times 10^{10}$ ± 0.01 particles/ml at $1500 \times g$ and decreased to $1.01 \times 10^{10}$ ± 0.01 particles/ml at $10000 \times g$. Notably, the gel EV sample measured at camera level (CL) 12 showed a size distribution (125.7 nm) comparable to UC isolates.

Table 2. NTA Size and Concentration of EVs

| Sample | Isolation | Centrifugation (g) | Size (nm) | Concentration (particles/ml) |
|---|---|---|---|---|
| Peel | UC | 150000 | 85 ± 1.00 | $1.63 \times 10^{11} \pm 0.05$* |
| Peel | PEG | 1500 | 83.7 ± 1.00 * | $4.71 \times 10^{9} \pm 0.01$* |
| Peel | PEG | 10000 | 86.6 ± 1.00 | $2.80 \times 10^{10} \pm 0.01$* |
| Gel | UC | 150000 | 125.8 ± 1.00 * | $4.970 \times 10^{11} \pm 0.01$* |
| Gel | PEG | 1500 | 106.2 ± 1.00 * | $1.53 \times 10^{10} \pm 0.01$ |
| Gel | PEG | 10000 | 48.1 ± 1.00 * | $1.01 \times 10^{10} \pm 0.01$* |
| Gel | PEG | 10000 (CL12) | 125.7 ± 1.00 | $3.33 \times 10^{10} \pm 0.01$* |

All data are presented as mean ± standard deviation (SD).

Statistical comparisons among groups were performed using One-way ANOVA. * $p < 0.05$ was considered statistically significant.

## Zeta potential and pH

Zeta potential and pH values are summarized in Table 3. UC-derived gel EVs exhibited strongly positive zeta potentials (38.85 ± 0.95 mv), indicating good colloidal stability. In contrast, the zeta potential of UC-derived peel EVs showed a significant decrease of 10.78 ±1.02 ($p < 0.05$) compared to UC-derived gel EVs. PEG precipitation significantly altered surface charge characteristics. Gel-derived PEG EVs collected at 1500 × g displayed 24.95 ± 1.17 mv, whereas samples collected at 10000 ×g exhibited a significant increase in zeta potential (40.40 ±2.11 mv). A similar pattern was observed for peel-derived EVs, where low-speed PEG pellets showed a zeta potential value of 11.26 ±1.60 mv, and high-speed PEG pellets demonstrated significantly increased surface charge ($p < 0.05$) of 39.90 ± 2.87 mv when compared to low-speed PEG peel-derived EVs. Results from Table 3 showed that the pH of all EV suspensions remained acidic and relatively stable (pH 4.5 to 4.7), indicating that differences in zeta potential were primarily attributable to isolation method and centrifugal force rather than pH variation. Collectively, these results demonstrate that both tissue source and isolation strategy significantly influence surface charge and colloidal stability of EVs.

Table 3. Zeta potential and pH of Aloe vera EVs

| **Sample** | **Isolation** | **Centrifugation (g)** | **Zeta Potential (mV)** | **pH** |
|---|---|---|---|---|
| Gel | UC | 150000 | 38.850 ± 0.95* | 4.6 |
| Peel | UC | 150000 | 10.78 ± 1.02 | 4.7 |
| Gel | PEG | 1500 | 24.950 ± 1.17* | 4.5 |
| Gel | PEG | 10000 | 40.40 ± 2.11* | 4.6 |
| Peel | PEG | 1500 | 11.26 ± 1.60 | 4.6 |
| Peel | PEG | 10000 | 39.90 ± 2.87* | 4.6 |

All data are presented as mean ± standard deviation (SD).

Statistical comparisons among groups were performed using One-way ANOVA. * $p < 0.05$ was considered statistically significant.

## Discussion

Plant-derived extracellular vesicles exhibit intrinsic bioactive properties, including anti-inflammatory and antioxidant activities, which can contribute directly to their biological efficacy. The isolation strategy of PDEVs is a key factor influencing vesicle purity, yield, and biological functionality, due to the complex nature of

plant tissues and coexisting biomolecules. Therefore, selecting and optimizing an appropriate isolation method is essential to ensure reproducibility and maximize the translational potential of PDEVs across biomedical and industrial applications.

The present study aimed to investigate how different isolation techniques influence the physicochemical characteristics and functional potential of Aloe vera-derived nanovesicles. Previous studies have shown that Aloe vera is rich in phenolic compounds, including cinnamic acids, chromones, anthracene derivatives, and flavonoids, many of which contribute to its well-documented antioxidant and anti-inflammatory (Mensah et al., 2025; Abid et al., 2025). In this study, EVs were isolated from Aloe vera peels and gel using both UC and PEG precipitation methods.

As summarized in Table 1, NanoDrop analysis revealed marked differences in protein concentration and absorbance ratios between UC and PEG precipitation methods for both Aloe vera gel and peel-derived EVs. UC-isolated peel EVs exhibited a relatively low protein concentration (0.713 mg/ml). In contrast, gel-derived EVs showed higher protein levels (2.359 mg/ml), indicating intrinsic differences in vesicle abundance and soluble protein content between the two plant tissues. In contrast, PEG precipitation resulted in substantially higher apparent protein concentrations across all samples (Table 1). A study has shown that the PEG precipitation method yields a higher protein concentration (Rahmatinejad et al., 2024). PEG precipitation relies on chemical aggregation to isolate vesicles at lower centrifugal forces, offering a faster and more scalable approach, with slightly lower purity due to co-isolated proteins and plant polysaccharides (Ludwig et al., 2018; Zhu et al., 2024).

Peel-derived EVs isolated by PEG showed protein concentrations ranging from 2.54 mg/ml at 1500 × g to 3.31 mg/ml at 10000 × g, while gel-derived PEG isolates reached even higher values (4.32 to 5.43 mg/ml). These findings are consistent with previous reports indicating that PEG-based isolation enhances total recoverable material by soluble proteins, polysaccharides, and other macromolecules (Huang et al., 2025).

The A260/280 ratios presented in Table 1 further support this interpretation. UC-isolated peel EVs displayed a low A260/280 ratio, reflecting relatively high protein purity and minimal nucleic acid or carbohydrate contamination. In contrast, PEG-isolated samples showed elevated A260/280 ratios, particularly in gel-derived EVs, suggesting co-isolation of nucleic acid, phenolic compounds, and polysaccharides, which are abundant in Aloe vera gel. Previous studies have shown that PEG precipitation can lead to lower purity of the isolated EV population (Martínez-Greene et al., 2021). It has been demonstrated in previous studies that ultracentrifugation is the method of choice for applications demanding high purity and precise characterization of extracellular vesicles (Mu et al., 2023).

The NTA results presented in Table 2 highlight apparent differences in particle size distribution and vesicle concentration between isolation methods and plant tissues. UC-isolated peel-derived EVs exhibited a mean particle size of approximately 85 nm with a concentration of 1.63 × 1011 particles/ml, and UC-isolated gel EVs showed a larger size (125.8 nm) and substantially higher concentration (4.97 × 1011 particles/ml). These values fall within the expected size range of small EVs and indicate efficient enrichment of intact vesicles using UC. PEG-isolated samples, as shown in Table 2, exhibited more variable size distributions and lower particle concentrations compared to UC isolates, which may reflect selective pelleting of smaller vesicles or interference from PEG residues during NTA measurement. Notably, despite higher protein concentrations observed in PEG isolates (Table 1), particle concentrations measured by NTA were consistently lower than those obtained by UC (Table 2). In contrast to the results obtained in the present study, another researcher indicates that the concentration of EV particles is higher when using PEG precipitation (Gharavi et al., 2024). This discrepancy emphasizes that protein content alone does not accurately reflect EV yield and reinforces the necessity of particle-based quantification when evaluating isolation efficiency. The gel EV sample measured at CL12 highlighting the sensitivity of PEG-derived samples to

measurement conditions. Overall, UC produced more concentrated and size-consistent EV populations, whereas PEG precipitation resulted in lower particle recovery and greater variability in size measurements, particularly at higher centrifugal forces.

Zeta potential is a key indicator of the surface charge and colloidal stability of EVs in a dispersed system. The net negative charge of nonfunctionalized EVs influences particle-particle and particle-medium interactions, affecting their tendency to aggregate. A higher absolute zeta potential promotes electrostatic repulsion and improves dispersion stability. Surface charge also plays a vital role in biological processes such as cellular uptake and cytotoxicity. Therefore, zeta potential provides valuable insight into the stability and in vivo behaviour of EVs, supporting their application in nanomedicine (Midekessa et al., 2020; Rogers et al., 2023).

This study, zeta potential and pH values reported in Table 3 provide insight into the colloidal stability and surface charge characteristics of Aloe vera-derived EVs. UC-isolated gel EVs demonstrated consistently high positive zeta potentials, indicative of strong electrostatic repulsion and excellent colloidal stability. Such values suggest that vesicle membranes and preserved surface chemistry following UC isolation. In contrast, UC-isolated peel EVs exhibited significantly lower zeta potentials, suggesting lower electrostatic stability, a higher tendency toward aggregation, and possible differences in membrane composition between gel- and peel-derived vesicles. This difference likely reflects tissue-specific variations in lipid composition, surface proteins, and associated phytochemicals among PDEVs from different tissues (Huang et al., 2025). PEG-isolated EVs showed zeta potential values that varied with centrifugal force, as summarized in Table 3. Low-speed PEG isolates exhibited moderate zeta potentials for gel-derived EVs and lower values for peel-derived EVs. Notably, high-speed PEG pelleting resulted in zeta potential values comparable to or exceeding those of UC-isolated gel EVs, suggesting selective enrichment of more stable vesicle populations or removal of loosely bound contaminants.

PDEVs have been reported to have higher stability against enzymatic degradation compared to mammalian drive EVs; thus, they are a potential candidate for oral drug administration due to their stability in both normal and acidic pH (Feng et al., 2023). Yang et al. (2020) reported that PDEVs from lemon using PEG precipitation increase their circulation time due to the attachment of PEG to the surface of EVs. Also, PEG improved EVs' stability in acidic pH (Yang et al., 2020).

Variations in PEG concentration can strongly affect precipitation efficiency and the extent of co-isolated proteins and polysaccharides, thereby impacting EV purity. A study has shown that concentration range of PEG (8%, 10%, 12%, and 15%) could increase the exosomes size (Kalarikkal et al., 2020). Finally, differences between Aloe vera gel and peel tissues (matrix complexity and biochemical composition) may contribute to variability in EV yield and physicochemical properties.

In the present study, the pH of all samples remained stable between 4.5 and 4.7 (Table 3), consistent with the native acidity of Aloe vera tissues. The absence of significant pH variation across isolation methods indicates that neither UC nor PEG precipitation altered the chemical environment of the EV preparations. Thus, results demonstrated that both the isolation method and tissue source profoundly influence the physicochemical properties of Aloe vera EVs. UC consistently produced preparations with higher particle concentrations, lower protein contamination, and more predictable zeta potential profiles, supporting its suitability for high-purity EV research. PEG precipitation, while yielding higher apparent protein concentrations, resulted in lower particle counts and greater variability in surface charge, reflecting co-precipitation of non-vesicular components. Nevertheless, PEG offers advantages in scalability and operational simplicity, making it attractive for applications where yield is prioritized over purity.

Gel-derived EVs consistently outperformed peel-derived EVs across all parameters, including particle concentration, protein yield, and colloidal stability, underscoring Aloe vera gel as a superior source of plant-derived nanovesicles for downstream applications.

## Conclusion

This study provides a comprehensive comparative evaluation of ultracentrifugation and polyethylene glycol precipitation for the isolation of extracellular vesicles (EVs) from Aloe vera gel and peel tissues. Integrating protein quantification, nanoparticle tracking analysis, and zeta potential measurements demonstrated that both the isolation method and plant tissue source significantly influence the yield, purity, and physicochemical stability of plant-derived nanovesicles. UC consistently produced EV preparations with higher particle concentrations, narrower size distributions within the expected range of small EVs, and lower levels of co-isolated proteins, indicating superior purity and structural integrity. These characteristics make UC-isolated Aloe vera EVs particularly suitable for mechanistic studies, molecular profiling, and applications requiring well-defined vesicle populations. In contrast, PEG precipitation resulted in substantially higher apparent protein concentrations but lower particle counts, reflecting co-precipitation of soluble proteins, polysaccharides, and other plant macromolecules. While this reduces purity, PEG-based isolation offers practical advantages in terms of simplicity, reduced equipment requirement, and scalability, which are critical for translational and industrial applications. The isolation of Aloe vera tissues highlights the gel as a superior and more reliable source of Aloe vera nanovesicles, likely due to its rich biochemical composition and lower structural complexity compared to peel tissue. Methodological limitations include the lack of standardized EV isolation protocols, which reduces reproducibility and cross-study comparability. In addition, ultracentrifugation has limited industrial scalability due to high cost and low throughput, while PEG precipitation is more scalable but suffers from lower purity and requires further steps. Future studies should focus on integrating molecular cargo analysis, functional bioactivity assays, industrial scalability, standardization of methods, and additional purification steps to optimize Aloe vera EVs.

## Acknowledgments

The authors express their gratitude to the University of Jiroft for their support.

## Conflict of Interest

The authors declare that there is no conflict of interest.

## References

Abdal Dayem, A., Kwak, Y., Jeun, H. and Cho, S.G., 2025. Recent Insights into Organoid-Derived Extracellular Vesicles and Their Biomedical Applications. *Journal of Personalized Medicine*, *15*(10), p.492.

Abid, A., Javed, M., Zafar, S., Hamdani, S.A.Z., Shah, S.H.B.U., Abid, J. and Ahmad, A.M.R., 2025. The green healer; an updated review on the phytochemical profile and therapeutic potential of Aloe vera. *Frontiers in Nutrition*, *12*, p.1689700.

Battistelli, M. and Falcieri, E., 2021. Apoptotic bodies: particular extracellular vesicles involved in intercellular communication. *Advances in Medical Biochemistry, Genomics, Physiology, and Pathology*, pp.473-486.

Choi, S.H., Eom, J.Y., Kim, H.J., Seo, W., Kwun, H.J., Kim, D.K., Kim, J. and Cho, Y.E., 2023. Aloe-derived nanovesicles attenuate inflammation and enhance tight junction proteins for acute colitis treatment. *Biomaterials Science*, *11*(16), pp.5490-5501.

Fawzy, M.P., Hassan, H.A., Amin, M.U., Preis, E., Bakowsky, U. and Fahmy, S.A., 2025. Deploying nucleic acids-loaded plant-derived exosomes as green nano gadget in cancer gene therapy. *Materials Advances*.

Feng, J., Xiu, Q., Huang, Y., Troyer, Z., Li, B. and Zheng, L., 2023. Plant-derived vesicle-like nanoparticles as promising biotherapeutic tools: present and future. *Advanced Materials*, *35*(24), p.2207826.

Gharavi, A.T., Niknejad, A., Irian, S., Rahimi, A. and Salimi, M., 2024. Polyethylene Glycol-Mediated Exosome Isolation: A Method for Exosomal RNA Analysis. *Iranian Biomedical Journal*, *28*(2-3), p.132.

Huang, D., Chen, J., Zhao, M., Shen, H., Jin, Q., Xiao, D., Peng, Z., Chen, T., Zhang, Y., Rao, D. and Liu, M., 2025. Plant-derived extracellular vesicles: composition, function and clinical potential. Journal of Translational Medicine, 23(1), pp.1-17.

Huang, Q., Wang, J., Ning, H., Liu, W. and Han, X., 2025. Exosome isolation based on polyethylene glycol (PEG): a review. Molecular and Cellular Biochemistry, 480(5), pp.2847-2861.

Kalarikkal, S.P., Prasad, D., Kasiappan, R., Chaudhari, S.R. and Sundaram, G.M., 2020. A cost-effective polyethylene glycol-based method for the isolation of functional edible nanoparticles from ginger rhizomes. Scientific reports, 10(1), p.4456.

Kim, M. and Park, J.H., 2022. Isolation of aloe saponaria-derived extracellular vesicles and investigation of their potential for chronic wound healing. Pharmaceutics, 14(9), p.1905.

Kim, M.K., Choi, Y.C., Cho, S.H., Choi, J.S. and Cho, Y.W., 2021. The antioxidant effect of small extracellular vesicles derived from aloe vera peels for wound healing. Tissue engineering and regenerative medicine, 18(4), pp.561-571

Langellotto, M.D., Rassu, G., Serri, C., Demartis, S., Giunchedi, P. and Gavini, E., 2025. Plant-derived extracellular vesicles: a synergetic combination of a drug delivery system and a source of natural bioactive compounds. Drug delivery and translational research, 15(3), pp.831-845.

Lo, K.J., Wang, M.H., Ho, C.T. and Pan, M.H., 2024. Plant-derived extracellular vesicles: a new revolutionization of modern healthy diets and biomedical applications. Journal of agricultural and food chemistry, 72(6), pp.2853-2878.

Ludwig, A.K., De Miroschedji, K., Doeppner, T.R., Börger, V., Ruesing, J., Rebmann, V., Durst, S., Jansen, S., Bremer, M., Behrmann, E. and Singer, B.B., 2018. Precipitation with polyethylene glycol followed by washing and pelleting by ultracentrifugation enriches extracellular vesicles from tissue culture supernatants in small and large scales. *Journal of extracellular vesicles*, *7*(1), p.1528109.

Martínez-Greene, J.A., Hernández-Ortega, K., Quiroz-Baez, R., Resendis-Antonio, O., Pichardo-Casas, I., Sinclair, D.A., Budnik, B., Hidalgo-Miranda, A., Uribe-Querol, E., Ramos-Godínez, M.D.P. and Martínez-Martínez, E., 2021. Quantitative proteomic analysis of extracellular vesicle subgroups isolated by an optimized method combining polymer-based precipitation and size exclusion chromatography. Journal of Extracellular Vesicles, 10(6), p.e12087.

Matei, C.E., Visan, A.I. and Cristescu, R., 2025. Aloe Vera Polysaccharides as Therapeutic Agents: Benefits Versus Side Effects in Biomedical Applications. Polysaccharides, 6(2), p.36.

Mensah, E.O., Adadi, P., Asase, R.V., Kelvin, O., Mozhdehi, F.J., Amoah, I. and Agyei, D., 2025. Aloe vera and its byproducts as sources of valuable bioactive compounds: Extraction, biological activities, and applications in various food industries. *PharmaNutrition*, p.100436.

Midekessa, G., Godakumara, K., Ord, J., Viil, J., Lattekivi, F., Dissanayake, K., Kopanchuk, S., Rinken, A., Andronowska, A., Bhattacharjee, S. and Rinken, T., 2020. Zeta potential of extracellular vesicles: toward understanding the attributes that determine colloidal stability. *ACS omega*, *5*(27), pp.16701-16710.

Mitra, A., Singh, M., Banga, A., Pandey, J., Tripathi, S.S. and Singh, D., 2023. Bioactive compounds and therapeutic properties of Aloe vera—A review. *Plant Science Today*, *10*, pp.1-7.

Mu, N., Li, J., Zeng, L., You, J., Li, R., Qin, A., Liu, X., Yan, F. and Zhou, Z., 2023. Plant-derived exosome-like nanovesicles: current progress and prospects. *International Journal of Nanomedicine*, pp.4987-5009.

Naini, M.A., Zargari-Samadnejad, A., Mehrvarz, S., Tanideh, R., Ghorbani, M., Dehghanian, A., Hasanzarrini, M., Banaee, F., Koohi-Hosseinabadi, O., Tanideh, N. and Iraji, A., 2021. Anti-inflammatory, antioxidant, and healing-promoting effects of Aloe vera extract in the experimental colitis in rats. *Evidence-Based Complementary and Alternative Medicine*, 2021(1), p.9945244.

Rahmatinejad, F., Kharat, Z., Jalili, H., Renani, M.K. and Mobasheri, H., 2024. Comparison of morphology, protein concentration, and size distribution of bone marrow and Wharton's jelly-derived mesenchymal stem cells exosomes isolated by ultracentrifugation and Polymer-based precipitation techniques. *Tissue and Cell*, *88*, p.102427.

Ramírez, O., Pomareda, F., Olivares, B., Huang, Y.L., Zavala, G., Carrasco-Rojas, J., Álvarez, S., Leiva-Sabadini, C., Hidalgo, V., Romo, P. and Sánchez, M., 2024. Aloe vera peel-derived nanovesicles display anti-inflammatory properties and prevent myofibroblast differentiation. *Phytomedicine*, *122*, p.155108.

Rawat, S., Arora, S., Dhondale, M.R., Khadilkar, M., Kumar, S. and Agrawal, A.K., 2025. Stability Dynamics of Plant-Based Extracellular Vesicles Drug Delivery. *Journal of Xenobiotics*, *15*(2), p.55.

Rogers, N.M., Hicks, E., Kan, C., Martin, E., Gao, L., Limso, C., Hendren, C.O., Kuehn, M. and Wiesner, M.R., 2023. Characterizing the transport and surface affinity of extracellular vesicles isolated from yeast and bacteria in well-characterized porous media. Environmental Science & Technology, 57(35), pp.13182-13192.

Ruf, A., Oberkofler, L., Robatzek, S. and Weiberg, A., 2022. Spotlight on plant RNA-containing extracellular vesicles. Current Opinion in Plant Biology, 69, p.102272.

Shen, J., Wei, T., Li, M., Jiang, Y., Zhang, J., Qi, Y., Chen, C., Li, X., Huang, P. and Qu, J., 2025. Aloe vera-derived extracellular vesicle-like particles suppress pancreatic carcinoma progression through triggering pyroptosis via ROS-GSDMD/E signaling pathway. *Chinese Medicine*, *20*(1), p.101.

Solaberrieta, I., Jiménez, A. and Garrigós, M.C., 2022. Valorization of Aloe vera skin by-products to obtain bioactive compounds by microwave-assisted extraction: antioxidant activity and chemical composition. *Antioxidants*, *11*(6), p.1058.

Yang, M., Liu, X., Luo, Q., Xu, L. and Chen, F., 2020. An efficient method to isolate lemon derived extracellular vesicles for gastric cancer therapy. *Journal of nanobiotechnology*, *18*(1), p.100.

Zhu, Y., Zhao, J., Ding, H., Qiu, M., Xue, L., Ge, D., Wen, G., Ren, H., Li, P. and Wang, J., 2024. Applications of plant-derived extracellular vesicles in medicine. *MedComm*, *5*(10), p.e741.

University of Jiroft

**Biospecies Research**

Journal homepage: bsr.ujiroft.ac.ir

Iranian Biology Society

# Morphological and physiological performance of petunia (*Petunia hybrida*) cultivated in a growth substrate derived from Tehran pine (*Pinus eldarica*) cone peat

Mehrdad Babarabie[1*], Atoosa Danyaei[2], Sediqeh Afsharipour[3*]

https://doi.org/10.22034/bsr.2026.570455.1014

[1]*Department of Agriculture, Minab Higher Education Complex, University of Hormozgan, Bandar Abbas, 7916193145, Iran. Mehrdad.babarai@hormozgan.ac.ir*

[2]*PhD in Horticultural Sciences, National Skill University, Tehran, Iran. atoosadanyaei@yahoo.com*

[3]*Department of Horticultural Sciences, University of Hormozgan, Bandar Abbas, Iran. s.afshari996@gmail.com*

**ARTICLE INFO**

**Article Type**
Original Article

**Article History**
Received: 03 January 2026
Accepted: 02 February 2026
Published: 15 February 2026


***Corresponding author**
s.afshari996@gmail.com

**ABSTRACT**

Petunia is a widely cultivated ornamental plant whose growth and flowering performance are strongly affected by the physical and chemical properties of the growing substrate. Increasing costs and limited availability of cocopeat have encouraged the use of low-cost, locally available alternatives. This study investigated the morphological and physiological responses of petunia grown in Tehran pine cone–based peat (*Pinus eldarica*) compared with cocopeat. The experiment was conducted as a completely randomized design with two substrate treatments, perlite–cocopeat and perlite–pine cone peat, with three replications. Plant height, flower number and diameter, flowering time, shoot and root biomass, leaf chlorophyll and carotenoid contents, total soluble sugars, and petal anthocyanin concentration were evaluated. The results showed that the pine cone peat–perlite mixture increased flower number by 85.7% and significantly enhanced leaf chlorophyll and carotenoid contents by 45.4% and 25.5%, respectively, while cocopeat promoted higher accumulation of soluble sugars. Overall, composted *P. eldarica* cone peat appears to be a sustainable and economically viable alternative to cocopeat for petunia production.

**Keywords**: growth substrate; pine cone peat; cocopeat; ornamental quality; chlorophyll.

**How to cite this paper**

Babarabie, B., Danyaei, A., Afsharipour, S. 2026. Morphological and physiological performance of petunia (*Petunia hybrida*) cultivated in a growth substrate derived from Tehran pine (*Pinus eldarica*) cone peat. *Biospecies Research*, 1, pp. 80-87.

## Introduction

Petunia (*Petunia hybrida*) is an annual or perennial ornamental species in the family Solanaceae, native to Argentina. It is extensively cultivated across the world and is considered a key element in landscaping for gardens, parks, and urban green spaces (Chehregani et al., 2016). Petunias were among the earliest ornamental plants to be commercially propagated in the ornamental plant market, starting from the 1950s (Hoda et al., 2014). The flowers of petunia display a wide array of colors, including white, red, purple, pink, yellow, blue, and variegated forms, and this broad color variation has made them one of the most favored bedding plants globally (Hoda et al., 2014).

Nowadays, the use of appropriate growing media is recognized as a critical factor in the production and cultivation of ornamental plants (Tzortzakis et al., 2020). The choice of substrate significantly influences the fulfillment of plant requirements, promotes vegetative growth, and improves overall plant performance and productivity (El-Kazzaz et al., 2017; Prasad et al., 2019). An ideal growing medium should ensure efficient oxygen exchange between roots and the surrounding atmosphere, while providing adequate water retention, nutrient availability, and mechanical support for plant anchorage (Al-Far et al., 2019). In greenhouse production, soilless substrates are widely employed because they are lighter, disease-free, readily available, and more suitable for containerized plants compared with mineral soils (Nelson, 1991).

Beyond physical, chemical, and biological suitability, an optimal growing medium should be cost-effective, sustainable, and lightweight to facilitate handling and transportation, while remaining economically practical (Davidson et al., 2000). Various soilless substrates are commonly used for cultivating flowering plants, including peat, peat moss, perlite, vermiculite, coco peat, zeolite, rockwool, sand, and composts derived from diverse organic sources (Fussy et al., 2022). However, limited availability and high import costs of cocopeat, peat moss, and other foreign substrates have created a need for locally available, cost-effective alternatives that can replace expensive imports and reduce production costs (Carpenter et al., 2011; Fox, 2011; Gruda, 2019). In this context, several studies have suggested that materials such as wood chips (Durand et al., 2021), tree barks, including palm peat (Ahmad et al., 2023), and plant fibers (Vandecasteele et al., 2018) may serve as effective substitutes for imported substrates and can be successfully applied in soilless cultivation systems.

According to Akbarzade et al., (2023), incorporating wood waste compost into the growing medium effectively enhanced flower diameter, plant height, leaf number, and chlorophyll content in plants. Similarly, Woznicki et al., (2024) reported that strawberry plants cultivated in a medium containing spruce wood fibers exhibited higher sugar accumulation along with improved quality and overall performance. Other studies have shown that adding tea waste to the substrate of cut *Anthurium* flowers not only lowered the costs of greenhouse soilless cultivation but also positively influenced growth parameters and quality indices (Asghari, 2017). Furthermore, Česonienė et al., (2023) indicated that the inclusion of pine and spruce fibers in blueberry cutting media can reduce the reliance on peat.

Recently, in Iran, a cellulose-based substrate derived from the cones of *Pinus eldarica* (Tehran pine) has been developed and patented. Considering its promising properties, evaluating its potential as a growing medium is essential. *P. eldarica*, a pine species native to the Eldar region of Georgia, has been cultivated in Iran for several centuries and is commonly referred to as Iranian pine, Tehran pine, or formal pine (Soltanian et al., 2016). Babarabie et al., (2025) reported that a cellulose-based cone peat substrate from *P. eldarica* increased germination rates of *Adenium*, ornamental sunflower, and *Osteospermum* compared to cocopeat. Another study demonstrated that Tehran pine cone peat could replace cocopeat as a propagation medium for *Zamiifolia*, enhancing root and rhizome length and reducing leaf cutting germination time (Babarabie et al., 2025). Given the significance of ornamental plants, particularly petunia, identifying a suitable growing medium for this species is of considerable importance. Accordingly, the present study aimed to compare the effects of *P. eldarica* cone peat and imported cocopeat on the quantitative and qualitative traits of petunia, and to evaluate their potential as substitutes for cocopeat.

## Materials and Methods

The present study was conducted in December 2024 at the Laboratory of Hormozgan University, using a completely randomized design with two treatments and three replications, with each replication consisting of three plants. The first treatment consisted of a 1:1 (v/v) mixture of perlite and cocopeat, while the second treatment consisted of a 1:1 (v/v) mixture of perlite and *Pinus eldarica* cone compost. The properties of these

growing media are presented in Table 1, including measurements of some essential macro- and micronutrients, pH, electrical conductivity, and cation exchange capacity, which differed between the two substrates.

Table 1 - Characteristics of the used growth media in the experiment

| Substrate | pH | EC | CEC | N (%) | P (ppm) | K (ppm) | Ca (ppm) | Mn (ppm) | Mg (ppm) | Fe (ppm) | Cu (ppm) |
|---|---|---|---|---|---|---|---|---|---|---|---|
| Cocopeat | 6.57 | 0.53 | 207 | 3.14 | 382 | 396 | 1380 | 10 | 597 | 362 | 16 |
| Pine Cone Peat | 6.43 | 0.61 | 241 | 2.85 | 413 | 419 | 1438 | 58 | 1770 | 800 | 309 |

Forty-five-day-old petunia seedlings (‘Burgundy’ F1) with six leaves were obtained from Shokoofeh Isfahan Company. Seedlings were transplanted into pots with a diameter of 14 cm and a height of 12 cm and grown in a research greenhouse with an average light intensity of 11,000 lux, 70 ± 5% relative humidity, and temperatures of 26 ± 2 °C during the day and 18 ± 2 °C at night. Upon transplanting, humic acid was applied during the first irrigation to reduce transplant shock. Plants were monitored daily, and each pot was irrigated with 100 mL of water whenever the growing medium began to dry.

One week after transplanting and continuing until the end of the growth and flowering period (95 days), all plants were fertilized weekly with Hoagland’s nutrient solution. At the end of the experiment, the following traits were measured: plant height, number of flowers, flower diameter, fresh and dry weight of roots, fresh and dry weight of shoots, total soluble sugars, total chlorophyll and leaf carotenoid contents, and petal anthocyanin content. Flowering onset was also recorded daily throughout the experimental period.

**Plant height and Flower diameter**

Plant height and flower diameter were recorded using a digital caliper. Fresh biomass of shoots and roots was determined with a digital balance. For dry weight measurements, shoot and root samples were separately placed in paper bags and oven-dried at 72 °C for 48 hours, after which the dry weights were measured using a digital balance.

**Chlorophyll and Carotenoids**

Chlorophyll extraction from leaf tissue was carried out using 80% acetone. Fresh leaf samples (0.1 g) were homogenized with 5 mL of 80% acetone to obtain a uniform solution. The homogenate was centrifuged at 4,800 rpm for 20 minutes, and the supernatant volume was then adjusted to 10 mL with 80% acetone. Absorbance was measured using a spectrophotometer at 645 and 663 nm for chlorophyll and at 480 and 510 nm for carotenoids. Total chlorophyll and carotenoid concentrations were calculated in mg $g^{-1}$ fresh weight according to the formulas described by Arnon (1949).

**Total Sugars**

For the measurement of total sugars, 100 mg of fresh leaf sample was hydrolyzed in 5 mL of 2.5 N hydrochloric acid in a boiling water bath for 3 hours and then neutralized with sodium carbonate. The volume was adjusted to 100 mL, and the solution was centrifuged at 5,000 rpm for 10 minutes. One milliliter of the supernatant was taken for analysis. Four milliliters of anthrone reagent were added, and the mixture was incubated in a water bath at 70 °C for one minute. The sample was then rapidly cooled, during which the color changed from green to gray, and absorbance was

measured at 630 nm. Total sugar content was calculated in mg $g^{-1}$ dry weight (Thimmaiah, 1999).

**Anthocyanin**

For anthocyanin measurement, 0.1 g of fresh petal tissue was ground with 10 mL of acidic methanol (a 1:99 v/v mixture of pure methanol and concentrated hydrochloric acid) using a porcelain mortar. The extract was transferred to test tubes and incubated in the dark at 25 °C for 48 hours. After incubation, the tubes were centrifuged at 4,000 rpm for 10 minutes, and the absorbance of the supernatant was measured at 550 nm using a spectrophotometer. Anthocyanin concentration was calculated in mg $g^{-1}$ fresh weight using a molar absorption coefficient of 33,000 $cm^{-1}$ M (Wagner, 1979).

**Data Analysis**

The experiment was designed as a completely randomized design (CRD). Statistical analyses were carried out using SAS software (version 9.4). Treatment means were compared using the LSD multiple range test at a 5% significance level ($P \leq 0.05$), and statistically significant differences were denoted by different letters. Graphs were generated using Microsoft Excel.

**Results**

The analysis of variance (ANOVA) indicated that the type of growing medium did not have a significant effect on flower diameter, plant height, fresh and dry weights of roots and shoots, flowering onset, or petal anthocyanin content. In contrast, the treatments significantly influenced the number of flowers at the 5% level. Moreover, total chlorophyll content, leaf carotenoid content, and total soluble sugar concentration were significantly affected by the substrate at the 1% level (Tables 2 and 3).

Table 2 - Analysis of variance of the effect of growing media on morphological traits of petunia.

| Source of Variation | df | Flower Diameter | Plant Height | Number of Flowers | Fresh Root Weight | Fresh Shoot Weight | Dry Root Weight | Dry Shoot Weight |
|---|---|---|---|---|---|---|---|---|
| Treatment | 1 | 0.054$^{ns}$ | 0.881$^{ns}$ | 96$^{*}$ | 0.074$^{ns}$ | 6.468$^{ns}$ | 0.005$^{ns}$ | 0.564$^{ns}$ |
| Error | 2 | 0.056 | 0.611 | 1.50 | 0.027 | 1.981 | 0.002 | 0.265 |
| CV% | - | 9.399 | 2.945 | 9.185 | 9.868 | 3.093 | 8.686 | 10.701 |

$^{*}$ and $^{ns}$ indicate significance at the 5% probability level and non-significance, respectively.

Table 3 – Analysis of variance of the effect of growing media on physiological and biochemical traits of petunia.

| Source of Variation | df | Petal anthocyanin content | Total sugar | Total Chlorophyll | Leaf carotenoid | Flowering time |
|---|---|---|---|---|---|---|
| Treatment | 1 | 0.001 $^{ns}$ | 0.014 $^{**}$ | 0.087 $^{**}$ | 0.052 $^{**}$ | 0.166 $^{ns}$ |
| Error | 2 | 0.0001 | 0.00003 | 0.0004 | 0.00006 | 0.067 |
| CV% | – | 2.056 | 1.872 | 3.140 | 1.977 | 1.108 |

$^{*}$ and $^{ns}$ indicate significance at the 5% probability level and non-significance, respectively.

**Number of Flowers**

The mean comparison results (Table 4) revealed that petunia plants grown in the 50:50 (v/v) mixture of *Pinus eldarica* cone peat and perlite produced the highest number of flowers. This increase in flower production supports the study's goal of identifying a locally available, nutrient-rich substrate that can match or surpass the performance of imported cocopeat. These results suggest that this medium not only enhances the reproductive performance of petunia but also offers a potential strategy to reduce reliance on foreign substrates.

Table 4. Means Comparison for the effect of growing media on physiological and biochemical traits of petunia.

| growing media | Number of flowers | Total sugar | Total Chlorophyll | Leaf carotenoid |
|---|---|---|---|---|
| Pine cone peat + perlite (50 + 50 v/v) | 17.333[a] | 0.630[b] | 0.772[a] | 0.926[a] |
| Cocopeat + perlite (50 + 50 v/v) | 9.333[b] | 0.729[a] | 0.531[b] | 0.738[b] |

Different letters indicate significant differences at the 5% probability level.

**Leaf Chlorophyll and Carotenoid Content**

The mean comparison results (Table 4) showed that petunia plants grown in a 50:50 (v/v) mixture of *Pinus eldarica* cone peat and perlite exhibited the highest leaf chlorophyll and carotenoid contents.

Regarding physiological traits, leaf chlorophyll and carotenoid contents were highest in plants grown in the pine cone peat + perlite medium (0.772 and 0.926 mg $g^{-1}$ FW, respectively), whereas plants grown in cocopeat + perlite exhibited lower levels (0.531 and 0.738 mg $g^{-1}$ FW, respectively).

**Total Sugar Content**

The mean comparison results (Table 4) showed that petunia plants grown in the 50:50 (v/v) mixture of cocopeat and perlite exhibited the highest total sugar content. This result highlights the effect of the growing medium and nutrient availability on soluble sugar accumulation. Cocopeat improves plant growth by enhancing water retention, which indirectly supports carbohydrate and sugar synthesis.

**Discussion**

The higher flower number in the pine cone peat + perlite treatment demonstrates the potential of this locally produced, nutrient-rich substrate to improve reproductive performance in petunia and reduce dependence on imported cocopeat. Nutrient availability, especially of potassium, phosphorus, nitrogen, and other macro- and micronutrients (Ca, Mg, Fe, Mn, Cu), is crucial for flower development and yield (Gülser et al., 2019; Hussain et al., 2017; Rahmani et al., 2020). The elevated cation exchange capacity and nutrient content of pine cone peat likely contributed to the observed increase in flower number.

Previous studies support the positive effect of organic substrates on flower production. Rahmani et al., (2020) reported that wood chip compost increased bud numbers in the lily, while Asghari (2017) observed higher flower numbers in Anthurium with tea waste in the medium. In contrast, pine wood fiber was reported to reduce flower production in petunia (Dickson et al., 2022; Harris et al., 2020), possibly due to allelopathic compounds or differences in material composition. In the present study, *P. eldarica* cone peat had a positive impact on flower number, highlighting its suitability compared with pine wood fiber (*P. taeda*).

The higher leaf chlorophyll and carotenoid contents in plants grown in pine cone peat + perlite are likely related to the increased availability of iron, manganese, and magnesium, which are essential for pigment biosynthesis (Marschner, 2012; Mohammadzadeh Toutounchi et al., 2016; Verbruggen et al., 2013). These findings are consistent with previous reports showing enhanced chlorophyll and carotenoid accumulation in

plants grown with organic amendments such as wood ash, green compost, and wood waste compost (Akbarzade et al., 2023; Mohsenzadeh et al., 2023; Nabeela et al., 2015; Sardoei, 2014).

Although pine cone peat provided adequate porosity and water retention, total soluble sugar content was higher in cocopeat + perlite. This effect may result from the superior water-holding capacity of cocopeat, which indirectly supports carbohydrate synthesis and translocation (Tiwari, 2015). Similar trends were reported in strawberry and Stevia plants grown in cocopeat-containing substrates (Asghari, 2017; Sharifi et al., 2019). Overall, the results indicate that pine cone peat is a promising alternative to imported cocopeat, improving flower number, chlorophyll, and carotenoid content, while cocopeat may favor sugar accumulation.

## Conclusion

The findings of this study indicate that the choice of growing medium significantly affects the quantitative and qualitative traits of petunia. Pine cone peat–based media had a more pronounced positive effect on most traits, including flower number, chlorophyll, and carotenoid contents, compared with cocopeat. Considering that pine cone peat is locally produced, reduces dependence on imported substrates, is more cost-effective, and contains higher nutrient levels, it can be recommended as a sustainable and economical alternative to imported cocopeat for petunia seedling production. Although this study was conducted under controlled greenhouse conditions, results may differ under field conditions; therefore, further field-based research is recommended to validate and generalize these findings.

## Reference

Ahmad, M., Al-Far, M.J., Tadros, & I.M. (2019). Evaluation of different soilless media on growth, quality, and yield of cucumber (Cucumis sativus L.) grown under greenhouse conditions. Australian *Journal of Crop Science*, 13(8), 1388–1400.

Akbarzade, S. S., Karimi, M., & Chalavi, V. (2023). Investigating the effect of wood waste compost and humic acid on the morphological and physiological characteristics of Zinnia (Zinnia elegans). *Journal of Plant Process and Function*, 12(56), 379–392.

Al-Far, A. M., Tadros, M. J., & Makhadmeh, I. M. (2019). Evaluation of different soilless media on growth, quality, and yield of cucumber (“Cucumis sativus” L.) grown under greenhouse conditions. *Australian Journal of Crop Science*, 13(8), 1388–1400.

Arnon, D. I. (1949). Copper enzymes in isolated chloroplasts. Polyphenoloxidase in Beta vulgaris. *Plant Physiology*, 24(1), 1.

Asghari, R. (2017). The compared effect of nutrient treatment and growth bed on some of the phytochemical characters of stevia. *Journal of Plant Research (Iranian Journal of Biology)*, 30(2), 264–272.

Babarabie, M., Rava, F., Ahmadizadeh Zahraei, A., & Danyaei, A. (2025). Pinus eldarica Cone Cellulosic Peat: A New Healthy, Organic, and Eco-friendly Substrate for Seed Germination of some Ornamental Plants (Report for the First Time). *Journal of Chemical Health Risks*, 500(1000).

Carpenter, N., & Rosenthal, W. (2011). The essential urban farmer. Penguin.

Česonienė, L., Krikštolaitis, R., Daubaras, R., & Mažeika, R. (2023). Effects of mixes of peat with different rates of spruce, pine fibers, or perlite on the growth of blueberry saplings. *Horticulturae*, 9(2), 151.

Chehregani, A., & Ramezani, H. (2016). The study of anther and pollen developmental stages in Petunia hybrida. *Journal of Plant Research (Iranian Journal of Biology)*, 29(1), 65–79.

Davidson, H., Mecklenburg, R., & Peterson, C. (2000). Nursery management: Administration and culture. *Prentice Hall Upper Saddle River, NJ*.

Dickson, R. W., Helms, K. M., Jackson, B. E., Machesney, L. M., & Lee, J. A. (2022). Evaluation of peat blended with pine wood components for effects on substrate physical properties, nitrogen immobilization, and growth of petunia (Petunia× hybrida Vilm.-Andr.). *HortScience*, 57(2), 304–311.

Durand, S., Jackson, B. E., Fonteno, W. C., & Michel, J.-C. (2021). The use of wood fiber for reducing risks of

hydrophobicity in peat-based substrates. *Agronomy*, 11(5), 907.

El-Kazzaz, K. A., & El-Kazzaz, A. A. (2017). Soilless agriculture a new and advanced method for agriculture development: an introduction. *Agric. Res. Technol.* Open Access J, 3, 63–72.

Fox, T. (2011). Urban farming: Sustainable city living in your backyard, in your community, and in the world. *CompanionHouse Books*.

Fussy, A., & Papenbrock, J. (2022). An overview of soil and soilless cultivation techniques—chances, challenges and the neglected question of sustainability. *Plants*, 11(9), 1153.

Gruda, N. S. (2019). Increasing sustainability of growing media constituents and stand-alone substrates in soilless culture systems. *Agronomy*, 9(6), 298.

Gülser, F., Çığ, A., Gökkaya, T. H., & Atmaca, H. (2019). Effects of different growing media on plant growth and nutrient contents of petunia (Petunia hybrida). *International Journal of Secondary Metabolite*, 6(4), 302–309.

Harris, C. N., Dickson, R. W., Fisher, P. R., Jackson, B. E., & Poleatewich, A. M. (2020). Evaluating peat substrates amended with pine wood fiber for nitrogen immobilization and effects on plant performance with container-grown petunia. *HortTechnology*, 30(1), 107–116.

Hoda, E. El, & Mona, S. (2014). Effect of bio and chemical fertilizers on growth and flowering of Petunia hybrida plants.

Hussain, R., Younis, A., Riaz, A., Tariq, U., Ali, S., Ali, A., & Raza, S. (2017). Evaluating sustainable and environment friendly substrates for quality production of potted Caladium. *International Journal of Recycling of Organic Waste in Agriculture*, 6(1), 13–21.

Marschner, H. (2012). Mineral nutrition of higher plants. *Academic*. Elsevier.

Mohammadzadeh Toutounchi, P., & Amirnia, R. (2016). Effect of foliar application of micronutrients on some morphological traits of Fenugreek (Trigonella foenum-graecum L.). *Iranian Journal of Medicinal and Aromatic Plants Research*, 32(2), 301–308.

Mohsenzadeh, S., Karmidarenjani, M., Mirahmadinejad, E. A., & Robati, R. (2023). The effect of green compost processed organic fertilizer and Chlorella microalgae solution on chlorophyll a, chlorophyll b, carotenoid and proline content of tropaeolum majus under drought stress. *Annual Research & Review in Biology*, 17–27.

Nabeela, F., Murad, W., Khan, I., Mian, I. A., Rehman, H., Adnan, M., & Azizullah, A. (2015). Effect of wood ash application on the morphological, physiological and biochemical parameters of Brassica napus L. *Plant Physiology and Biochemistry*, 95, 15–25.

Nelson, P. V. (1991). Greenhouse operation and management.

Prasad, M., Chrysargyris, A., McDaniel, N., Kavanagh, A., Gruda, N. S., & Tzortzakis, N. (2019). Plant nutrient availability and pH of biochars and their fractions, with the possible use as a component in a growing media. *Agronomy*, 10(1), 10.

Rahmani, F., Karimi, M., & Moradi, H. (2020). Effect of Wood Chips Compost and Humic Acid on Growth, Flowering and Vase Life of Lily (Longiflorum × Asiatic) Cv. Nashville. *Journal of Agricultural Science and Sustainable Production*, 30(3), 185–202.

Sardoei, A. (2014). Vermicompost effects on the growth and flowering of marigold (Calendula officinalis). *European Journal of Experimental Biology*, 4(1), 651–655.

Sharifi, A., Ghaderi, N., Khorshidi, J., & Javadi, T. (2019). Investigation of the Quantity and Quality of Strawberry Fruit (cv. Aromas) in Different Harvesting Periods as Affected by Culture Medium and Humic Acid. *Journal of Soil and Plant Interactions-Isfahan University of Technology*, 10(3), 81–100.

Soltanian, F. K., Kiani, B., Meybodi, M. H. H., & Saravi, A. T. (2016). Comparing growth and success of Eldarican pine (Pinus eldarica Medw.) in pure and mixed stands with river red gum (Eucalyptus camadulensis Dehnh.) in Shahid-Paidar Park, Ardakan.

Thimmaiah, S. K. (1999). Carbohydrates. Standard Methods for Biochemical Analysis. *Kalyani Publishers*, New Delhi, India, 55–57.

Tiwari, P. (2015). Coco peat: A new era of soil less urban farming. *Cellulose*, 26(7), 10.

Tzortzakis, N., Nicola, S., Savvas, D., & Voogt, W. (2020). Soilless cultivation through an intensive crop production scheme. Management strategies, challenges and future directions. *In Frontiers in Plant Science* (Vol. 11, p. 363). Frontiers Media SA.

Vandecasteele, B., Muylle, H., De Windt, I., Van Acker, J., Ameloot, N., Moreaux, K., Coucke, P., & Debode, J. (2018). Plant fibers for renewable growing media: Potential of defibration, acidification or inoculation with biocontrol fungi to reduce the N drawdown and plant pathogens. *Journal of Cleaner Production*, 203, 1143–1154.

Verbruggen, N., & Hermans, C. (2013). Physiological and molecular responses to magnesium nutritional imbalance in plants. *Plant and Soil*, 368(1), 87–99.

Wagner, G. J. (1979). Content and vacuole/extravacuole distribution of neutral sugars, free amino acids, and anthocyanin in protoplasts. *Plant Physiology*, 64(1), 88–93.

Woznicki, T., Kusnierek, K., Vandecasteele, B., & Sønsteby, A. (2024). Reuse of coir, peat, and wood fiber in strawberry production. *Frontiers in Plant Science*, 14, 1307240.